



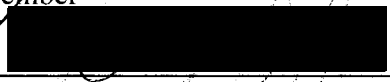
School of Medicine
Oregon Health & Science University


CERTIFICATE OF APPROVAL


This is certify that the Ph.D. dissertation of
Cynthia Wei-Sheng Lee
has been approved




Mentor/Advisor


Member


Mem


Member


Member


Member

INTERACTION BETWEEN SK CHANNEL CALMODULIN
BINDING DOMAIN AND CALMODULIN

by
Cynthia Wei-Sheng Lee

A DISSERTATION

Presented to the Neuroscience Graduate Program
and the Oregon Health & Science University
School of Medicine
in partial fulfillment of
the requirements for the degree of
Doctor of Philosophy
April 2006

TABLE OF CONTENTS

I. CHAPTER 1.....	1
INTRODUCTION.....	1
A. Overview.....	1
B. SK Channels Contribute to the Medium Afterhyperpolarization.....	2
C. Cloned SK Channels.....	4
D. Calcium-gating and Calmodulin.....	6
E. Structure of the CaMBD/CaM Complex.....	8
F. Ca ²⁺ /CaM Inhibition in CNG Channels.....	12
G. Relating Functional Data to Crystal Structure.....	14
II. CHAPTER 2.....	19
SMALL CONDUCTANCE CA ²⁺ -ACTIVATED K ⁺ CHANNELS AND CALMODULIN: CELL SURFACE EXPRESSION AND GATING.....	19
Summary.....	20
Introduction.....	21
Material and Methods.....	23
<i>Molecular Biology</i>	23
<i>Electrophysiology</i>	23
<i>Immunocytochemistry</i>	24
Results.....	26
<i>SK2:64/67 channels require cotransfected CaM for function</i>	26
<i>Exogenous CaM rescues SK2:64/67 activity in excised patches</i>	27
<i>Compensatory mutations in CaM restore association with SK2:64/67 channels</i> ...	29
<i>Ca²⁺-dependence</i>	30
<i>CaM is required for SK channel cell surface localization</i>	31
Discussion.....	33
III. CHAPTER 3.....	43
SMALL CONDUCTANCE CA ²⁺ -ACTIVATED K ⁺ CHANNEL CALMODULIN: CHALLENGING THE ‘DIMER-OF-DIMERS’ MODEL FOR SK CHANNEL GATING.....	43
Summary.....	44
Introduction.....	45
Material and Methods.....	47
<i>Molecular Biology and Biochemistry</i>	47

<i>Reactivity Measurements of Cysteine Mutants with PyMPO</i>	48
<i>Immunocytochemistry</i>	49
<i>Electrophysiology</i>	49
Results.....	51
<i>Forming CaMBD-CaM Complex from Isolated Peptides</i>	51
<i>Crosslinking of Cysteine-Substituted CaMBD</i>	51
<i>Site-directed Fluorescence Labeling of Adjacent Residues of W432 on CaMBD</i> ..	52
<i>rSK2 L457C Cross-linked by Homobifunctional MTS Compounds</i>	54
<i>The rSK2 K472 Truncation Is Fully Functional and Gated by Ca²⁺</i>	57
Discussion.....	59
<i>The Architecture of Calcium-Gated Potassium Channels</i>	59
<i>Factors affecting cysteine modification by PyMPO maleimide</i>	60
<i>Calmodulin-modulated Channel Activities</i>	62
<i>Altered Ca²⁺-sensitivity of SK Channels and Plausible Mechanisms</i>	62
<i>A Role for Hydrophobic Residues in Ca²⁺-sensitivity of SK Channels</i>	63
IV. DISCUSSION	80
A. CaM Activation Mechanisms.....	80
B. CaM-facilitated Trafficking of SK Channels.....	82
C. Reconcile the Functional Data to the Crystal Structure.....	84
D. Hydrophobic Residues in SK Channels.....	85
E. Future Experiments.....	86
V. SUMMARY AND CONCLUSIONS	87
VI. REFERENCES	88

LIST OF FIGURES AND TABLES

Figure 1: Dendrogram of the 71 cloned mammalian K⁺ channels

Figure 2: Topology, nomenclature and chromosomal localization of the KCNN family

Figure 3: Structure of the gating domain of SK2 (CaMBD) complexed with Ca²⁺/CaM

Figure 4: SK2:64/67 requires co-expressed CaM for function.

Figure 5: Ca²⁺-CaM rescues SK2:64/67 in excised patches.

Figure 6: Ca²⁺-free CaM associates with SK2:64/67 SK channels and calmodulin.

Figure 7: CaM:84/87 compensates for SK2:64/67.

Figure 8: Ca²⁺ dose-responses.

Figure 9: CaM is required for surface expression.

Figure 10: As isolated peptides, CaMBD-CaM complex retains the specific interaction and the 1:1 stoichiometry.

Figure 11: Site-directed fluorescence labeling (SDFL) of adjacent residues of W432 on CaMBD.

Figure 12: The rSK2 L457C single mutant was able to be modified and crosslinked upon addition of MTS compounds, altering the calcium sensitivity of the channel.

Figure 13: The rSK2 K472* channel harboring a truncation of the C-terminal domain was fully functional, displaying normal Ca²⁺-gating.

Table 1: Alteration of Ca²⁺-sensitivity after cross-linking/modification with MTS compounds

LIST OF ABBREVIATIONS

SK channel: small conductance Ca^{2+} -activated potassium channel

CaM: calmodulin

CaMBD: Calmodulin binding domain

AHP: afterhyperpolarization

K_{Ca} currents: Ca^{2+} -dependent K^+ conductance

IK channel: intermediate conductance Ca^{2+} -activated potassium channel

BK channel: Ca^{2+} -activated K^+ channels of large conductance

CNG channel: cyclic nucleotide-gated channel

HCN channel: hyperpolarization-activated, cyclic nucleotidemodulated channel

GIRK channel: G-protein-coupled inwardly rectifying K^+ channel

RCK domain: regulator of conductance for K^+

SK2:64/67: SK2 R464E;K467E

CaM:84/87: CaM E84R;E87K

CaM1,2, CaM3,4, CaM1,2,3,4: calmodulins with mutations in the first position of the indicated E-F hands, effectively abolishing Ca^{2+} binding.

SK2:472*: rSK2 K472 truncation

SK2:475*: rSK2 D475 truncation

SK2:477*: rSK2 A477 truncation

PyMPO-maleimide: 1-(2-maleimidylethyl)-4-(5-(4-methoxyphenyl)oxazol-2-yl)pyridinium
methanesulfonate

MTS: methanethiosulfonate

MTSBn: benzyl methanethiosulfonate

MTSEA: 2-(aminoethyl) methanethiosulfonate

MTSES: Sodium (2-Sulfonatoethyl)methanethiosulfonate

MTSET: [2-(trimethylammonium)ethyl] methanethiosulfonate

M2M: 1,2-ethanediyl bismethanethiosulfonate

M3M: 1,3-propanediyl bismethanethiosulfonate

M4M: 1,4-butanediyl bismethanethiosulfonate

M5M: 1,5-pentanediyl bismethanethiosulfonate

M6M: 1,6-hexanediyl bismethanethiosulfonate

SDFL: site-directed fluorescence labeling

ACKNOWLEDGEMENTS

First and foremost, I thank my mentor Dr. John Adelman who has invested so much time and energy supporting my advancement through graduate school. I also thank Dr. James Maylie and Dr. David Farrens for their scientific training. I especially would like to thank Dr. Andrew Bruening-Wright who has taught me electrophysiology, critical thinking, and provided technical support and friendship. And finally, to my parents, who never stop encouraging and supporting higher education.

ABSTRACT

Small conductance Ca^{2+} -activated K^+ channels (SK channels) are heteromeric complexes of pore-forming alpha subunits and constitutively bound calmodulin (CaM). Structure-function analysis demonstrated that the interaction between SK channels and CaM occurs at the CaM binding domain (CaMBD) residing in the proximal region of the intracellular C terminus of the alpha subunit. Using electrophysiological recordings and immunochemistry on the SK channel double charge reversal mutant, SK2 R464E/K467E (SK2:64/67), that has dramatically reduced calmodulin binding affinity due to disrupted salt bridges with E84 and E86 on CaM, we demonstrated that the Ca^{2+} -independent constitutive association of CaM and SK channel subunits is required for surface expression, but not for channel gating. Residues on the first helix of the helix-turn-helix CaMBD peptide, containing the tryptophan residue in its central region and hydrophobically contacting the C-lobe of CaM, were cysteine-substituted in the attempts to define the interaction sites between the SK channel CaMBD and CaM with site-directed fluorescence labeling (SDFL) on isolated peptides. Application of methanethiosulfonate (MTS) reagents onto SK2 L457C revealed the charge-dependent modulation of Ca^{2+} -sensitivity, and MTS crosslinkers rescued the decreased Ca^{2+} -sensitivity of SK2 L457C. Therefore, both electrostatic and hydrophobic interactions contribute to the close association between the SK channel CaMBD and CaM.

I. CHAPTER 1

Introduction

A. Overview

Ion channels are macromolecular pores that conduct currents by carrying ions through the cell membrane. They are the fundamental elements of the excitable cells, responsible for the electrical signaling in nerves, muscles, and synapses. In response to extracellular stimuli such as a membrane potential change, a neurotransmitter binding, or a mechanical deformation, channels open or close the pores to permit or block the ion flow. This gating process is selective, allowing restricted classes of small ions to flow passively down their electrochemical activity gradients at the extremely high rate of $> 10^6$ per second. With their extraordinary sensitivity, selectivity and speed, diverse ion channels work in concert to shape the signals and responses of the nervous system (Hille, 2001).

The Na^+ , K^+ , Ca^{2+} , and Cl^- channels are major ion classes in the nervous system. Being named after their most permeant ion, Na^+ , K^+ , Ca^{2+} , and Cl^- channels are further classified by their kinetics, pharmacology, response to ion substitution, and more recently, genetic sequences (Hille, 2001). K^+ channels are the most diverse superfamily of ion channels (Figure 1). This diversity originates from the large number of genes coding K^+ channel principal subunits, as well as alternative splicing that generates multiple mRNA transcripts from a single gene, possible RNA editing, posttranslational modifications, and heteromeric assembly of different principal subunits (Coetzee et al., 1999). Ca^{2+} -activated K^+ channels (K_{Ca} channels), first described in red blood cells, play an

important part in the maintenance of the blood's physiological ion balance (Gardos, 1958). They were also implicated to underlie the afterhyperpolarization (AHP) that follows bursts of action potentials in the mammalian hippocampus (Alger and Nicoll, 1980). All K_{Ca} currents are activated or modulated by Ca^{2+} , whereas they are different in their voltage sensitivity and pharmacology (Sah, 1996). Small conductance K_{Ca} channels (SK channels) are gated solely by intracellular Ca^{2+} via the constitutively-bound calmodulin within their intracellular C-terminal domain (Xia et al., 1998). This dissertation will focus on the structure and function of SK channels, especially in their interaction with calmodulin (CaM), the gating element of SK channels and the ubiquitous Ca^{2+} sensor inside the cell.

B. Small Conductance Ca^{2+} -activated K^+ Channels (SK Channels) Contribute to the Medium Afterhyperpolarization

The K_{Ca} currents characterized in different systems give rise to a similar physiological consequence: hyperpolarization of the membrane potential. Depending on their time courses, K_{Ca} currents contribute either to the repolarization of the action potential or to one or more phases of the afterhyperpolarization (fast, medium and slow AHP) following single or bursts of action potentials (Stocker et al., 2004). The fast AHP typically lasts for 1-10 milliseconds, and is primarily due to the activation of voltage-gated K^+ currents and big conductance K_{Ca} channels (BK channels). As intracellular Ca^{2+} levels increase during an action potential, a long lasting AHP that usually has two Ca^{2+} -dependent components, medium and slow, ensues (Sah, 1996). Recordings from CA1 neurons in the

hippocampus show that a sustained stimulus elicits a train of action potentials. With each action potential, the AHP increases in depth and duration, causing increased interspike intervals and, ultimately, accommodation where the cell is no longer able to reach the action potential threshold. Blocking SK channels with apamin reduces the medium AHP, increases the number of elicited action potentials, and shortens interspike intervals while not affecting accommodation (Stocker et al., 1999). The contribution of SK channels to somatic mAHP in CA1 hippocampal pyramidal cells (Bond et al., 2004; Sailer et al., 2002; Stackman et al., 2002) was recently disputed (Gu et al., 2005), but this inconsistency did not preclude that SK channels can generate mAHP in other types of neurons (Abel et al., 2004; Schwindt et al., 1988). Intriguingly, although the molecular identities of the fast and medium AHP currents have been assigned to the big conductance K_{Ca} channels (BK channels) (Shao et al., 1999) and the SK channels (Bond et al., 2004), respectively, the slow AHP remains an apamin-insensitive calcium-modulated K^+ current without known molecular identity.

Four models of SK channel function in the central nervous system have been drawn from recent work (Bond et al., 2005): (i) SK channels contribute to the AHP (Stocker et al., 1999) and synaptic integration in pyramidal neurons of the hippocampus (Ngo-Anh et al., 2005). (ii) SK channels are involved in pacemaker activity and synaptic response in dopamine neurons of the substantia nigra (Wolfart et al., 2001). (iii) SK channels enable rapid firing and mode switching in Purkinje neurons of the cerebellum (Edgerton and Reinhart, 2003; Swensen and Bean, 2003). (iv) SK channels convert an excitatory neurotransmitter signal into inhibition in hair cells of the Organ of Corti (Marcotti et al.,

2004; Oliver et al., 2000). Different cells dictate the timing and position of SK channel influence on membrane potential by employing specific subsets of Ca^{2+} sources. In addition, the phosphorylation state of SK-bound CaM, which might reflect the recent activity of the cell, also affects SK channel activity (Bildl et al., 2004).

C. Cloned SK Channels

Four genes encode the structurally and functionally related members of the SK channel family: $\text{K}_{\text{Ca}2.1}$ (SK1), $\text{K}_{\text{Ca}2.2}$ (SK2), $\text{K}_{\text{Ca}2.3}$ (SK3) and $\text{K}_{\text{Ca}3.1}$ (SK4/IK1) (Ishii et al., 1997b; Joiner et al., 1997; Kohler et al., 1996) (Figure 2). SK1, SK2, and SK3 are apamin-sensitive, calcium-activated, and voltage-independent channels with unit conductance of about 10 pS in symmetrical K^+ solution (Hirschberg et al., 1998; Kohler et al., 1996). With overlapping but distinct profiles, these channels are widely expressed in the central nervous system (Sailer et al., 2002; Stocker and Pedarzani, 2000). The apamin-sensitivity of the cloned SK channels strongly suggests that one or more of them underlie the apamin-sensitive component of the medium AHP in central neurons. SK4, the fourth member of the family, is also calcium-activated and voltage-independent, but not apamin-sensitive, and with a larger unitary conductance of about 40 pS (Ishii et al., 1997b; Joiner et al., 1997). SK4 expression is restricted to peripheral tissues (Ishii et al., 1997b; Logsdon et al., 1997). The topology of SK channels has not been directly mapped, but their primary amino acid sequences predict a serpentine architecture like Shaker K_V channels. The SK channels have six transmembrane domains (S1-S6) with the N- and C-termini residing in the cytoplasm,

and a pore region between S5 and S6 bearing the signature sequences of the selectivity and conduction pathway for potassium channels (Kohler et al., 1996). Functional SK channels are probably tetramers analogous to most other potassium channels. Among SK channels, the primary sequences of the transmembrane domains are conserved, yet the sequences vary in the extreme termini, suggesting that these distal domains confer the physiological specificity of each subtype of SK channels (Bond et al., 1999).

Transgenic mice models have been generated to investigate the physiological functions of cloned SK channels. SK2 null mice completely lack the apamin-sensitive component of the mAHP current in CA1 neurons (Bond et al., 2004). Furthermore, transgenic mice that overexpress SK2 subunits by 10-fold have 4-fold increased apamin-sensitive current in CA1 neurons relative to wild-type littermates. In addition, the amplitude of synaptically evoked EPSPs recorded from SK2 overexpressing CA1 neurons increased twice in response to SK channel blockade. Consistent with this, SK2 overexpression reduced long-term potentiation after high-frequency stimulation and severely impaired learning in both hippocampus- and amygdala-dependent tasks (Hammond et al., 2006). SK3 expression can be manipulated using a transgenic mouse that harbors a tetracycline-regulated SK3 gene (Bond et al., 2000). Absence of SK3 does not present overt phenotypic consequences. However, SK3 overexpression induces abnormal respiratory responses to hypoxia and compromised parturition (Bond et al., 2000). Electromyographic (EMG) recordings from this transgenic mice demonstrate that SK3 channels are necessary but not sufficient for denervation-induced skeletal muscle hyperexcitability (Jacobson et al., 2002). Examining bladder function in these mice

reveals that SK3 channels have a significant role in the control of non-voiding contractions *in vivo*. Hence, activation of SK3 channels could be a therapeutic approach for management of non-voiding contractions, a condition which characterizes many types of urinary bladder dysfunctions including urinary incontinence (Herrera et al., 2003). In a transgenic mouse expressing a truncated SK_{Ca} subunit (SK3-1B) as a dominant negative for SK_{Ca}-IK_{Ca} channels, SK3-1B expression profoundly inhibits mAHP but has no discernable effect on sAHP. This result is consistent with the proposal that SK_{Ca} channels do not mediate sAHP in pyramidal cells (Villalobos et al., 2004).

D. Calcium-gating and Calmodulin

Calmodulin (CaM) has been found to be the constitutive or dissociable Ca²⁺-sensing subunit of various ion channels in a wide range of species from *Homo sapiens* to *Paramecium*. These ion channels include voltage-gated Ca²⁺ channels, cyclic nucleotide-gated (CNG) channels (Grunwald et al., 1999; Hsu and Molday, 1993), NMDA receptors (Ehlers et al., 1996; Zhang et al., 1998), ryanodine receptors (RyR) (Rodney et al., 2000) and inositol 1,4,5-trisphosphate receptors (IP₃R) (Michikawa et al., 1999), Ca²⁺-activated K⁺ channels of small or intermediate conductance (SK or IK), Trp family channels, gap junction channels, human EAG channels (hEAG1) (Schonherr et al., 2000), and even Ca²⁺-induced Ca²⁺ release channels from organelles (Smith et al., 1989). For Ca²⁺-activated K⁺ channels of large conductance (BK), the precise Ca²⁺ interaction site is still not known (Qian et al., 2002), but have been suggested to use a “Ca²⁺-bowl” structure (Schreiber and Salkoff, 1997) or the RCK domain (regulator of conductance for

K⁺) (Xia et al., 2002) in the C-terminus of the pore-forming domain to detect cytoplasmic Ca²⁺, and hence do not belong to this category (Saimi and Kung, 2002).

The unique feature of SK channels is that they are solely gated by calcium, the ubiquitous second messenger in the cell. The channels are highly calcium-sensitive, with K_D values of about 0.5 μM (Hirschberg et al., 1998; Kohler et al., 1996). Fast application of saturating Ca²⁺ revealed rapid channel gating, occurring in a few milliseconds. Surprisingly though, the primary sequences of the SK channels do not contain obvious Ca²⁺-binding motifs. Xia *et al.*, using a yeast two hybrid approach, demonstrated that the proximal domains of the C-termini interact with the ubiquitous Ca²⁺ sensor, CaM (Xia et al., 1998). Biochemical experiments revealed that the calmodulin binding domain (CaMBD), a stretch of 92 amino acids, interacts with CaM in the presence or absence of Ca²⁺. The SK channel-CaM complex is extremely stable, requiring harsh denaturing conditions to separate them. CaM possesses two E-F hand¹ motifs in each globular N- and C-terminal region, separated by a flexible linker. Mutagenesis studies showed that the two N-terminal E-F hands are necessary and sufficient for normal Ca²⁺-gating, whereas the C-terminal E-F hands are dispensable for gating (Keen et al., 1999; Xia et al., 1998). Thus, the crystallographic and biochemical data suggest that SK channels are heteromeric complexes of four pore-forming α-subunits and constitutively bound β-subunit, calmodulin, which senses the change of intracellular Ca²⁺ concentration and rapidly gates the pore-forming α-subunits. Further experiments using a double charge reversal mutant

¹ An E-F hand is consisted of an N-terminal helix (the E helix) immediately followed by a centrally located Ca²⁺-coordinating loop and a C-terminal helix (the F helix). The three-dimensional arrangement of these domains is reminiscent of the thumb, index and middle fingers of a hand, hence denoted 'E-F hand'. Chin, D., and Means, A. R. (2000a). Author correction. *Trends Cell Biol* 10, 428, Chin, D., and Means, A. R. (2000b). Calmodulin: a prototypical calcium sensor. *Trends Cell Biol* 10, 322-328.

of the SK2 channel with reduced affinity for CaM illustrated that the constitutive associations between CaM and the pore-forming α -subunits are not required for channel gating, as exogenous CaM could be applied to restore the gating in SK2 channels lacking pre-associated CaM. However, the Ca^{2+} -independent interactions are necessary for cell-surface expression of SK2 channels (Lee et al., 2003). Therefore, CaM has dual functions— as the β -subunit of SK channels, Ca^{2+} -mediated gating, and proper trafficking to the cell surface.

In addition to CaM constitutively bound to the intracellular C terminus of SK channels, the cytoplasmic N and C termini of the channel protein form a polyprotein complex with the catalytic and regulatory subunits of protein kinase CK2 and protein phosphatase 2A. Within this complex, CK2 phosphorylates CaM at threonine 80, reducing by 5-fold the apparent Ca^{2+} sensitivity and accelerating channel deactivation. The results demonstrate that native SK channels are polyprotein complexes; the balance between kinase and phosphatase activities within the protein complex shapes the hyperpolarizing response mediated by SK channels (Bildl et al., 2004).

E. Structure of the CaMBD/CaM Complex

The 1.60 Å crystal structure of the SK channel CaMBD/ Ca^{2+} /CaM complex revealed that the CaMBD forms an elongated dimer with a CaM molecule bound at either end. There are electrostatic interactions, hydrogen-bond tethers, and hydrophobic patches between the two proteins, and each CaM wraps around three α -helices, two from one CaMBD

subunit and one from the other. The CaMBD/Ca²⁺/CaM complex is distinct from other CaM/peptide complexes because CaM binds three α -helices instead of one, and the N-lobe and C-lobe of each CaM contact different CaMBD monomers. Furthermore, as only the CaM N-lobe has bound Ca²⁺, the CaMBD/Ca²⁺/CaM structure details both Ca²⁺-dependent and Ca²⁺-independent CaM interactions in a single complex. According to the crystal structure, a possible chemo-mechanical gating model was proposed. Ca²⁺ binding to each CaM N-lobe exposes its hydrophobic patch, allowing it to interact with the adjacent CaMBD monomer. As each N-lobe on adjacent monomers grabs the other CaMBD C-terminal region, a rotary force is created and transmitted to the attached S6 pore helices in the gate region. In this model, two CaMBD serve as levers to drive opening of the channel activation gate (Schumacher et al., 2004; Schumacher et al., 2001). Therefore, the SK channel might gate as a dimer-of-dimers (Figure 3).

CaM interactions with Ca²⁺ channels mediate Ca²⁺ regulation of channels. L-type (Ca_v1) Ca²⁺ channels possess Ca²⁺-dependent inactivation (CDI) which reflects activation of preassociated CaM in response to Ca²⁺ entry (Erickson et al., 2001; Erickson et al., 2003; Peterson et al., 1999; Zuhlke et al., 1999). Additionally, P/Q-type (Ca_v2.1), R-type (Ca_v2.3), and N-type (Ca_v2.2) channels also undergo CDI (DeMaria et al., 2001; Liang et al., 2003). In L-type channels, CDI is mediated by the high-affinity C-terminal lobe of CaM and is consequently insensitive to buffering of intracellular Ca²⁺. For non-L-type channels, CDI relies on the lower-affinity N-terminal lobe of CaM, and hence aggregate increases in intracellular Ca²⁺ from multiple sources (channels or internal stores) are required (Zamponi, 2003). Crucial to this function is the number of CaMs regulating each

channel, and the number of CaMs privy to the local Ca^{2+} signal from each channel. To resolve these parameters, L-type Ca^{2+} channels were fused to single CaM molecules, revealing that a single CaM directs L-type channel regulation. Similar fusion proteins were also used to estimate the local CaM concentration near Ca^{2+} channels (Mori et al., 2004). To examine the stoichiometry of CaM required for SK channel function, SK1 and SK2:64/67 subunits were linked together by a Q_{10} linker, and the dimer mRNA was injected into *Xenopus* oocytes. In contrast to a dimer of SK1 and wild-type SK2 (Ishii et al., 1997a), channel gating was not observed; suggesting that CaM must be bound constitutively to at least three α -subunits for channel function (Keen et al., 1999). Assuming that SK channels are tetramers, the fluorescence measurements and functional data suggest that CaM is bound to each α -subunit, and Ca^{2+} binding to either one or both E-F hands 1 or 2 on CaM molecules results in channel gating (Keen et al., 1999). A model describing Ca^{2+} -dependent gating of SK2 was proposed according to the single-channel kinetics (Hirschberg et al., 1998), EC_{50} for Ca^{2+} (Keen et al., 1999), and kinetics of activation and deactivation (Xia et al., 1998). The complete form of the model shows the conformational changes in the channel comprising fifteen closed states and five identical open states, implicating that these substates of SK channels (Hirschberg et al., 1998) could represent the different CaM stoichiometries.

Despite of biochemical assays revealing CaMBD and CaM as a 1:1 molar ratio complex (Keen et al., 1999; Schumacher et al., 2004; Schumacher et al., 2001), the functional stoichiometry of Ca^{2+} /CaM regulation of SK channels is unknown. An experiment similar to that used in determining distinct functional stoichiometry of potassium channel β

subunits would be the best approach to answer this question. In these experiments concatenated tetramers of SK subunits would be expressed in which the number of subunits harboring mutations that eliminate CaM binding would be varied, i.e. utilizing the SK channel lacking the CaMBD which loses its Ca^{2+} /CaM activation, combined with 12CA5 monoclonal epitope tagged CaM, to investigate the stoichiometry of α and β subunits in functional SK channels (Xu et al., 1998). The difficulty in applying this methodology is due to the non-functionality of tandem SK channel constructs which constrain subunit stoichiometry (Bruening-Wright et al., unpublished data) and the abundance of endogenous CaM inside the oocytes and mammalian cells.

According to the crystal structure, at least two CaM molecules are required to form a CaMBD/ Ca^{2+} /CaM dimer to fulfill the ‘dimer-of-dimers’ gating model. Therefore, the functional stoichiometry of SK channels should be 2 or 4 if the model is correct. Biophysical techniques involving resonance energy transfer, FRET (fluorescence resonance energy transfer) and BRET (bioluminescence resonance energy transfer), have enabled monitoring the formation of dynamic G protein-coupled receptor(s) (GPCR)-protein complexes in living cells in real time (Pfleger and Eidne, 2005). Hence, a possible future experiment to elucidate to functional SK stoichiometry is to utilize fusions SK channel-Rluc (*Renilla luciferase*²) and SK channel-YFP constructs expressed in HEK-293 cells and assess the occurrence of BRET (Angers et al., 2000). Another potential experiment is to coinject *Xenopus* oocytes with different ratios of mRNAs of

² BRET is a naturally occurring phenomenon resulting from the nonradiative energy transfer between luminescent donor and fluorescent acceptor proteins. In the sea pansy *Renilla reniformis*, the luminescence generated by the catalytic degradation of coelenterazine by luciferase is transferred to the green fluorescence protein (GFP), which emits fluorescence upon dimerization of two proteins.

intact and CaM binding deficient SK channels, and access the functionality by recording the currents from excised inside-out patches (Ishii et al., 1997a).

The substituted cysteine accessibility method (SCAM) and block by intracellular quaternary amines were used to probe the topology of the SK2 channel inner vestibule and compare the location of SK channel gate with those of K_V and K_{CSA} channels. Data from internal application of quaternary amines indicated that the inner vestibules of K_V and SK channels share structural similarity. The charged sulfhydryl specific alkylating agent, 2-(aminoethyl) methanethiosulfonate (MTSEA), modified a position predicted to lie in the lumen immediately intracellular to the selectivity filter in the open and closed states equivalently. The pore blocker tetrabutylammonium impeded MTSEA access to this position either in open or closed channels, suggesting that the SK channel activation gate is not constituted by the cytoplasmic end of S6 as for K_V and K_{CSA} channels, but resides deep in the ion-conducting pore in or near the selectivity filter (Bruening-Wright et al., 2002).

F. Ca^{2+} /CaM Inhibition in CNG Channels.

Cyclic nucleotide-gated (CNG) ion channels mediate sensory transduction in olfactory sensory neurons and retinal photoreceptor cells. Internal Ca^{2+} /CaM inhibits CNG channels, thereby having a putative role in sensory adaptation (Trudeau and Zagotta, 2003). Currently, six types of mammalian CNG channel subunits are divided into two classes; the CNGA class contains CNGA1, CNGA2, CNGA3, and CNGA4 subunits, and the CNGB class contains the CNGB1 and CNGB3 subunits. CNGB also contains

CNGB1b, an olfactory-specific splice variant of CNGB1. Channel subunits are 35–75% similar, and all have the same proposed transmembrane arrangement with intracellular N- and C-terminal regions and six transmembrane domains. Like SK channel, four subunits coassemble to form a tetrameric CNG channel with a central pore region (Liu et al., 1996).

CNG channels in olfactory sensory neurons are formed by three different channel subunits, CNGA2, CNGA4, and CNGB1b; whereas the native retinal rod CNG channel is formed exclusively by co-assembly of CNGA1 and CNGB1 subunits into heteromeric channels. For both olfactory and rod channels, $\text{Ca}^{2+}/\text{CaM}$ binds to an N-terminal region of the channel and disrupts an interaction between this region and a C-terminal region, causing inhibition. Olfactory CNGA2 subunits contain an archetypal “1-8-14” site in their N-terminal region that is necessary and sufficient to bind to $\text{Ca}^{2+}/\text{CaM}$ (Chen and Yau, 1994). Rod CNGB1 subunits have an N-terminal site similar to those in the IQ motifs that is necessary for $\text{Ca}^{2+}/\text{CaM}$ binding, and also contain a C-terminal region that binds to $\text{Ca}^{2+}/\text{CaM}$ in biochemical assays (Grunwald et al., 1998).

An interdomain interaction in CNGA2 olfactory channels involves an N-terminal 1-8-14 motif and the C-terminal C-linker and CNBD. In contrast, intersubunit interaction in rod channels involves the $\text{Ca}^{2+}/\text{CaM}$ -binding site in the N-terminal region from CNGB1 and the distal C-terminal region of CNGA1. Inhibition is due to disruption of the interaction in the presence of $\text{Ca}^{2+}/\text{CaM}$ (Trudeau and Zagotta, 2002; Varnum and Zagotta, 1997). Different from the cloned channels, native olfactory CNG channels are comprised of two

CNGA2 subunits, a CNGA4 subunit, and a CNGB1b subunit. CaM constitutively binds to sites on CNGB1b N-terminal and CNGA4 C-terminal domains. Ca^{2+} binds to CaM upon Ca^{2+} influx through the channel, rendering the channel less sensitive to Ca^{2+} . (Adelman and Herson, 2004; Bradley et al., 2004)

The hyperpolarization-activated, cyclic nucleotidemodulated (HCN) channels are nonselective cation channels, underlying the I_f , I_h and I_q currents of heart and nerve cells. They are activated by membrane hyperpolarization and modulated by the binding of cyclic nucleotides such as cAMP and cGMP. The mechanism underlying this modulation depends on a carboxy-terminal fragment of HCN2 containing the cyclic nucleotide-binding domain (CNBD) and the C-linker region that connects the CNBD to the pore. X-ray crystallographic structures of this C-terminal fragment bound to cAMP or cGMP, together with equilibrium sedimentation analysis, identify a tetramerization domain and the mechanism for cyclic nucleotide specificity, and suggest a model for ligand-dependent channel modulation. Due to amino acid sequence similarity to HCN channels, the CNG channels are probably related to HCN channels in structure and mechanism (Zagotta et al., 2003).

G. Relating Functional Data to Crystal Structure

Whether the dimer-of-dimers model of SK channels is correct or not, the crystal structure and complementary biochemical data not only reveal the physical interactions between the CaMBD and CaM, but also suggest domains and residues that undergo

conformational changes as a function of Ca^{2+} . To benefit from the insight gained through the crystal structure, we investigated the physical properties of SK channels by generating compensatory mutations of CaM to rescue an SK channel mutant that has dramatically reduce CaM binding affinity. Further immunocytochemical studies revealed the role of CaM-association in appropriate surface expression of SK channels. Attempts to define the interaction sites between SK channel calmodulin binding domain (CaMBD) and calmodulin were made via cysteine substitution of interested residues on isolated peptides. Site-directed fluorescence labeling and cross-linking of cysteine-substituted CaMBD peptides were performed. Further, inside-out patch clamp recordings using monofunctional and homobifunctional MTS agents led to the identification of a vital leucine residue on the SK channel CaM binding domain.

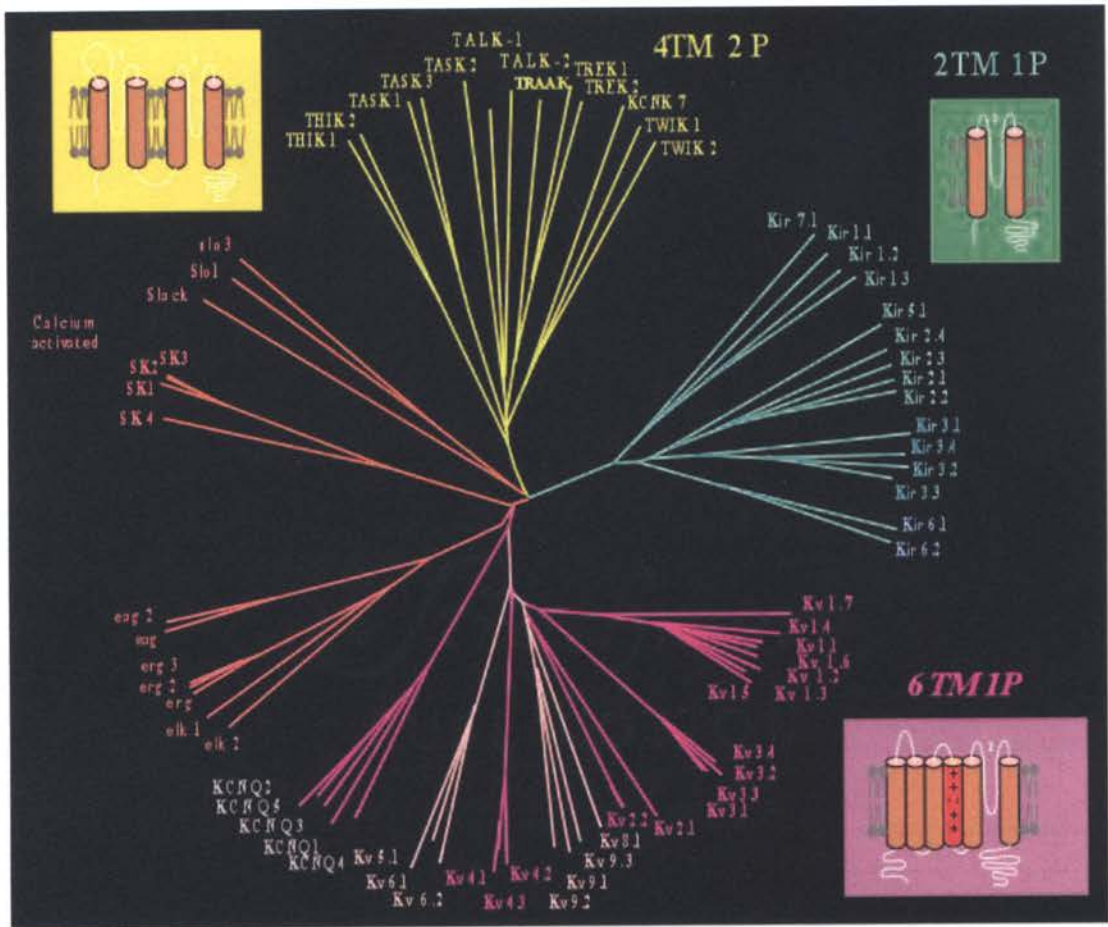
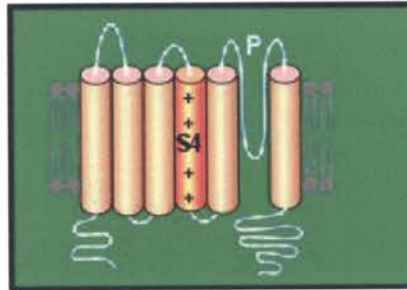


Figure 1: Dendrogram of the 71 cloned mammalian K⁺ channels

Legend: TM; Transmembrane segment, P; pore domain

(Adapted from <http://www.ipmc.cnrs.fr/~duprat/ipmc/nomenclature.htm>, Fabrice Duprat, 16 / 12 / 2003)

KCNN FAMILY



Assembly:

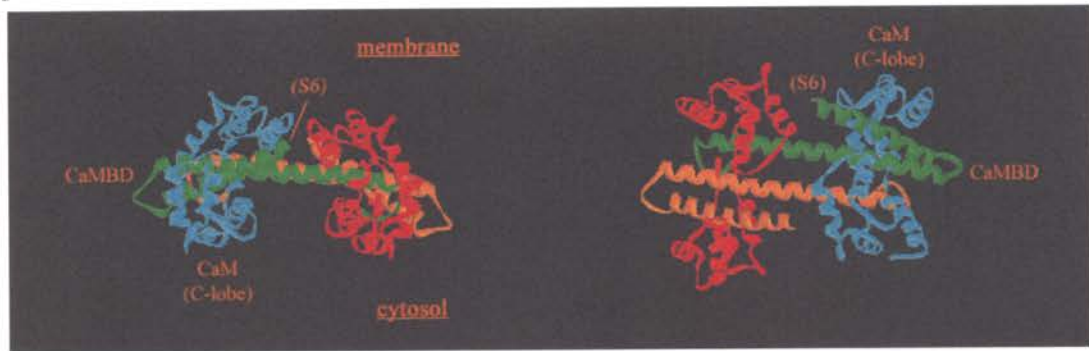
x4

Calcium-activated: intermediate and small conductance			
Human gene names	Channel names (IUPHAR)	Other names	Chromosomal localization
<i>KCNN1</i>	KCa2.1	SK1, SKCa1	19p13.1
<i>KCNN2</i>	KCa2.2	SK2, SKCa2	5q23.1-23.2
<i>KCNN3</i>	KCa2.3	SK3, SKCa3, hKCa3	1q21.3
<i>KCNN4</i>	KCa3.1	SK4, Kca4, IKCa1, IK1	19q13.2

Figure 2: Topology, nomenclature and chromosomal localization of the KCNN family

(Adapted from <http://www.ipmc.cnrs.fr/~duprat/ipmc/nomenclature.htm>, Fabrice Duprat, 16 / 12 / 2003)

A



B

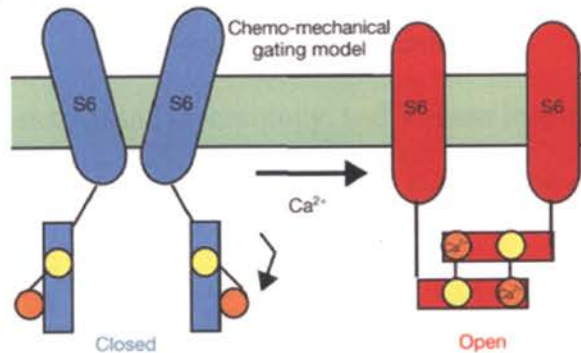


Figure 3. Structure of the gating domain of SK2 (CaMBD) complexed with $\text{Ca}^{2+}/\text{CaM}$

(A) (*Left*) Ribbon diagram of the CaMBD/ Ca^{2+} /CaM dimeric complex. CaMBD subunits are in green and orange, and CaM molecules are in blue and red. The orientation of the complex relative to the membrane is indicated. (*Right*) Top view of the crystal structure.

(B) Cartoon of proposed chemo-mechanical gating model. The CaM C-lobe and N-lobe are yellow and orange. The CaMBD/CaM complex is monomeric in the absence and dimeric in the presence of Ca^{2+} . A rotary movement resulted from the formation of the dimeric complex would drive a rotation between the S6 helices to open the gate. Adapted from (Schumacher et al., 2001).

II. CHAPTER 2

Small conductance Ca²⁺-activated K⁺ channels and calmodulin: Cell surface expression and gating

Wei-Sheng Lee, Thu Jennifer Ngo-Anh, Andrew Bruening-Wright,

James Maylie\$, John P. Adelman*

\$ Department of Obstetrics and Gynecology, and Vollum Institute, Oregon Health
& Science University, Portland, Oregon, USA

running title: SK channels and calmodulin

Corresponding author:

Dr. John P. Adelman

Vollum Institute, Oregon Health & Science University

3181 SW Sam Jackson Park Road

Portland, Oregon, 97239

(503)-494-5450

(503)-494-4353 (fax)

adelman@ohsu.edu

Copyright 2003 by The American Society for Biochemistry and Molecular Biology, Inc.

JBC Papers in Press. Published on May 6, 2003 as Manuscript M302091200

Summary

Small conductance Ca^{2+} -activated K^+ channels (SK channels) are heteromeric complexes of pore-forming α subunits and constitutively bound calmodulin (CaM). The binding of CaM is mediated in part by the electrostatic interaction between residues R464 and K467 of SK2 and E84 and E87 of CaM. Heterologous expression of the double charge reversal in SK2, SK2R464E;K467E (SK2:64/67), did not yield detectable surface expression or channel activity in whole cell or inside-out patch recordings. Coexpression of SK2:64/67 with wild type CaM or CaM1,2,3,4, a mutant lacking the ability to bind Ca^{2+} , rescued surface expression. In patches from cells coexpressing SK2:64/67 and wild type CaM, currents were recorded immediately following excision into Ca^{2+} -containing solution but disappeared within minutes after excision or immediately upon exposure to Ca^{2+} -free solution, and were not reactivated upon reapplication of Ca^{2+} -containing solution. Channel activity was restored by application of purified recombinant Ca^{2+} -CaM, or exposure to Ca^{2+} -free CaM followed by application of Ca^{2+} -containing solution. Coexpression of the double charge reversal E84R;E87K in CaM (CaM:84/87) with SK2:64/67 reconstituted stable Ca^{2+} -dependent channel activity that was not lost with exposure to Ca^{2+} -free solution. Therefore, Ca^{2+} -independent interactions with CaM are required for surface expression of SK channels, while the constitutive association between the two channel subunits is not an essential requirement for gating.

Introduction

Small conductance Ca^{2+} -activated K^+ channels (SK channels) are fundamental components of cell excitability. SK channels are voltage-independent and activated by elevated intracellular Ca^{2+} levels that occur during an action potential. In many neurons, SK channels remain open after the action potential and contribute to an afterhyperpolarization, thereby influencing interspike interval and burst duration (Alger and Nicoll, 1980; Lancaster and Nicoll, 1987; Madison and Nicoll, 1984; Stocker et al., 1999). SK channels are also important in peripheral tissues, regulating hormone release from gland cells (Tse and Hille, 1992; Tse et al., 1995) and smooth muscle tone (Doughty et al., 1999; Herrera et al., 2000; Murphy and Brayden, 1995). Four genes comprise the SK channel gene family. SK1, 2, and 3, are expressed in the central nervous system and peripheral tissues, while expression of the structurally and functionally similar intermediate conductance channel, IK1, is limited to peripheral tissues (Ishii et al., 1997b; Joiner et al., 1997; Kohler et al., 1996). SK and IK channel α subunits share the serpentine architecture of voltage-gated K^+ channels, each bearing six transmembrane domains, with the N- and C-termini residing within the cell. The SK subunits are highly homologous, but vary in their extreme N- and C-terminal domains. The only striking primary sequence homology between SK channel subunits and other K^+ channels is in the pore region located between the fifth and sixth transmembrane domains. Functional SK channels are heteromeric complexes of four pore-forming α subunits and calmodulin (CaM) that mediates Ca^{2+} -gating. In inside-out patches containing cloned SK channels, Ca^{2+} -dependent gating persists in the absence of applied CaM suggesting that CaM is constitutively bound to the native complex (Xia et al., 1998). Structure-function studies

are consistent with this model and have shown that the interaction occurs at the CaM binding domain (CaMBD), a highly conserved stretch of 92 amino acids residing in the proximal region of the intracellular C-terminus of the α subunits (Keen et al., 1999; Wissmann et al., 2002). The structure of the complex between the CaMBD and Ca^{2+} -CaM partitions CaM into distinct functional domains. Through interactions with the CaMBD, CaM adopts an extended conformation with the globular N- and C-lobes that harbor the E-F hand motifs separated by an elongated linker region. Ca^{2+} binding to the N-lobe E-F hands 1 and 2 of CaM is necessary and sufficient for Ca^{2+} -gating (Keen et al., 1999; Schumacher et al., 2001). Residues in the linker domain and the C-lobe maintain Ca^{2+} -independent interactions, including salt bridges between R464 and K467 on the CaMBD and E84 and E87 on CaM. Indeed, the spatial orientation of the residues in E-F hands 3 and 4, usually the higher affinity Ca^{2+} binding sites, is disrupted by extensive interactions with CaMBD residues and cannot adopt a chelating configuration. Therefore, it is likely that these interactions account for the constitutive association between the proteins (Schumacher et al., 2001). The constitutive association between the channel subunits and CaM permits rapid gating in response to Ca^{2+} (Hirschberg et al., 1998; Xia et al., 1998). To determine whether the constitutive association between the CaMBD and CaM is required for SK channel gating, mutations that disrupt the constitutive interaction were introduced into SK2. Expression studies show that SK channels can undergo Ca^{2+} -CaM dependent gating in the absence of a constitutive association with CaM. Surprisingly, Ca^{2+} -independent interactions with CaM are required for cell surface expression of SK channels.

Material and Methods

Molecular Biology

Proteins expressed in transfected cells were cloned in the CMV-based vector, pJPA. Site-directed mutagenesis was performed using Pfu DNA polymerase (Stratagene, La Jolla, CA). The tandem triple myc epitope (EQKLISEEDL) was inserted at the S3-S4 loop of rSK2 using complementary oligonucleotides cloned into a BamHI site that had been introduced by site-directed mutagenesis at position 246 of rSK2. All sequences were verified by DNA sequence analysis.

Electrophysiology

COSm6 or HEK293 cells were grown in Dulbecco's Modified Eagle Medium (DMEM) supplemented with penicillin-streptomycin and 10% heat-inactivated fetal bovine serum (all from Invitrogen, Carlsbad, CA). Cells were transfected SK channels and calmodulin with pJPA expression plasmids encoding CD4, the indicated SK2 channel, and CaM (ratios of DNAs were 1: 8: 8, respectively) using calcium phosphate for HEK293 cells, or lipofection (Qiagen, Valencia, CA) for COSm6 cells. Recordings were performed at room temperature 1-3 days after transfection. Transfected cells were identified by CD4 antibody-coated microspheres (Dynabeads, M-450 CD4, Dynal, Oslo, Norway). When filled, pipettes prepared from thin-walled borosilicate glass (World Precision Instruments, Sarasota, FL) had resistances of 1.8-3 M Ω . Voltage-clamp recordings were performed with an Axopatch-1B patch clamp amplifier (Axon Instruments, Foster City, CA). Currents were filtered at 5 kHz (-3 dB). For whole-cell recordings pipettes were filled with (in mM) 140 KCl, 10 HEPES, 1 MgCl₂, 10 EGTA, pH-adjusted to 7.2 with KOH, after adding CaCl₂ to 100 μ M. The bath solution was 30 KCl, 110 NaCl, 10 HEPES, 1

MgCl₂, 1 CaCl₂ (pH-adjusted to 7.2 with NaOH). For excised patch recordings, the pipette solution was (in mM) 30 KOH, 120 NaOH, 10 HEPES, and 1 MgCl₂, pH-adjusted to 7.2 with methanesulfonic acid. Excised patches were superfused with an intracellular solution containing (in mM): 150 KOH, 10 HEPES, and 1 EGTA, supplemented with CaCl₂, pH-adjusted to 7.2 with methanesulfonic acid; the amount of CaCl₂ required to yield the indicated concentrations was calculated according to Fabiato and Fabiato (1979). Current amplitudes were measured at -80 mV unless otherwise indicated.

Rat CaM, and the indicated mutants were cloned into pET23b, expressed in BL21 (DE3), and purified on a low-substitution phenyl sepharose column (Amersham, Piscataway, NJ). CaMs were added to the bath solution at 10 μM SK channels and calmodulin immediately prior to use. The SK-MLCK M13 peptide (KRRWKKNFIAVSAANRFKKISSSGAL) was synthesized by Genemed Synthesis (South San Francisco, CA).

Immunocytochemistry

COSm6 cells were grown to ~15% confluency in a 60-mm dish on microscope cover glasses and incubated for 5 hours with the transfection mixture of 2.75 μg of DNA (a ratio of GFP:SK2:CaM=1:5:5) in 1 ml of DMEM and 8 μl of DMRIE-C reagent (Invitrogen) in another 1 ml of DMEM. The mixture was incubated at room temperature for 20 minutes prior to cell treatment. After transfection, cells were washed and fed with complete medium and incubated at 37°C in a 5% CO₂. Immunocytochemistry was performed 1-2 days post-transfection.

Non-permeabilized immunostaining was performed by incubating the cells at 37°C with

1:250 dilution of anti-myc monoclonal antibody (Invitrogen) in complete medium for 1 hour. After 3 washes in complete medium and 2 washes in PBS⁺ (1X phosphate-buffered saline containing 1 mM MgCl₂ and 0.1 mM CaCl₂), cells were fixed with 4% paraformaldehyde at room temperature for 15 minutes. After quenching with 2 washes with 50 mM NH₄Cl in PBS⁺, cells were washed once with PBS⁺. Nonspecific binding was then blocked by incubating the cells with 10% bovine serum albumin (BSA) in PBS⁺ at room temperature for 30 minutes. The excess BSA was removed, and the secondary antibody (1:500 dilution of Texas Red-conjugated horse anti-mouse IgG (H+L), Vector, Burlingame, CA) was applied at 4°C overnight. Cells were then washed 3 times with PBS⁺ and mounted (ProLong Antifade Kit, Molecular Probes, Eugene, OR) for imaging. For permeabilized labeling, cells were washed with PBS⁺ and fixed with 4% paraformaldehyde at 4°C for 30 minutes. After washing 3 times with ice-cold PBS⁺, cells were permeabilized with 0.2% Triton X-100 in PBS⁺ at room temperature for 15 minutes. To remove excess Triton X-100, cells were washed 5 times with PBS⁺ at room temperature. Nonspecific binding was then blocked by incubating the cells with 10% BSA in PBS⁺ at room temperature for 30 minutes and primary antibody was then added and incubated at 4°C overnight. The next day, the cells were washed and incubated with the secondary antibody at room temperature for 1 hour. Cells were washed again, and mounting was performed as described for non-permeabilized cells. Images were acquired with epifluorescence using an optical microscope Axioplan2 (Zeiss, Thornwood, NY) and OpenLab program (Improvision, Lexington, MA).

Results

SK2:64/67 channels require cotransfected CaM for function

The crystal structure of the CaMBD-Ca²⁺/CaM complex from SK2 revealed strong electrostatic contacts between the SK channel CaMBD residues R464 and K467 and CaM E84 and E87 in the CaM linker region close to the C-lobe implicated in constitutive CaM binding (Schumacher et al., 2001). Consistent with this observation, the CaMBD peptide harboring the double charge reversal R464E;K467E did not retain CaM in Ca²⁺-free pull-down assays, while the Ca²⁺-dependent interaction was still detected (Keen et al., 1999). To further investigate the role of the constitutive interaction between SK channels and CaM, whole cell recordings were performed from cells transiently transfected with SK2 wild type or SK2:64/67 mutant channels, with or without cotransfected CaM (Fig. 4). Five minutes after whole-cell patch formation with Ca²⁺ (100 μ M) in the patch pipette, cells transfected with wild type SK2 and recorded in asymmetrical K⁺ showed large currents (-4.4 ± 0.5 nA; n=5; Fig. 4A) that reversed in response to voltage ramp commands close to the predicted K⁺ reversal potential (-40 mV). Cotransfection with CaM did not obviously affect current responses (-4.4 ± 1.0 nA, n=5; Fig 4B). Point mutation charge reversals at either of R464 or K467 resulted in functional channels that were not obviously different from wild type (not shown), while only small currents that were not different from mock-transfected cells were recorded from cells transfected with SK2:64/67 (-30.0 ± 10.0 pA; n=5; Fig. 4C). However, when SK2:64/67 was cotransfected with CaM, robust currents were recorded within one minute of whole-cell patch formation, and increased to a steady state by 5 minutes (-5.3 ± 1.0 nA; n=5; Fig 4D), indicating that SK2:64/67 channels retain an ability to interact with Ca²⁺-CaM.

Exogenous CaM rescues SK2:64/67 activity in excised patches

To more closely examine the interaction between CaM and SK2:64/67, inside-out patches were excised from transiently transfected COS cells into Ca^{2+} -containing solution (10 μM ; $E_{\text{K}}=-40$ mV). In the absence of cotransfected CaM, currents measured at -80 mV (-31.3 ± 5.7 pA, $n=13$) were not different from mocktransfected cells (-23.3 ± 6.8 pA, $n=4$; $p=0.5$, unpaired t-test). In contrast, patches from cells cotransfected with SK2:64/67 and CaM yielded channel activity immediately after excision (-638.3 ± 109.3 pA; $n=19$) but channel activity diminished even while maintaining the patches in Ca^{2+} solution such that within 3 minutes the current measured at -80 mV decayed to $40.2 \pm 5.7\%$ of the initial current amplitudes (-294.9 ± 81.8 pA; $n=19$). If patches were excised into Ca^{2+} solution (-887.5 ± 214.7 pA; $n=10$) and then exposed to Ca^{2+} -free solution (0 Ca^{2+}) for 1 min, SK currents disappeared (-38.4 ± 12.3 pA; $n=10$) and, different from wild type, returning to Ca^{2+} solution did not re-evoked SK currents (-42.0 ± 9.9 pA; $n=10$).

One possible reason for the rapid decay of SK2:64/67 channel activity in patches and the inability to repeatedly activate the channels by exposure to Ca^{2+} is that the channels are weakly associated with CaM prior to and immediately after excision into Ca^{2+} solution, but channel activity is lost as CaM dissociates from the channels. To test this possibility, patches from cotransfected cells were excised into Ca^{2+} solution, and currents were evoked as described above. Ca^{2+} -dependent channel activity was abolished by exposure to Ca^{2+} -free solution. However, when exposed to Ca^{2+} solution additionally containing 10 μM CaM (Ca^{2+} -CaM solution), $56.7 \pm 12.8\%$ of the initial channel activity was reconstituted ($n=10$; Fig. 5A,B). Upon re-exposure to 0 Ca^{2+} solution and return to Ca^{2+}

solution, currents could not be evoked, nor were currents evoked by exposure to CaM solution in the absence of Ca^{2+} . The time course of Ca^{2+} -CaM binding and unbinding was examined by three sequential applications of Ca^{2+} -CaM solution separated by exposure to Ca^{2+} solution lacking CaM (Fig. 5C). The amplitude of the currents sampled at -80 mV increased on addition of Ca^{2+} -CaM and decreased upon switching to Ca^{2+} solution without CaM. Fitting the data with single exponentials yielded time constants of 1.2 ± 0.2 , 1.7 ± 0.3 , and 1.8 ± 0.4 min for Ca^{2+} -CaM association and 0.7 ± 0.1 , 1.4 ± 0.4 , and 2.1 ± 0.8 min. for Ca^{2+} -CaM dissociation ($n=7$). The maximum current amplitudes decreased over the course of the experiment, consistent with channel rundown (Khawaled et al., 1999).

To determine whether CaM could associate with SK2:64/67 channels in the absence of Ca^{2+} , patches were excised into Ca^{2+} solution, verifying functional channels, and then exposed to 0 Ca^{2+} solution during which time CaM dissociated as confirmed by subsequent exposure to Ca^{2+} solution. Patches were then exposed to Ca^{2+} -free CaM (10 μM) for five minutes. Upon switching to Ca^{2+} solution lacking CaM, currents were rapidly evoked indicating that CaM had assembled with the channels during the Ca^{2+} -free incubation (Fig 6A). After CaM dissociation and decay of the currents, reapplication of Ca^{2+} -CaM for 5 min again rescued the currents (Fig 6B). The percentage of the current evoked upon exposure to Ca^{2+} following Ca^{2+} -free CaM compared to the current subsequently evoked by Ca^{2+} -CaM was $29.7 \pm 3.8\%$ ($n=4$). This result shows that Ca^{2+} -free CaM can associate with SK2:64/67 channels, and suggests that the CaM affinity is increased by the presence of Ca^{2+} . CaM antagonists such as the M13 peptide (Klevit et al., 1985) or calmidazolium (Lamers and Stinis, 1983) do not interfere with the Ca^{2+} -dependent gating process of wild type SK2 (Xia et al., 1998). It is likely that the

constitutive interaction of CaM with SK2 does not present an exposed hydrophobic domain on CaM for antagonist binding (Schumacher et al., 2001). However, the interaction between SK2:64/67 and CaM is less stable in the absence of Ca^{2+} . Therefore, patches containing wild type SK2 or SK2:64/67 channels were exposed to Ca^{2+} -CaM solution (1.2 ± 0.3 nA, for wild type, n=9; -486.0 ± 187.2 pA for SK2:64/67, n=10), and then exposed to the same solution additionally containing the M13 peptide (100 μM). In contrast to wild type SK2 channels, the M13 peptide blocked the ability of Ca^{2+} -CaM to activate SK2:64/67 channels (-1.1 ± 0.3 nA for wild type, n=9; -32.4 ± 7.9 pA for SK2:64/67; n=10). Interestingly, the rate of current inhibition (0.28 ± 0.04 min, n=8) was greater than removal of CaM from the bath solution (see figure 5C) suggesting that the excess M13 peptide enhanced the dissociation of SK2:64/67-bound CaM.

Compensatory mutations in CaM restore association with SK2:64/67 channels

To test whether the double charge reversal E84R;E87K in CaM (CaM:84/87) might compensate for the R464E;K467E double charge reversal in SK2, cells were cotransfected with SK2:64/67 and CaM:84/87. Inside-out patches exposed to Ca^{2+} , displayed SK currents (-1.7 ± 0.6 nA; n=8) that disappeared upon subsequent exposure to 0 Ca^{2+} solution (-43.3 ± 12.2 pA; n=8). Distinctly different from cotransfection of SK2:64/67 with wild type CaM, returning the patch to Ca^{2+} solution reactivated the channels, rescuing $62.2 \pm 12.0\%$ of the initial current (Fig. 7).

Cotransfection of wild type SK2 with CaM:84/87 resulted in channels that activated upon patch excision into Ca^{2+} solution (-594.2 ± 225.4 pA, n=8) and rapidly decreased without CaM in the bath solution. Unlike coexpression of SK2:64/67 with wild type CaM, currents did not completely disappear, plateauing at $53.2 \pm 6.4\%$ of the initial current. This

current may reflect channels that have assembled with wild type CaM. Following exposure to 0 Ca^{2+} solution, reexposure to Ca^{2+} solution evoked $62.2 \pm 5.3\%$ of the initial current. Subsequent exposure to Ca^{2+} -CaM solution rescued the currents (-740.7 ± 317.6 , $n=8$; Fig. 7B). These results suggest that the E84R;E87K charge reversals in CaM act destabilize the interaction between SK2 and CaM, and that in patches, CaM:84/87 is lost and may be replaced by wild type CaM.

Ca^{2+} -dependence

Coexpression studies with wild type SK2 and CaMs harboring point mutations in the E-F hand domains showed that E-F hands 1 and 2 are necessary and sufficient for Ca^{2+} -gating. Mutations in E-F hands 3 and 4 (CaM3,4) that abolish Ca^{2+} binding do not alter Ca^{2+} sensitivity while mutations in either E-F hands 1 or 2 (CaM1 or CaM2) shift the sensitivity from ~ 0.5 to $\sim 1 \mu\text{M}$, and the double mutant, CaM1,2, eliminated Ca^{2+} gating. Functional studies were confirmed by the crystal structure of the CaMBD- Ca^{2+} /CaM complex that showed E-F hands 1 and 2 occupied by Ca^{2+} ions while E-F hands 3 and 4 were uncalcified (Keen et al., 1999; Schumacher et al., 2001). To examine the Ca^{2+} dependence of SK2:64/67 channels, and whether exogenous application of Ca^{2+} -CaM reconstituted SK channel gating similar to wild type, cells were cotransfected with either WT CaM, CaM1,2, CaM3,4, CaM1,2,3,4, or CaM:84/87. One to three days later, patches were excised into an internal solution containing the same purified recombinant CaM ($10 \mu\text{M}$) and Ca^{2+} dose-responses were performed by changing between internal solutions containing CaM with varying concentrations of Ca^{2+} (Fig. 8). For either wild type or SK2:64/67, neither CaM 1,2 nor CaM1,2,3,4 supported Ca^{2+} gating (not shown). The Ca^{2+} -sensitivity of SK2:64/67 with wild type CaM was right-shifted ($K_d=0.82 \pm 0.07 \mu\text{M}$,

n=5) compared to wild type channels ($K_d=0.51\pm 0.02 \mu\text{M}$, n=7; $p=0.001$, unpaired t-test). Application of CaM:84/87 to wild type SK2 channels right-shifted the Ca^{2+} dose response ($K_d=0.82\pm 0.06 \mu\text{M}$, n=9) to the same extent as SK2:64/67 were right-shifted in the presence of wild type CaM ($p=0.97$, unpaired t-test). Coexpression of SK2:64/67 with CaM:84:87 rescued stable currents patches (see above) but with reduced Ca^{2+} affinity ($K_d = 1.38\pm 0.06 \mu\text{M}$, n=8). Application of CaM3,4 to either wild type or SK2:64/67 slightly leftshifted the apparent affinity compared to wild type CaM (not shown).

CaM is required for SK channel cell surface localization

Application of Ca^{2+} or Ca^{2+} -CaM to patches from cells transfected with SK2:64/67 alone did not yield currents, while patches from cells cotransfected with CaM yielded robust channel activity. These results suggest that in the absence of cotransfected CaM, SK2:64/67 channels may not be present on the cell surface. To test this possibility, three tandem copies of the myc epitope were inserted into the extracellular loop between transmembrane domains 3 and 4 in SK2 and SK2:64/67. Cells were transfected with the channel alone or in combination with CaM and then examined by immunocytochemistry with a monoclonal anti-myc antibody, either with or without permeablizing the cells; cotransfected GFP was used to identify transfected cells. For SK2 with or without cotransfected CaM, channel protein was detected on the cell surface when cells were not permeablized as well as in intracellular organelles after permeabilization (not shown). In contrast, SK2:64/67 protein was detected on the cell surface only when cotransfected with CaM, even though the protein was highly expressed as evidenced by the strong intracellular organelle staining in permeablized cells (Fig. 9, Top, middle panels).

To determine whether requires Ca^{2+} -CaM, cells were cotransfected with wild type SK2 or

SK2:64/67 and CaM1,2,3,4, a Ca^{2+} -independent form of CaM (Geiser et al., 1991; Xia et al., 1998). When cotransfected with CaM1,2,3,4, SK2:64/67 subunits were detected in the plasma membrane, demonstrating that Ca^{2+} binding to CaM is not essential for cell surface expression (Fig. 9 Lower panels). Patches from these cells were excised into Ca^{2+} solution but did not yield SK currents (-31.4 ± 4.5 pA; $n=9$). However application of exogenous wild type Ca^{2+} -CaM resulted in channel activation (-488.8 ± 85.1 pA; $n=9$) suggesting that the channels were in the plasma membrane and initially associated with nonfunctional CaM1,2,3,4 that was replaced by the exogenous functional Ca^{2+} -CaM. Consistent with this idea, patches from cells cotransfected with wild type SK2 and CaM1,2,3,4 were detected in the plasma membrane, and excision into Ca^{2+} solution did not result in channel activation (-13.3 ± 4.4 pA; $n=4$), nor could channel activity be restored by exogenous Ca^{2+} -CaM (-11.1 ± 3.0 pA; $n=4$). Therefore, wild type SK2 channels retain constitutively bound CaM1,2,3,4 that cannot bind Ca^{2+} and cannot be replaced by wild type CaM, but are properly trafficked to the cell surface.

Discussion

The results presented here show that Ca^{2+} -independent interactions between the CaMBD and CaM are essential for cell surface expression, and that the constitutive binding between the pore-forming α subunits of SK channels and CaM is not required for channel gating. The crystal structure of the complex between the CaMBD and Ca^{2+} -CaM showed strong interactions between R464 and K467 on the channel and E84 and E87 on CaM, in the region implicated in constitutive association (Schumacher et al., 2001). This was supported by the lack of channel function when the double mutant was expressed. In addition, the purified CaMBD R464E;K467E peptide failed to retain purified CaM in pull-down assays in the absence of Ca^{2+} (Keen et al., 1999). These results show that the CaMBD R464E;K467E is different from wild type in its ability to retain CaM but they do not distinguish between a complete lack of binding or a weakened affinity.

The crystal structure of the CaMBD- Ca^{2+} -CaM and functional studies with mutant CaMs (Keen et al., 1999; Schumacher et al., 2001) suggested a separation of function between the two lobes of CaM with the C-lobe mediating many of the Ca^{2+} -independent interactions with the CaMBD. Indeed, the shape of E-F hands 3 and 4 are altered through the multiple interactions with CaMBD residues and no longer coordinate Ca^{2+} ions. The N lobe E-F hands 1 and 2 bound Ca^{2+} and were comparable to other Ca^{2+} -CaM substrate structures (Babu et al., 1985; Ikura et al., 1992; Meador et al., 1992). Therefore, if the double mutation R464E;K467E eliminated all Ca^{2+} -independent interactions, Ca^{2+} gating in this channel might be mediated solely by interactions with either Ca^{2+} -loaded N- or C-lobes. However, application of mutant CaMs with different combinations of intact E-F hands to SK2:64/67 channels showed that, just as for wild type channels, E-F hands 1 and

2 are required while E-F hands 3 and 4 are dispensable. This implies that the double mutation, R464E;K467E, weakens the Ca^{2+} -independent interactions between the channel subunit and CaM, and that the reconstituted channels interact with exogenously applied CaM similar to that of wild type, but with a reduced Ca^{2+} -sensitivity. Therefore it is likely that overexpressed CaM rescues whole cell SK2:64/67 channels and surface expression by overcoming the weakened affinity.

The compensatory mutations in CaM reconstituted tighter binding between the two double mutants, SK2:64/67 and CaM:84/87, presumably by reinstating salt bridges between these positions. However, the reconstituted channels have reduced Ca^{2+} -sensitivity, with apparent K_d values even more right-shifted than SK2:64/67 with WT CaM suggesting that while the complex is stabilized, the conformational changes that open the channel gate subsequent to Ca^{2+} -binding are compromised.

A role for CaM in SK channel trafficking was also found. Immunocytochemistry clearly demonstrated surface expression of SK2:64/67 only with cotransfected CaM, and functional studies showed that the channels carried associated CaM. Joiner et al (Joiner et al., 2001) had observed that overexpressing a part of the C-terminal domain of IK1 that included the CaMBD redistributed the channels to the intracellular compartments and overexpressing CaM redeposited them in the plasma membrane. The present results extend the implications for trafficking by showing that the Ca^{2+} -independent interactions between the channel subunits and CaM are sufficient for cell surface expression. Patches from cells cotransfected with SK2:64/67 channels and CaM1,2,3,4 did not show channel activity when excised into Ca^{2+} solution, but channel activity was reconstituted upon subsequent application of Ca^{2+} -CaM. Immunocytochemistry verified surface expression

of SK2:64/67 channels when cotransfected with CaM1,2,3,4. This result is consistent with the ability of Ca²⁺-free CaM to associate with the channels in excised patches.

Since the CaM-dependent gating mechanism was described for SK channels, a variety of other channels have been shown to undergo Ca²⁺-free and Ca²⁺-dependent CaM interactions that alter their functions. For example, Ca²⁺-free CaM binds to an I-Q motif in the intracellular C-terminal domains of L-, N- and P/Q-type voltage-gated Ca²⁺ channels (Erickson et al., 2001; Peterson et al., 1999; Pitt et al., 2001; Zuhlke et al., 1999) and similar to SK channels the different lobes of CaM mediate different functions (DeMaria et al., 2001). CaM binds to and modulates specific isoforms of voltage-gated Na⁺ channels (Deschenes et al., 2002; Mori et al., 2000), CNG channels (Molday, 1996; Varnum and Zagotta, 1997), and CaM is an auxiliary subunit of KCNQ channels (Wen and Levitan, 2002; Yus-Najera et al., 2002). CaM also binds to and regulates the function of several ionotropic receptors, Ca²⁺-release channels, and TRP channels (Hamilton and Reid, 2000; Nadif Kasri et al., 2002; Saimi and Kung, 2002). CaM is not the only E-F hand Ca²⁺ binding protein that directly regulates ion channel function. Members of the Kv4 family of voltage-gated K⁺ channels interact with KChIPS that endow important biophysical properties as well as regulating trafficking to the plasma membrane (An et al., 2000). For SK channels, it remains to be determined just how the binding of CaM influences trafficking. However, the SK channels contain a conserved RKR motif in the intracellular N-terminus, immediately preceding the first transmembrane domain. An analogous situation exists for functional K_{ATP} channels in which the channel forming Kir 6.2 subunits require association with SUR1 for surface expression. In this case, trafficking is regulated by the RKR ER-retention signals present in each of the partner

subunits that is exposed prior to co-assembly and buried once the two subunits form the macromolecular complex (Zerangue et al., 1999). However, mutagenesis of the RKR motif to AAR in SK2:64/67 did not result in surface expression in the absence of cotransfected CaM, although channel subunits were detected inside the cell (not shown).

CaM is highly expressed in almost all cell types, yet the concentrations and subcellular localization of free CaM may vary dramatically depending upon the state of phosphorylation, anchoring to the plasma membrane, or association with CaM storage proteins such as GAP-43 (Persechini and Stemmer, 2002; Skene, 1990; Verkade et al., 1997). Moreover distinct CaM pools may be differentially mobilized, transiting long cellular distances, from dendrites to the nucleus (Deisseroth et al., 1998). In addition, local CaM concentrations may also be translationally regulated as CaM mRNA is differentially distributed, a process that likely reflects the conservation of three nonallelic mammalian CaM genes encoding identical proteins but distinct 5' and 3' noncoding sequences. For example, one pool of CaM mRNA, derived from a specific CaM gene (CALM1) is abundant in the apical dendrites of cerebellar pyramidal cells and may give rise to local reservoirs of CaM, while in NGF-stimulated PC12 cells, mRNAs derived from CALM1 and CALM2 genes are found in neurite outgrowths while CALM3-derived transcripts reside within the cell body (Palfi et al., 2002; Palfi et al., 1999; Toutenhoofd and Strehler, 2000). Based upon these factors, and the number and concentrations of CaM binding proteins, it is possible that CaM availability is rate limiting for SK channel surface expression (Persechini and Stemmer, 2002). In this case, metabolic processes that alter the concentrations of free CaM may dynamically regulate SK current density and cell excitability.

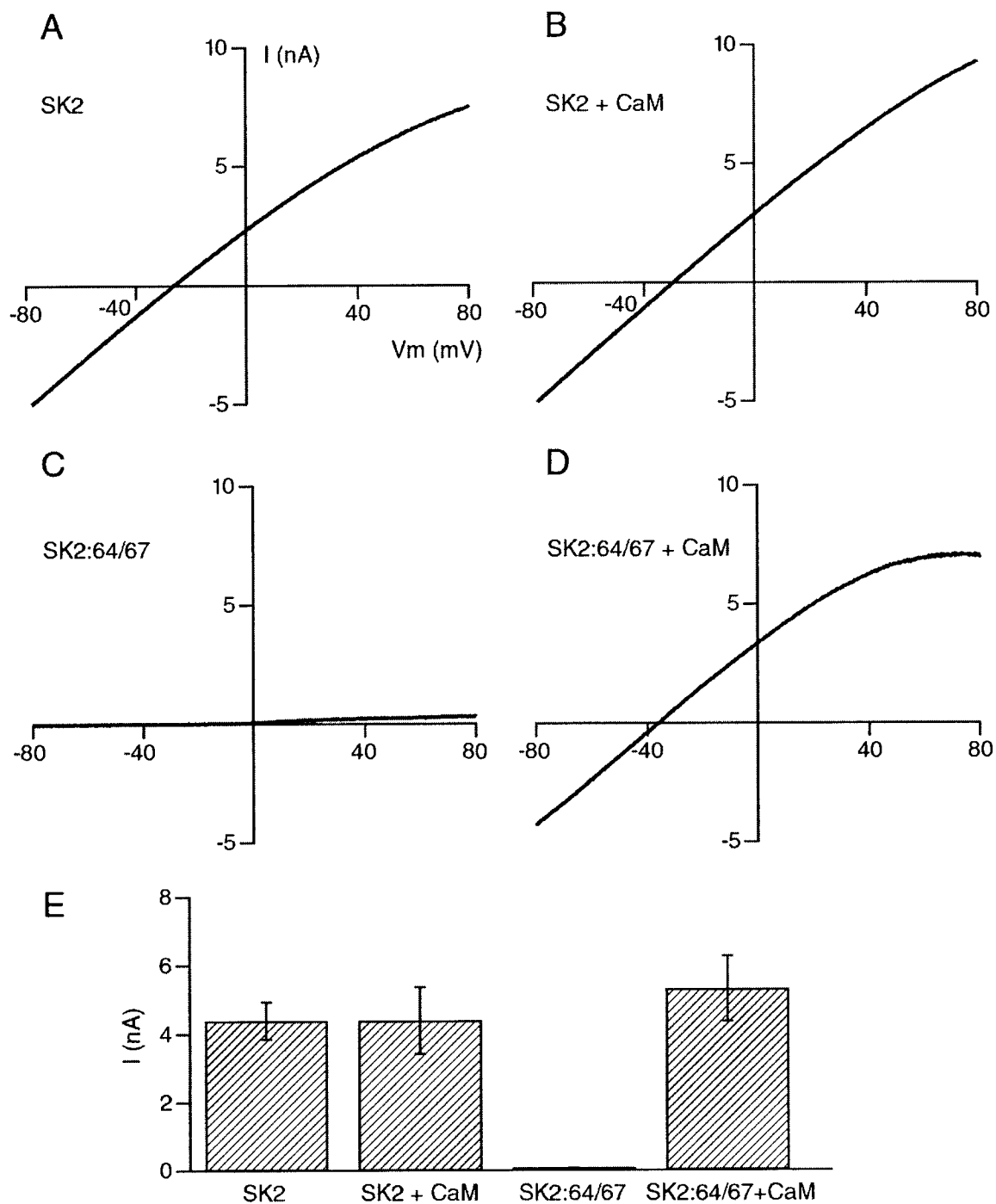


Figure 4. SK2:64/67 requires co-expressed CaM for function.

(A-D) Representative whole cell voltage clamp recordings from HEK293 cells transfected with the indicated expression plasmids, five minutes after whole-cell patch formation. To activate SK channels, Ca^{2+} (100 μM) was dialyzed into the cell through the patch pipette. The traces show responses to 2-second voltage ramp commands from -80 to 80 mV. (E) Whole cell current amplitudes \pm S.E.M measured at -80 mV ($n=5$).

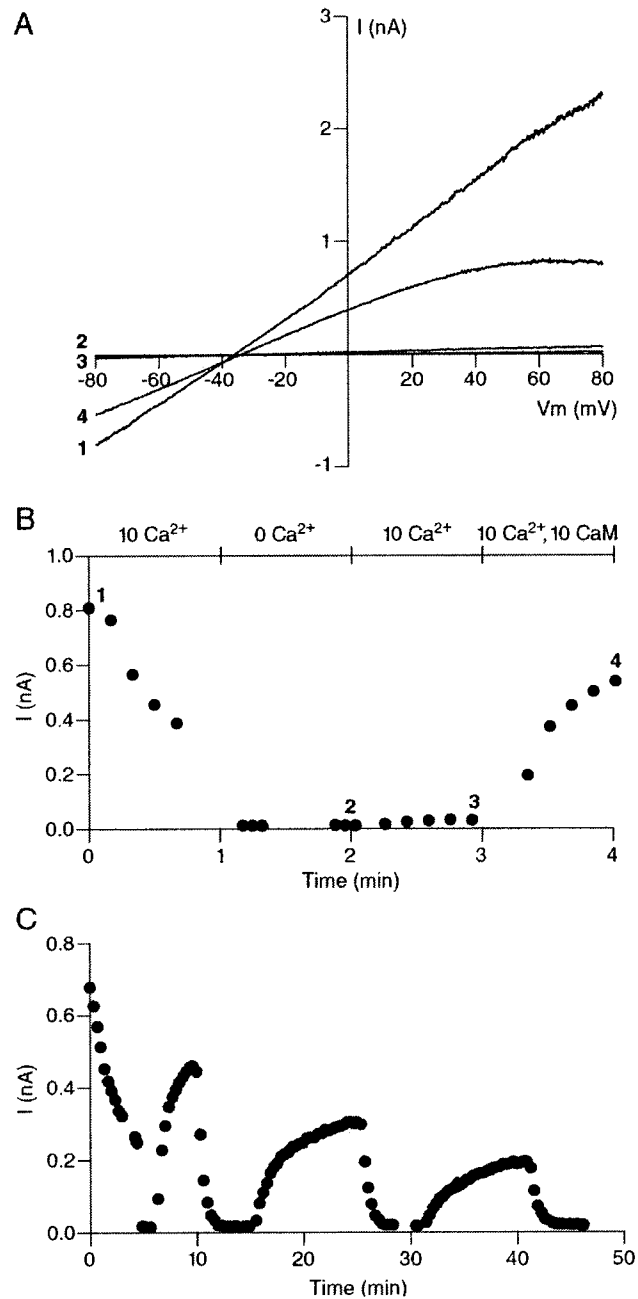


Figure 5. Ca^{2+} -CaM rescues SK2:64/67 in excised patches.

(A) Currents recorded from a representative inside-out patch excised from a COS cell cotransfected with SK2:64/67 and CaM. The patch was excised into (1) Ca^{2+} solution (10 μM), then exposed to (2) 0 Ca^{2+} solution, and returned to (3) Ca^{2+} solution, before (4) Ca^{2+} -CaM (10 μM) was applied, rescuing channel activity. (B) Diary plot of the current measured at -80 mV from the patch shown in (A). The numbers correspond to the current responses shown on the left. (C) Diary plot of the currents measured at -80 mV from a separate patch exposed to three sequential applications of Ca^{2+} -CaM (10 μM) separated by exposure to Ca^{2+} solution (10 μM) lacking CaM.

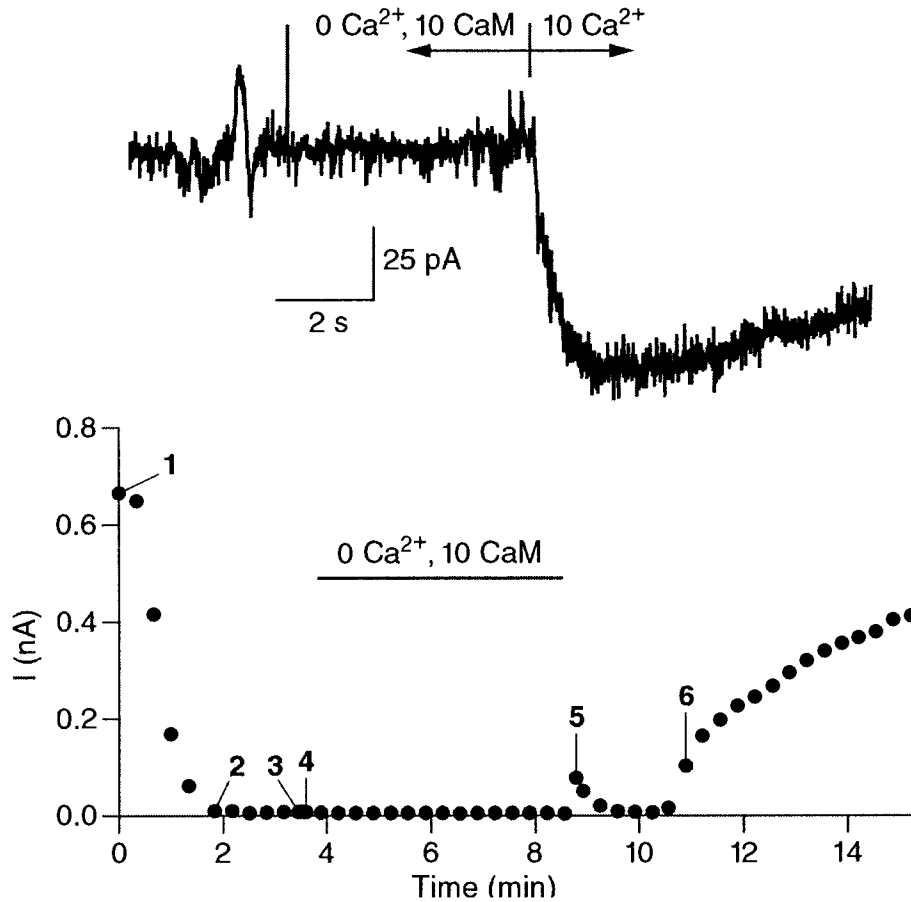


Figure 6. Ca^{2+} -free CaM associates with SK2:64/67 SK channels and calmodulin

Top: Continuous recording at -80 mV from an inside-out patch containing SK2:64/67 channels. After a 5 min application of CaM in the absence of Ca^{2+} , currents were evoked upon exposure to a solution lacking CaM but containing $10 \mu\text{M}$ Ca^{2+} (corresponds to point 5, below). Bottom: Diary plot of the patch shown above. The patch was excised into (1) Ca^{2+} solution ($10 \mu\text{M}$), then exposed to (2) 0Ca^{2+} solution, and returned to (3) Ca^{2+} solution, before (4) Ca^{2+} -free CaM ($10 \mu\text{M}$) was applied. Exposure to Ca^{2+} without CaM (5) evoked a current that decayed within 1.5 min. Channel activity was rescued (6) by a second application of Ca^{2+} -CaM.

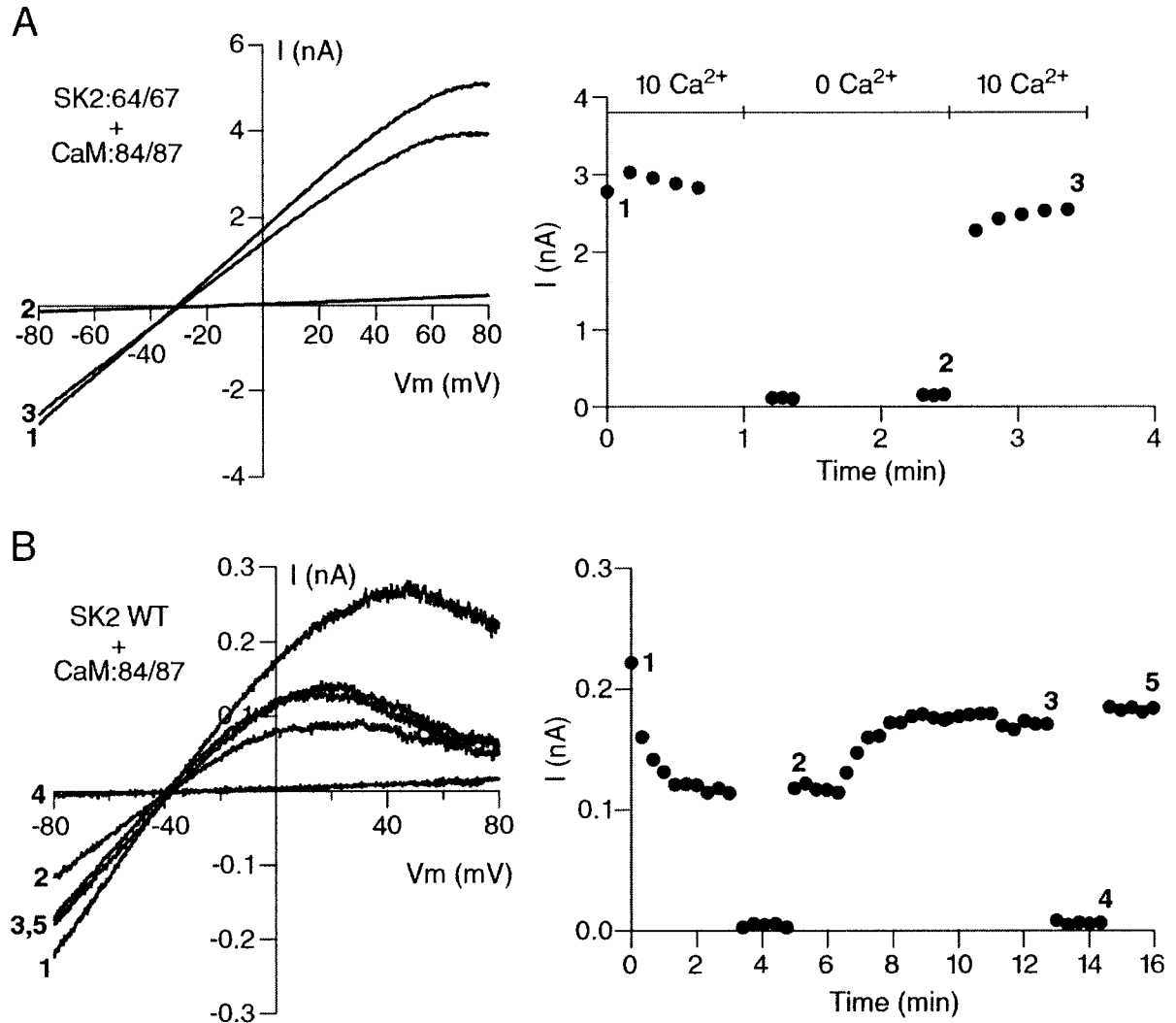


Figure 7. CaM:84/87 compensates for SK2:64/67.

(A) Left: Currents recorded from a representative inside out patch excised from a COS cell cotransfected with SK2:64/67 and CaM:84/87. The patch was excised into (1) Ca²⁺ solution (10 μM), then exposed to (2) 0 Ca²⁺ solution, and returned to (3) Ca²⁺ solution. Ca²⁺ alone is sufficient to reactivate the channels; application of Ca²⁺-CaM is not required. Right: Diary plot of the current measured at -80 mV from the patch shown on the left. The numbers correspond to the current responses shown on the left. (B) Left: Currents recorded from a representative inside out patch excised from a COS cell cotransfected with wild type SK2 and CaM:84/87. The patch was excised into (1) Ca²⁺ solution (10 μM), then exposed to 0 Ca²⁺ solution, returned to (2) Ca²⁺ solution, and (3) exposed to Ca²⁺-CaM before returning to 0 Ca²⁺ solution and (5) exposure to Ca²⁺. Right: Diary plot of the current measured at -80 mV from the patch shown on the left. The numbers correspond to the current responses shown on the left.

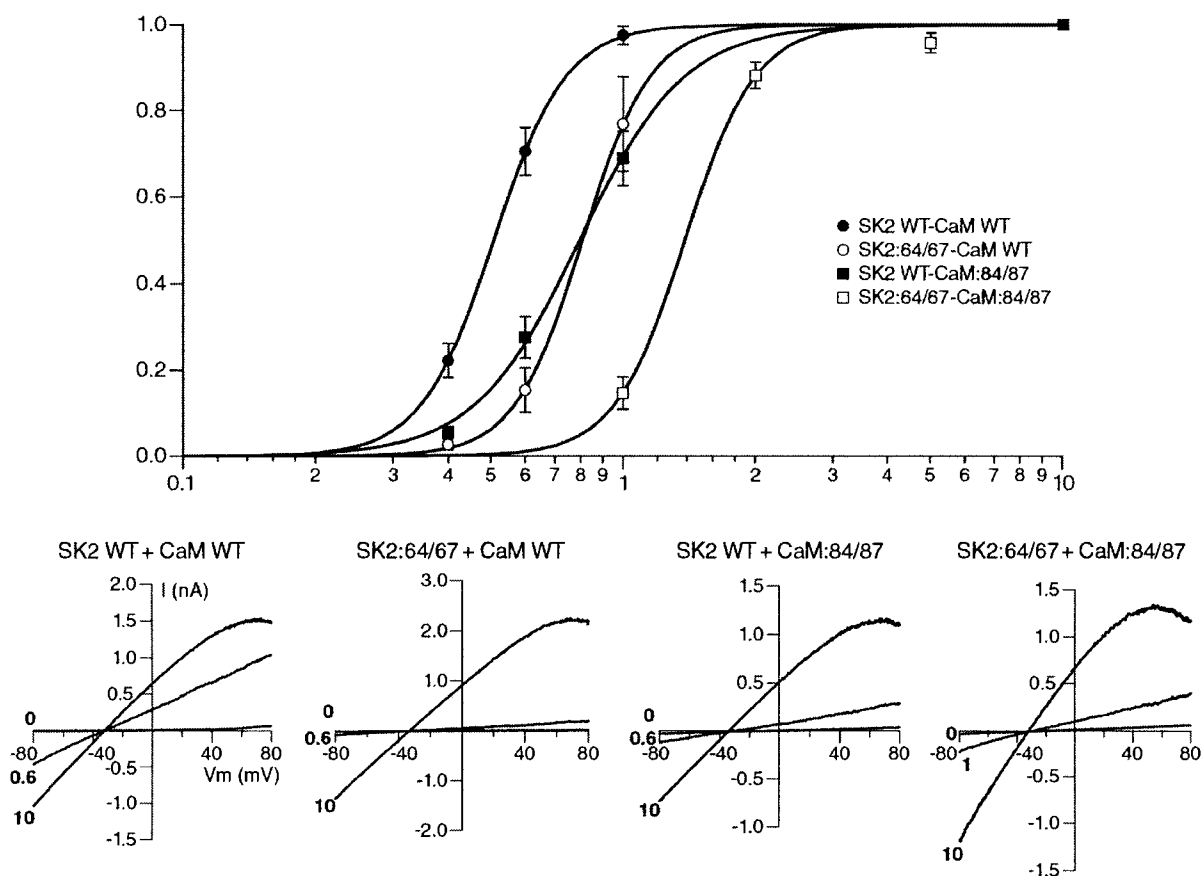


Figure 8. Ca^{2+} dose-responses.

Top: Normalized Ca^{2+} dose-response relationships. The indicated SK2 channel and CaM were coexpressed, and the same purified recombinant CaM was applied with different Ca^{2+} solutions to the inside face of patches. Relative current amplitudes measured at -80 mV from $n \geq 5$ patches for each combination of channel and CaM were averaged and plotted versus the intracellular Ca^{2+} concentration. The averaged data were fitted with a Hill equation (continuous lines) yielding an EC_{50} (μM) and (Hill coefficient) of 0.51 ± 0.02 (5.6) for wild type SK2 with wild type CaM, 0.82 ± 0.07 (7.1) for SK2:64/67 with wild type CaM, 0.82 ± 0.06 (4.2) for wild type SK2 with CaM:84/87, and 1.38 ± 0.07 (6.4) for SK2:64/67 with CaM:84/87. Bottom: Currents measured in response to voltage ramps in representative patches from cells coexpressing the indicated SK2 channel and CaM for 0, 0.6 or 1, and 10 μM Ca^{2+} .

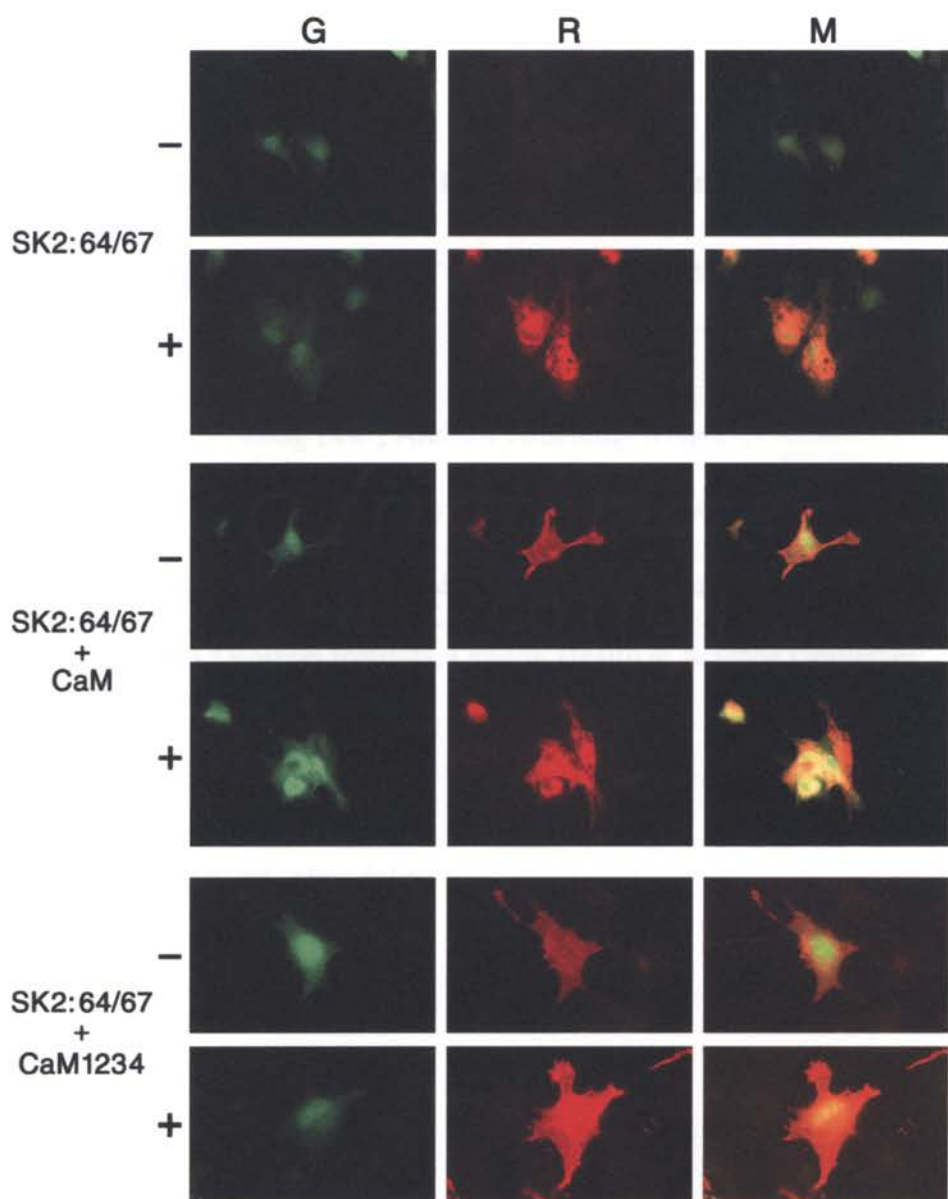


Figure 9. CaM is required for surface expression.

Immunocytochemistry of COS cells transfected with the indicated combinations of SK2:64/67, CaM, and a GFP expression plasmid. SK2:64/67 harbors three tandem copies of the myc epitope in the external loop between transmembrane domains 3 and 4. For each panel, transfected cells were visualized by expression of GFP (G; left), channel protein was detected with an anti-myc mouse monoclonal antibody and visualized by Texas Red-conjugated horse anti-mouse secondary antibody (R; middle) and the signals were merged (M; right). In each case, cells were examined either without (-) or with (+) the membrane permeabilization. (Top) SK2:64/67 was not detected on the cell surface (-) but channel protein was detected inside permeabilized cells (+). (Middle) SK2:64/67 was detected on the cell surface (-) as well as inside the cell (+) when transfected with wild type CaM or (Bottom) the Ca^{2+} -independent CaM mutant, CaM1,2,3,4.

III. CHAPTER 3

Small conductance Ca²⁺-activated K⁺ channels and calmodulin:

Challenging the ‘dimer-of-dimers’ gating model

Wei-Sheng Lee*, Andrew Bruening-Wright*,

David L. Farrens&, James Maylie\$, John P. Adelman*

&Department of Biochemistry and Molecular Biology, \$Department of Obstetrics and

Gynecology, and *Vollum Institute, Oregon Health & Science University,

Portland, Oregon, USA

running title: SK channels and calmodulin

Corresponding author:

Dr. John P. Adelman

Vollum Institute, Oregon Health & Science University

3181 SW Sam Jackson Park Road

Portland, Oregon, 97239

(503)-494-5450

(503)-494-4353 (fax)

adelman@ohsu.edu

Summary

Small conductance Ca^{2+} -activated K^{+} channels (SK channels) are heteromeric complexes of pore-forming α subunits and constitutively bound calmodulin (CaM). CaM is constitutively bound to a succinct domain of ~100 residues, the CaM binding domain (CaMBD) that resides C-terminal to the sixth transmembrane domain just inside the cell. We used cysteine substitutions in the isolated CaMBD as well as in functional channels to test structural predictions of solvent accessibility and proximity between specific residues. Residues on the first helix of the helix-turn-helix CaMBD peptide, containing the tryptophan residue in its central region and hydrophobically contacting the C-lobe of CaM, were cysteine-substituted in the attempts to define the interaction sites between the CaMBD and CaM with site-directed fluorescence labeling (SDFL) on isolated peptides. The proximity between residue pairs in the double cysteine mutants was assessed by evaluating their ability to form disulfide bonds. Neither the solvent accessibility nor proximity of substituted cysteines reflected the predictions based upon the structural data. Furthermore, a C-terminal truncation predicted to abolish Ca^{2+} gating resulted in fully functional Ca^{2+} -gated channels. Application of methanethiosulfonate (MTS) reagents onto SK2 L457C revealed the charge-dependent modulation of Ca^{2+} -sensitivity, and MTS crosslinkers rescued the decreased Ca^{2+} -sensitivity of SK2 L457C. Therefore, this hydrophobic residue also contributes to the close association between the SK channel CaMBD and CaM.

Introduction

Small conductance Ca^{2+} -activated K^+ channels (SK channels) are important regulators of numerous physiological processes such as neuronal excitability, synaptic plasticity, smooth muscle tone, and hormone secretion (Bond et al., 2004; Bond et al., 2005; Marrion and Tavalin, 1998; Stackman et al., 2002; Stocker, 2004; Taylor et al., 2003; Zhang et al., 2005). SK channels are gated solely by intracellular Ca^{2+} ions. The cloned SK channels revealed a family with four highly homologous members that have a six-transmembrane serpentine architecture, reminiscent of the voltage-gated K^+ channels despite their clear lack of voltage-dependence upon heterologous expression (Hirschberg et al., 1998; Ishii et al., 1997b; Joiner et al., 1997; Kohler et al., 1996). Functional studies showed that SK channel gating is due to a constitutive association between the alpha, pore-forming subunits and the ubiquitous Ca^{2+} sensor, calmodulin (CaM) (Xia et al., 1998). Ca^{2+} ions bind to the N-lobe E-F hands of CaM and initiate conformational changes in the channel protein that open the gate (Keen et al., 1999). Further structure-function experiments showed that CaM is constitutively bound to a succinct domain of ~100 residues, the CaM binding domain (CaMBD) that resides C-terminal to the sixth transmembrane domain just inside the cell (Keen et al., 1999). Based upon these results, the crystal structure of the isolated complex between the CaMBD and CaM was obtained in the presence of Ca^{2+} , a condition that may represent the 'open' configuration of the channel. The structure showed a remarkable dimer structure in which two CaMBDs are complexed with two CaMs such that the CaMBDs do not contact each other. Rather they are tightly associated by interwoven CaM. In the structure, Ca^{2+} ions are clearly resident in E-F hands 1 and 2, in the CaM N-lobe, but the C-lobe E-F hands 3 and

4 are uncalcified, consistent with previous structure-function experiments that used functioning channels (Keen et al., 1999; Schumacher et al., 2001). A previous NMR structure and more recently a crystal structure of the CaMBD-CaM complex in the absence of Ca^{2+} , presumably reflecting the closed state of the channel, have been presented. These results show the complex is monomeric in the absence of Ca^{2+} (Schumacher et al., 2004; Schumacher et al., 2001; Wissmann et al., 2002). Based upon the structure solved in the presence of Ca^{2+} , we proposed a model in which the channel is a ‘tetramer of monomers’ in the closed state, with one CaM attached to each of the pore-forming subunits. Upon Ca^{2+} binding to the N-lobe E-F hands, a large-scale reorganization may occur, forming the ‘dimer-of-dimers’. In the present study we used cysteine substitutions in the isolated CaMBD as well as in functional channels to test structural predictions of solvent accessibility and proximity between specific residues. The results show that neither the solvent accessibility nor proximity of substituted cysteines reflects the predictions based upon the structural data. Further, a channel harboring a truncation of the C-terminal domain that is predicted to drastically disrupt the dimer-of-dimers is fully functional, displaying normal Ca^{2+} -gating. Therefore, despite several previously reported consistencies between structural data and functional SK channels, the ‘dimer-of-dimer’ model for SK channel gating may need revision.

Material and Methods

Molecular Biology and Biochemistry

The rSK2 CaMBD peptides that were expressed in bacteria were cloned in pET33b, expressed in BL21 (DE3), and purified on HiTrap™ chelating HP columns (Amersham Biosciences, Piscataway, NJ). Rat CaM was cloned into pET23b, expressed in BL21 (DE3), and purified on a low substitution phenyl-Sepharose column (Amersham Biosciences, Piscataway, NJ). Proteins expressed in transfected mammalian cells were cloned in the CMV-based vector, pJPA. Site-directed mutagenesis was performed using *Pfu* DNA polymerase (Stratagene, La Jolla, CA). All sequences were verified by DNA sequence analysis.

For Western blots, proteins separated by native gels or SDS-PAGE were transferred to nitrocellulose membranes, probed with 6xHis mAb/HRP Conjugate (BD Biosciences, Palo Alto, CA), anti-CaM (mouse, Upstate Biotech, Lake Placid, NY), or anti-C8 (purified from the tissue culture supernatant of Chessie 8 hybridoma (Abacioglu et al., 1994)), incubated with horseradish peroxidase-conjugated secondary antibodies whenever necessary, and then developed with SuperSignal West Pico (Pierce).

In Tricine SDS-PAGE analysis of oxidized cysteine-substituted CaMBD peptides, oxidation with Cu-phenanthroline was initiated by addition of CuSO₄ and phenanthroline (to a final concentration of 0.5 and 1.5 mM, respectively) to 30 μM rSK2 CaMBD peptides and calmodulin in 10 mM HEPES, 130 mM NaCl, and 100 μM CaCl₂ (pH 7.2). The mixture was incubated at room temperature for 5 min, and the reaction was halted by adding EDTA to a final concentration of 12.5 mM.

During MTS cross-linking analysis, membranes were prepared from transfected CHO

cells and treated with 0.2 mM MTS cross-linker (Toronto Research Chemicals, Toronto, Ontario, Canada) for 15 min on ice. The reactions were stopped by addition of non-reducing SDS sample buffer containing *N*-ethylmaleimide (NEM) or dithiothreitol (DTT). The samples were separated on 6% SDS-PAGE and subjected to immunoblotting. Densitometry analysis of the gel images was performed with NIH Image.

Reactivity Measurements of Cysteine Mutants with PyMPO

The rSK2 CaMBD V427C peptide was allowed to react (at pH 6.8 in 100 mM HEPES and 50 μ M free Ca^{2+}) with a 4-fold excess of PyMPO maleimide (Molecular Probes, Eugene, OR) for 2 h at room temperature while the mutant was bound to the HiTrap™ chelating HP column. After extensive washing to remove unreacted PyMPO label, the sample was eluted from the column, and PyMPO labeling was determined by comparing its absorption spectrum with an unlabeled rSK2 CaMBD V427C spectrum. The unlabeled rSK2 CaMBD V427C spectrum was then subtracted from that of the labeled sample, allowing the amount of attached PyMPO to be determined from the remaining absorbance at 416 nm using an extinction coefficient of 23,000 for PyMPO.

2.5 μ g (0.25 nmol) of each cysteine-substituted rSK2 CaMBD peptide in 12.5 μ l was reacted with 3-fold excess PyMPO on ice for 10 min at pH 7.2 (100 mM HEPES) either in the presence or absence of 50 μ M free Ca^{2+} and/or 0.25 nmol CaM. The reaction was then quenched by adding cysteine to a final concentration of 1 mM, and the samples were then analyzed by SDS-PAGE. Gel was visualized using UV irradiation, and the amount of label incorporation was determined using Kodak 1D 2.0.2 by comparing the signal intensity with the PyMPO-labeled rSK2 CaMBD V427C standard of known concentration. The wild-type rSK2 CaMBD peptide (containing no reactive cysteine

residues) was used to show specificity in PyMPO labeling. The gels were subsequently subjected to Coomassie staining to check for equal distribution of protein in each sample well.

Solvent accessibility of the rSK2 CaMBD crystal structure was calculated using DeepView / Swiss-PdbViewer 3.7 (SP5).

Immunocytochemistry

Non-permeabilized immunostaining was performed as described previously (Lee et al., 2003). Briefly, COSm6 cells were transfected with pJPA expression plasmids encoding EGFP, the indicated SK2 channel, and CaM using DMRIE-C reagent (Invitrogen, Carlsbad, CA). Immunocytochemistry was performed 1–2 days post-transfection using anti-myc monoclonal antibody (Invitrogen, Carlsbad, CA) and Texas Red-conjugated horse anti-mouse IgG (H+L) (Vector, Burlingame, CA). Images were acquired with epifluorescence using an optical microscope (Axioplan2, Zeiss, Thornwood, NY) and the program OpenLab (Improvision, Lexington, MA).

Electrophysiology

CHO cells were grown in F-12 medium supplemented with penicillin, streptomycin, and 10% heat-inactivated fetal bovine serum (all from Invitrogen, Carlsbad, CA). Cells were transfected with pJPA expression plasmids encoding EGFP, the indicated SK2 channel, and CaM using FuGENE 6 (Roche Applied Science, Indianapolis, IN). Recordings were performed at room temperature 1–2 days after transfection. Transfected cells were identified by the green fluorescence. When filled, pipettes prepared from thin-walled borosilicate glass (World Precision Instruments, Sarasota, FL) had resistances of 1.8–3 M Ω . Rapid solution changes were performed using an RSC-200 (Molecular Kinetics,

Pullman, WA). Currents were measured and digitized with an EPC9 (Heka Elektronik, Lambrecht/Pfalz, Germany), currents were sampled and filtered at 0.33 kHz, digitalized at 1 kHz, and analysis was performed using Pulse (Heka Elektronik) and Igor (Wavemetrics, Lake Oswego, OR) software. For excised patch recordings, the pipette solution was (in mM) 150 KOH, 10 HEPES, 0.1 CaCl₂ and 2 MgCl₂, with pH adjusted to 7.2 with methanesulfonic acid. Excised patches were superfused with an intracellular solution containing (in mM): 150 KOH, 10 HEPES, and 1 EGTA, supplemented with CaCl₂, with pH adjusted to 7.2 with methanesulfonic acid; the amount of CaCl₂ required to yield the indicated concentrations was calculated according to Fabiato and Fabiato (Fabiato and Fabiato, 1979).

Results

Forming CaMBD-CaM Complex from Isolated Peptides

The rSK2 CaMBD peptide was reconstructed to remove the first 17 residues, which could not be resolved in the crystal structure of CaMBD/Ca²⁺/CaM (Schumacher et al., 2001). This new construct contains the SK2 CaMBD residues 411-487 along with the C-terminal 6xHis tag, and is herein referred as the CaMBD peptide.

To examine whether the CaMBD peptide is able to form the complex with CaM in aqueous solution, we mixed a set amount of CaM with increasing amounts of CaMBD or cytochrome c, a peptide of similar molecular weight and pI value (isoelectric point) to CaMBD. Native, nondenaturing gels revealed that higher molecular weight complexes only appeared in the samples containing both CaM and CaMBD, but not in the mixture of CaM and cytochrome c. Western blots further confirmed that this complex is composed of CaM and the CaMBD (Figure 10A). To determine the stoichiometry of the CaMBD-CaM complex, a set amount of CaM (0.25 nmol) was titrated by increasing amount of rSK2 CaMBD peptide either in the presence or absence of Ca²⁺. The samples were then separated on native gels, stained with Coomassie Blue, and subsequently subjected to densitometry analysis, demonstrating that CaMBD-CaM is an equimolar complex in both conditions (Figure 10B). Hence, the deletion of the first 17 amino acids did not affect the ability of the CaMBD to bind CaM with a 1:1 stoichiometry.

Crosslinking of Cysteine-Substituted CaMBD

The crystal structure of CaMBD/Ca²⁺/CaM suggested a chemo-mechanical gating model in which the channel opens as Ca²⁺ binds to CaM, inducing the formation of CaM-CaMBD dimer-of-dimers (Schumacher et al., 2001). To further assess this model,

we introduced pairs of cysteine residues at positions predicted to be in close proximity by the crystal structure of the CaMBD/Ca²⁺/CaM and evaluated their ability to form disulfide bonds. Based solely on their distances calculated according to the crystal structure of CaMBD/Ca²⁺/CaM, the sulfur atoms of M468C-M468C (situated in the middle of the CaMBD α 2 helix) and Q453C-T486C (positioned on the opposite sides of the CaMBD α 2 helix) were predicted to be approximately 2 Å apart, the length of a disulfide bond (Petersen et al., 1999). The double substitutions and single control substitutions were constructed. Equimolar CaMBD/CaM complexes were preformed by adding equivalent molar amount (determined by absorption spectroscopy) of CaMBD to CaM. Oxidation of the cysteine substituted peptides was then performed with the mild oxidizing reagent copper-phenanthroline in the presence of 100 μ M Ca²⁺ (Farrens et al., 1996; Kobashi, 1968). To assess crosslinking, samples were resolved by Tricine SDS-PAGE (Figure 10C). As expected, rSK2 CaMBD M468C-M468C formed a crosslinked product that could be reduced by the odorless and stable reducing agent TCEP (Tris(2-carboxyethyl)phosphine), whereas wild-type rSK2 CaMBD, which does not contain any cysteine residue, did not crosslink. Surprisingly, disulfide cross-links were formed by all cysteine-substituted CaMBD peptides including the Q453C and T486C single mutants. This result suggests that crosslinking occurred in cysteine-substituted CaMBD peptides, and the crosslinkable residues were not all predicted by the crystal structure.

Site-directed Fluorescence Labeling of Adjacent Residues of W432 on CaMBD

To further assess the structural model, we examined the solvent accessibility of the cysteine-substituted CaMBD residues in the presence of CaM with or without Ca²⁺. The

CaMBD peptide contains a single tryptophan residue, W432, which resides in a highly solvent-exposed environment as judged by its fluorescence emission maximum at 346.2 ± 0.8 nm (Keen et al., 1999; Lakowicz, 1999). Fluorescence emission measurements previously demonstrated that CaM binding to the CaMBD induces a change in the environment of W432, and subsequent Ca^{2+} binding to the CaMBD-CaM complex further alters the conformation of the CaMBD peptide (Keen et al., 1999). A cysteine-specific reagent, 1-(2-maleimidylethyl)-4-(5-(4-methoxyphenyl)oxazol-2-yl)pyridinium methanesulfonate (PyMPO-maleimide), has been used to determine the accessibility of cysteine mutants in dark state rhodopsin mutants. This large, rigid molecule successfully demonstrated differences in its ability to penetrate and react with cysteine residues in sterically constrained regions of the protein (Dunham and Farrens, 1999). Therefore, cysteine substitutions were made around W432 in the CaMBD (Figure 11A) to explore the conformational changes with site-directed fluorescence labeling using PyMPO as the fluorescent probe.

Twenty-one cysteine mutants N422C-K442C in the CaMBD were generated, affinity-purified with a Ni column, and labeled with PyMPO-maleimide with or without CaM or Ca^{2+} . Figure 11B shows the differential labeling of a representative CaMBD cysteine mutant, T438C, in the presence or absence of Ca^{2+} and/or CaM. The intensity of PyMPO fluorescence for the CaMBD alone was greatly reduced in the absence of Ca^{2+} , suggesting that T438 is more accessible when the CaMBD has bound Ca^{2+} . In contrast, the cysteine-less wild-type CaMBD showed no reactivity toward PyMPO in all four conditions. To determine the appropriate amount of proteins to be used in the PyMPO fluorescence assay, increasing amounts of T438C were labeled with PyMPO-maleimide

in the presence of Ca^{2+} without CaM (Figure 11B, middle panel). Analysis of the data indicated a linear relationship between the tested protein concentration range, 0.5-3.5 μg , and the resulting fluorescence intensity. Therefore, we decided to use 2.5 μg of each cysteine-substituted CaMBD in the following experiments.

To compare the labeling efficiencies among different cysteine mutants, PyMPO-labeled and subsequently column-purified V427C was used as a standard. The number of incorporated PyMPO molecules per CaMBD V427C molecule was determined with the absorption spectroscopy and found to be 0.48. The relative fluorescence intensity of the various cysteine substituted CaMBD peptides was compared with PyMPO-V427C to calculate the number of the incorporated PyMPO onto each CaMBD cysteine mutant under different conditions and to identify the residues that undergo large conformational changes upon binding to Ca^{2+} and/or CaM (Figure 11C). Interestingly, the reactivity profile of the CaMBD cysteine mutants in the presence of Ca^{2+} and CaM does not exactly correspond to the solvent accessibility predicted from the crystal structure (Figure 11D). For example, the solvent accessibility of W432C was predicted to be < 30% (monomer) or < 10% (dimer), yet its PyMPO reactivity was higher than any other cysteine-substituted residue.

rSK2 L457C Crosslinked by Homobifunctional MTS Compounds

The failure to crosslink residues that are predicted by the structure to be in close proximity suggested that either the structure does not reflect the interaction between CaMBD/ Ca^{2+} /CaM in solution or that screening for likely nearby residues based upon distance alone may not be adequate. Therefore, we used an algorithm that also accounts for bond angles (Dombkowski, 2003). This program identified 18 pairs of residues as

possible candidates, yet neither of the previously identified pairs, M468C-M468C and Q453C-T486C, was detected. To test whether these residues are in proximity in functional channels, two cysteines were introduced into full-length SK2 channels at positions L457 and D482 located on the N- and C-terminal of the second α -helix belonging to two separate CaMBD peptides and hence predicted to form inter-subunit disulfide bond (Figure 12A).

The rSK2 L457C/D482C double mutant retained Ca^{2+} -gating response to voltage commands in inside-out patch configuration; yet it had a lower Ca^{2+} -sensitivity ($1.24 \pm 0.24 \mu\text{M}$; $n=6$) than wild-type rSK2 channels. Addition of the homobifunctional MTS cross-linker, M4M (1,4-butanediyl bismethanethiosulfonate), with a cross-linking span of 7.8 Å (Loo and Clarke, 2001), increased the Ca^{2+} -sensitivity of rSK2 L457C/D482C to $0.76 \pm 0.06 \mu\text{M}$ ($n=6$; $p=0.003$, paired t-test). Further examination of the L457C and D482C single mutants, however, revealed that the single substitution L457C is responsible for the shift of Ca^{2+} -sensitivity (before M4M: $1.07 \pm 0.05 \mu\text{M}$, after M4M: $0.53 \pm 0.10 \mu\text{M}$; $n=4$; $p=0.004$, paired t-test). To distinguish cross-linking from modification, we applied the monofunctional MTS compound, MTSET, to rSK2 L457C. In contrast to M4M, MTSET decreased the Ca^{2+} -sensitivity of rSK2 L457C to $1.53 \pm 0.02 \mu\text{M}$ ($n=3$), and the effect was readily reversible by DTT ($0.91 \pm 0.01 \mu\text{M}$; $n=3$) (Figure 12B).

Since there are two endogenous intracellular cysteine residues in the wild-type rSK2 channel (CaM contains no cysteine residue), M4M might have cross-linked L457C and another endogenous intracellular cysteine residue. To exclude this possibility, we generated an intracellular cysteine-free mutant, rSK2 C4A/C386A, and the corresponding

rSK2 L457C/C4A/C386A mutant.

We further investigated the alteration of Ca^{2+} -sensitivity caused by MTS compounds using the intracellular cysteine-free mutant, rSK2 C4A/C386A, and the corresponding rSK2 L457C/C4A/C386A mutant (Figure 12D; Table 1). As the negative control, none of the MTS compounds significantly affected the Ca^{2+} -sensitivity of rSK2 C4A/C386A. Interestingly, all MTS cross-linkers and negatively-charged monofunctional MTSES increased the Ca^{2+} -sensitivity of rSK2 L457C/C4A/C386A channel, whereas positively-charged MTSEA decreased its Ca^{2+} -sensitivity. MTSET, a bulkier positively-charged MTS reagent, failed to decrease the Ca^{2+} -sensitivity of rSK2 L457C/C4A/C386A mutant in the absence of Ca^{2+} , yet did so in the presence of Ca^{2+} ; indicating that the L457C residue is more accessible to MTS modification in the open state. Correspondingly, the neutral MTSBn increased the Ca^{2+} -sensitivity of rSK2 L457C/C4A/C386A channel only in the presence of Ca^{2+} . Considering that the M4M-induced decrease in EC_{50} of rSK2 L457C/C4A/C386A was not state-dependent, homobifunctional neutral MTS reagents indeed cross-linked, instead of merely modified, the channel. Interestingly, DTT could fully reduce M4M cross-linked rSK2 L457C/C4A/C386A mutant only in absence of Ca^{2+} , hinting that the cross-linked sites are more inaccessible in the open state.

The M4M cross-linked products were then assayed via Western blots. CHO cells were transiently-transfected with an intracellular cysteine-free rSK2 and rSK2 L457C harboring an N-terminal C8 tag (Strassmaier et al., 2005). Membrane proteins were prepared, and the M4M cross-linking reaction was performed in the presence of 50 μM free Ca^{2+} . Following separation on SDS-PAGE and transfer to the nitrocellulose

membrane, the anti-C8 antibody recognized a higher molecular weight band, presumably the cross-linked rSK2 dimer, which was more resistant to DTT reduction in samples containing the rSK2 L457C mutant (Figure 12C). Therefore, M4M facilitated the formation of rSK2 L457C dimers that is more stable than rSK2 wild-type dimers in the presence of reducing agent, probably by joining adjacent L457C residues. The apparent proximity of L457C residues in functional channels is inconsistent with the structural prediction.

The rSK2 K472 Truncation Is Fully Functional and Gated by Ca²⁺

The chemo-mechanical gating model proposed that in the absence of Ca²⁺, the CaMBD peptide exists as a monomer; Ca²⁺ binding to the N-lobe of CaM induces the dimerization of CaMBD, thereby opens the SK channel gate (Figure 3). In the crystal structure of CaMBD/Ca²⁺/CaM, the Ca²⁺-bound N-lobe of CaM makes strong contacts with the C-terminus of the CaMBD via a 'hydrophobic anchor point' involving the L480 prong. In addition, a short CaM N-lobe loop (G40 and P43) reaches around the other subunit of the CaMBD dimer. Thus, the CaMBD/N-lobe interaction stabilizes the dimeric complex. According to the crystal structure, the loss of this interaction would be fatal to SK channel gating. To examine the importance of this predicted interaction, SK2 channel harboring truncation rSK2 K472 (SK2:472*) that is predicted to drastically disrupt the dimer-of-dimers was generated and transiently expressed in mammalian cells (Figure 13A). Since a Ca²⁺-independent interaction with CaM is vital for cell surface expression, we first examined whether the truncations are detrimental to the CaMBD/C-lobe interaction. Immunocytochemistry of COS cells transfected with SK channels harboring three tandem copies of the myc epitope in the external loop between transmembrane

domains 3 and 4 was performed in non-permeabilized cells. SK2:472* truncated channel retained the normal cell surface expression (Figure 13B), indicating constitutive CaM association. Inside-out patches were then used to examine channel function and Ca^{2+} -gating; SK2:472* remained functional and was gated by Ca^{2+} (Figure 13C). Using rapid solution exchange to apply intracellular solutions of different Ca^{2+} concentrations on inside-out patches, deactivation time constants (determined from mono-exponential fits) were 52.3 ± 5.8 , 18.2 ± 3.1 , 16.2 ± 2.8 and 12.5 ± 1.9 (mean \pm SEM) ms for wild-type, truncated rSK2 A477 (SK2:477*), rSK2 D475 (SK2:475*), and SK2:472* channels, respectively (Figure 13D). In other words, time constants for deactivation of rSK2 K472, D475 and A477 truncations increased toward that of the wild-type rSK2 channel as the number of the remaining residues increased. Ca^{2+} dose-responses were performed by changing between internal solutions containing varying concentrations of Ca^{2+} (Figure 13E). The steady-state Ca^{2+} -sensitivity of SK2:477*, SK2:475*, and SK2:472* was right-shifted ($K_d = 1.19 \pm 0.02$, 1.31 ± 0.05 , 1.43 ± 0.02 μM ; Hill coefficients = 4.45 ± 0.25 , 4.50 ± 0.28 , 4.34 ± 0.33 ; $n \geq 4$) compared to wild type channels ($K_d = 0.59 \pm 0.00$ μM , Hill coefficients = 5.45 ± 0.49 , $n=4$). Similar to deactivation time constants, steady-state Ca^{2+} -sensitivity of rSK2 K472, D475 and A477 truncations increased toward that of the wild-type rSK2 channel as the number of the remaining residues increased. Therefore, the interaction between the N-lobe of CaM and the C-terminus of the CaMBD is dispensable at the expense of normal Ca^{2+} affinity/sensitivity. It was interesting that the off rates were faster in the truncations – indicating that the N-lobe interactions may be important for slowing the closing rates of the channel.

Discussion

The Architecture of Calcium-Gated Potassium Channels

Chemo-mechanically gated SK channels belong to ligand-gated potassium channels that include high conductance Ca^{2+} -modulated K^+ channels (BK channels), K_{ATP} channels, and G-protein-coupled inwardly rectifying K^+ channels (GIRK channels). Different from the Ca^{2+} -gated MthK channel which possesses an octameric gating ring composed of eight intracellular ligand-binding RCK domains (Dong et al., 2005; Jiang et al., 2002), SK channels were proposed to form dimer-of-dimers with calcified CaM via the intracellular CaMBD immediately C-terminal to the pore in the open state (Schumacher et al., 2004; Schumacher et al., 2001). Our native gel assays (Figure 10) confirmed that the 1:1 molar ratio CaMBD-CaM complex retains the specific interaction in the aqueous solution as previous published results (Wissmann et al., 2002). Yet, SDFL and cross-linking experiments contradicted the predictions based on the crystal structure of CaMBD/ Ca^{2+} /CaM. The rSK2 K472 truncation, which disrupted the CaMBD/N-lobe interaction and thus dimerization as predicted by the chemo-mechanical gating model, is also fully functional and gated by Ca^{2+} . Therefore, the static crystal structure might not be a precise gauge in visualizing the dynamic movement during SK channel gating.

Disulfide trapping has been applied to study protein mobility and proximity relationships between residues in water soluble proteins. The disulfide bond formation rate depends on the collision frequency of the sulfhydryls, the energy of collision, and the presence of an oxidizing environment. Collision frequency depends on the average separation distance of the sulfhydryls, their relative orientation in the protein and the protein's mobility and/or flexibility (Careaga and Falke, 1992). The oxygen/ $\text{Cu(II)}(1,10\text{-phenanthroline})_3$

system is thought to oxidize by generation of an oxyradical (hydroxyl radical or superoxide anion), which diffuses to the vicinity of a sulfhydryl and removes an electron, yielding a sulfur radical capable of disulfide formation upon collision with a second thiol or sulfur radical. This scheme avoids modification of the reacting sulfhydryls with a covalent intermediate, such as those formed in disulfide exchange reactions, which might perturb backbone dynamics (Careaga and Falke, 1992). In the experiment shown in Figure 10C, the reaction mixture of 30 μM CaMBD and 30 μM CaM was sit at room temperature for 5 minutes, which is shorter than 15 minutes used for the crosslinking of 100 μM GABA_A receptor (Horenstein et al., 2001) and comparable to the incubation at 4°C for 7 min for oxidizing 1 μM double cysteine rhodopsin mutants (Farrens et al., 1996). Therefore, the result should not reflect nonspecific crosslinking owing to inappropriate protein concentration, high reaction temperature or extensive reaction time.

Factors affecting cysteine modification by PyMPO maleimide

Site-directed fluorescence labeling (SDFL) using PyMPO maleimide to modify cysteine-substituted residues was used to demonstrate light-dependent changes in PyMPO reactivity of the rhodopsin V250C mutant (Dunham and Farrens, 1999), and subsequently, the high affinity peptide analogue of the G_{T α} C terminus W23SV (sequence WVLEDLKS_VGLF) blocked labeling of V250C by PyMPO maleimide (Janz and Farrens, 2004). Yet, PyMPO did not generate voltage-dependent fluorescence signals at the prokaryotic sodium channel NaChBac L112 position (Blunck et al., 2004). Hence, the reactivity of PyMPO maleimide is highly dependent on the environment of the targeted cysteine within each individual protein. Although the PyMPO reactivities of cysteine-substituted rSK2 CaMBD mutants appeared to be inconsistent with the crystal

structure (Figure 11), several factors affecting the cysteine modification by PyMPO maleimide may explain the discrepancies. First, the observed pK_a values of surface groups on the proteins might be shifted by the nature of the surrounding residues (Schutz and Warshel, 2001), making the cysteine residue more or less prone to maleimide modification. Second, the solvent accessibility of the positions on the CaMBD was calculated based on the crystal structure for either the wild-type or with the site-directed cysteine mutation. Therefore, possible structural distortions induced by the cysteine mutation were ignored and not considered in the prediction. Third, the readout of the assay is PyMPO fluorescence, not the labeling efficiency. If the PyMPO fluorescence is quenched by neighboring side chains, such as tryptophan, the readout would be smaller than the actual modification. In this regard, the surprisingly high reactivity of W432C is likely resulted from the elimination of tryptophan by changing it into cysteine. Therefore, the PyMPO reactivity profile presented here might not faithfully reflect the actual solvent accessibility of the investigated positions. Other fluorescent dyes, such as cyanine 3 monofunctional bihexanoic acid Mono-MTSEA (Cy3) and Texas Red methanethiosulfonate (TxRed), may be used to confirm the results of PyMPO reactivity.

Interestingly, the intensity of PyMPO fluorescence for the CaMBD alone was increased in the presence of Ca^{2+} alone for seventeen of the nineteen purified cysteine-substituted CaMBD peptides (Figure 11C). Considering that CaMBD is constitutively bound to CaM in functional SK channels, the Ca^{2+} induced conformational change suggested by the changes in solvent accessibility of CaMBD by Ca^{2+} alone probably has no direct functional implication. However, this result suggests that Ca^{2+} might regulate a CaMBD conformation that may affect things other than channel gating, such as protein-protein

interaction between the SK channel and other associated proteins.

Calmodulin-modulated Channel Activities

Calmodulin has been demonstrated to modulate the rat olfactory CNG channels (Bradley et al., 2004), L-type Ca^{2+} channels (Mori et al., 2004), TRPC5 channels (Ordaz et al., 2005), and SK channels. The uniqueness of SK channels is that CaM activates, not inhibits their functionality, in the presence of Ca^{2+} via filling the N- but not C-lobe (Keen et al., 1999; Schumacher et al., 2001). Intriguingly, our truncation experiments revealed that the N-lobe contact is not required for SK channel gating; or that the interaction as described by the crystal structure cannot be applied to functional channels, leaving whether there is an N-lobe/CaMBD contact uncertain (Figure 13C). An interesting observation is that Ca^{2+} sensitivity is reduced in truncated SK channels (Figure 13E), and the close rates of truncated SK channels (Figure 13D) closely resembles the steady-state Ca^{2+} sensitivity. This implicated that Ca^{2+} /CaM association to the C-terminal of CaMBD stabilizes the interaction between Ca^{2+} /CaM and SK channels, housekeeping the high Ca^{2+} sensitivity. Overall, despite previously reported consistencies between structural data and functional SK channels, such as the compensatory CaM E84R/E87K mutant successfully stabilized the Ca^{2+} -dependent channel activity of the SK2 R464E/K467E double charge reversal mutant (Lee et al., 2003), the ‘dimer-of-dimer’ model for SK channel gating has been challenged.

Altered Ca^{2+} -sensitivity of SK Channels and Plausible Mechanisms

Why do rSK2 L457C mutant and 472* truncated channel have reduced Ca^{2+} -sensitivity? One explanation is that the mutation/truncation caused reduced CaM binding affinity; subsequently, rSK2 CaMBD became less sensitive to the conformational change of CaM

induced by Ca^{2+} -binding. Another possibility is that the mutation/truncation resulted in some conformation distortion of bound CaM, decreasing the Ca^{2+} -binding affinity of CaM. To distinguish between these two mechanisms, two kinds of experiments should be performed: (1) measuring the CaM affinity of CaMBD containing L457C mutation or 472* truncation, (2) assessing the Ca^{2+} affinity of CaM bound to CaMBD peptide containing L457C mutation or 472* truncation. [^{35}S]CaM binding assay has been used for measuring the CaMBD affinity by incubating type-3 ryanodine receptor derived from transfected HEK 293 cells (Yamaguchi et al., 2005). Similarly, this assay could be applied for rSK2 L457C or 472* channel proteins derived from transfected CHO cells. On the other hand, the Ca^{2+} dissociation constant (K_d) was determined by following changes in signals in the ^{15}N - ^1H HSQC NMR spectra of the human cardiac voltage-gated sodium channel $\text{Na}_v1.5$ truncated construct as Ca^{2+} was titrated into Ca^{2+} -free, BAPTA-free peptide (Shah et al., 2006). This approach might be appropriate to measure the Ca^{2+} dissociation constant (K_d) of the mutated/truncated CaMBD-bound CaM.

A Role for Hydrophobic Residues in Ca^{2+} -sensitivity of SK Channels

The Western blot of rSK2 L457C demonstrated that M4M could facilitate the formation of stable rSK2 L457C dimers relative to dimers formed by wildtype rSK2 (Figure 12C), further strengthens the interpretation that M4M increases the Ca^{2+} -sensitivity of rSK2 L457C on excised inside-out patches via crosslinking (Table 1). This crosslinking is probably resulted from disulfide bonds formed between introduced L457C mutations on two individual α -subunits, although there is still minor possibility that L457C interacts with another cysteine residue embedded on the transmembrane domain of either the same or another α -subunit. Interestingly, the intensity of the dimer band is highest in the

sample containing 2 mM DTT, not 2.5 mM NEM; indicating that the formation of the dimer might be preferable in the presence of low concentration of reducing agent, which removes non-specific protein aggregation.

The charge-dependent modification by MTSET (positively-charged) and MTSES (negatively-charged) of rSK2 L457C implies possible charge-charge interaction between this position and neighboring residues. Because the positively-charged MTSET decreases the Ca^{2+} -sensitivity whereas negatively-charged MTSES increases it, there might be a positively-charged residue interacting with this position and thus destabilizing or stabilizing the CaM-CaMBD interaction. The residue originally predicted by the crystal structure in close proximity, rSK2 D482, is negatively-charged and hence precluded to be the candidate. Further experiments, such as using a photoactivatable reagent N-[(2-pyridyldithio)-ethyl] 4-azido salicylamide (PEAS) attached to L457C via a disulfide-exchange reaction with the pyridylthio group to map contact sites by covalent crosslinking (Cai et al., 2001), should be performed to define the surrounding positively-charged residue(s).

The finding of MTS compound-modified rSK2 L457C Ca^{2+} -sensitivity (Figure 12) suggests that this hydrophobic residue L457 of the CaMBD could be vital in stabilizing protein-protein interaction of SK channels, leading to the alteration in the efficiency of transforming the chemical energy into mechanical gating. Although the leucine-heptad-repeat region of the Shaker K^+ channel has been demonstrated to be essential in the transduction of charge movement into channel opening and closing (McCormack et al., 1991), no comparable discovery has been reported in ligand-gated K^+ channels except L344 in $\text{G}_{\beta\gamma}$ activation of GIRK2 channels (Finley et al., 2004).

Hence, our data pioneered in revealing the importance of the overlooked hydrophobic residues.

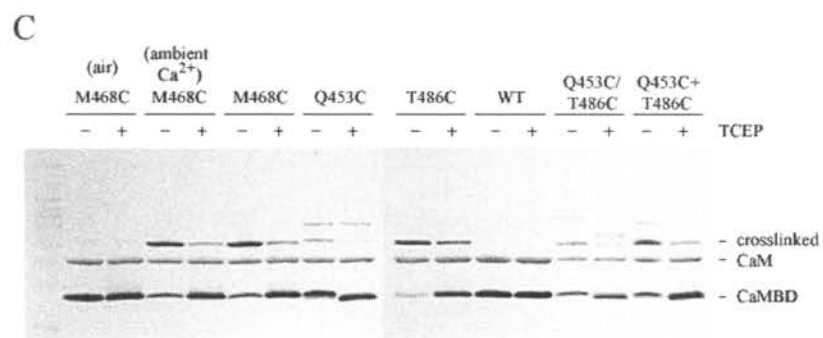
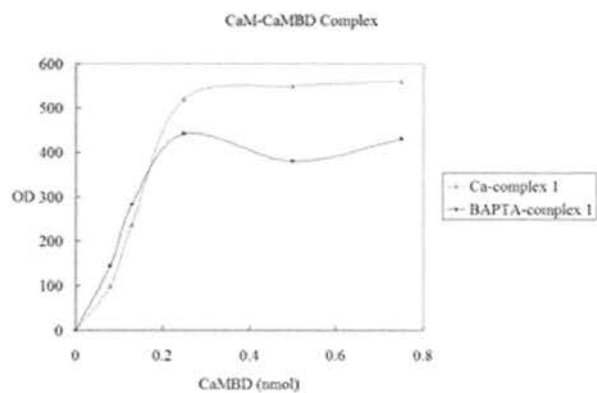
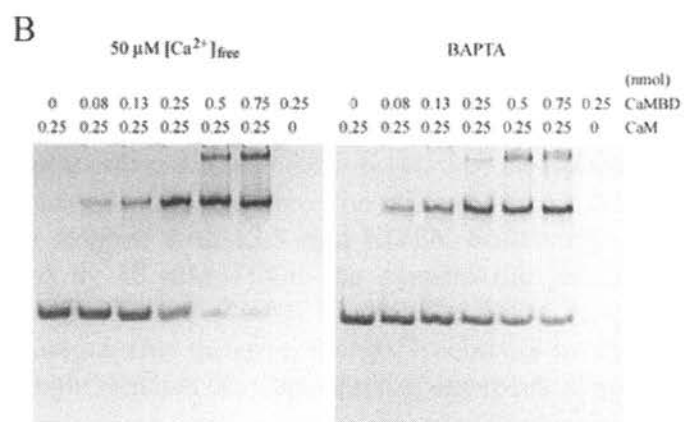
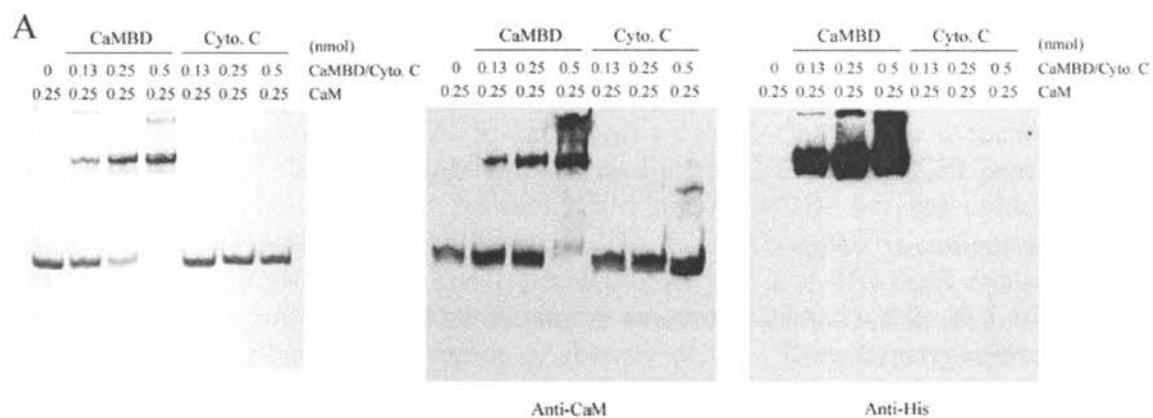
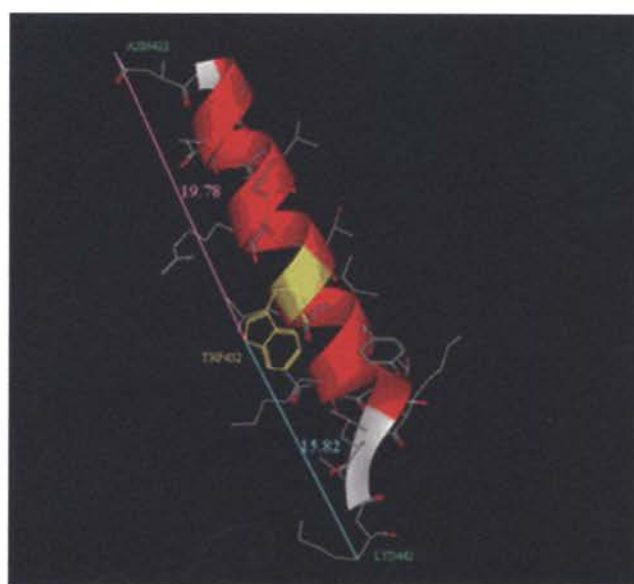


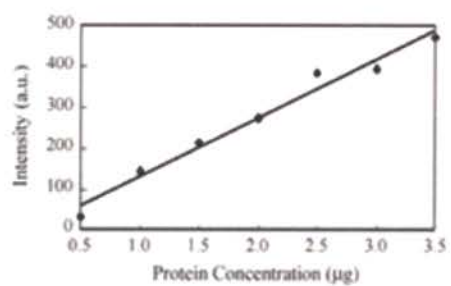
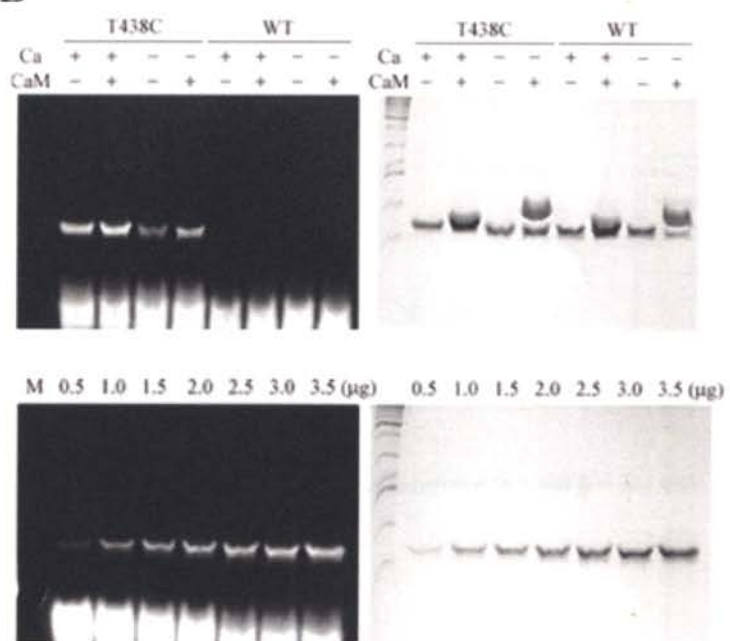
Figure 10. As isolated peptides, CaMBD-CaM complex retains the specific interaction and the 1:1 stoichiometry.

(A) CaM forms complex with rSK2 CaMBD specifically. 0.25 nmol of CaM was titrated by increasing amount (0, 0.13, 0.25, 0.5 nmol) of rSK2 CaMBD or cytochrome c, a peptide of similar molecular weight and pI value to rSK2 CaMBD. (Left panel) Native gel showing complex formation between CaM and CaMBD, but not cytochrome c. (Middle and Right panels) Western blot revealing that the complex is composed of CaM and 6xHis-tagged CaMBD. (B) The 1:1 stoichiometry of CaMBD-CaM complex. 0.25 nmol of CaM was further titrated by increasing amount (0.08, 0.13, 0.25, 0.5, 0.75 nmol) of rSK2 CaMBD either in the presence or absence of Ca^{2+} . Densitometry analysis of the Coomassie-stained native gels indicates that CaMBD-CaM is an equimolar complex in both conditions. (C) $\text{Cu}(\text{phenanthroline})_3$ accelerated crosslinking in the presence of $100\mu\text{M}$ added Ca^{2+} . Residues predicted to be in close proximity based on the crystal structure were substituted by cysteines, and the disulfide-bond formation between cysteine-substituted CaMBD peptides was accelerated by $\text{Cu}(\text{phenanthroline})_3$. $30\mu\text{M}$ CaM and $30\mu\text{M}$ CaMBD peptides were mixed in 130 mM NaCl buffered with 10 mM HEPES pH 7.2. Subsequently, 0.5 mM CuSO_4 and 1.5 mM phenanthroline, along with $100\mu\text{M}$ CaCl_2 , were added to the reaction. The mixture was sit at room temperature for 5 minutes before being stopped with 12.5 mM EDTA. Following either quenched by 2.5 mM NEM or reduced by 10 mM TCEP, the crosslinking products were separated on non-reducing Tricine-SDS-PAGE (16.5% T, 6% C). While M468C is able to form a crosslinked product across two different CaMBD subunits as predicted by the model, Q453C and T486C single mutants also demonstrate unexpected crosslinking.

A

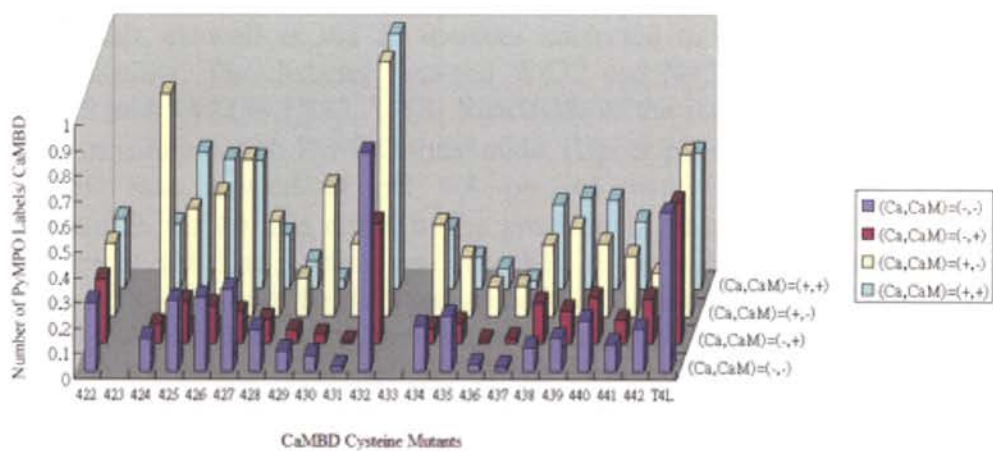


B



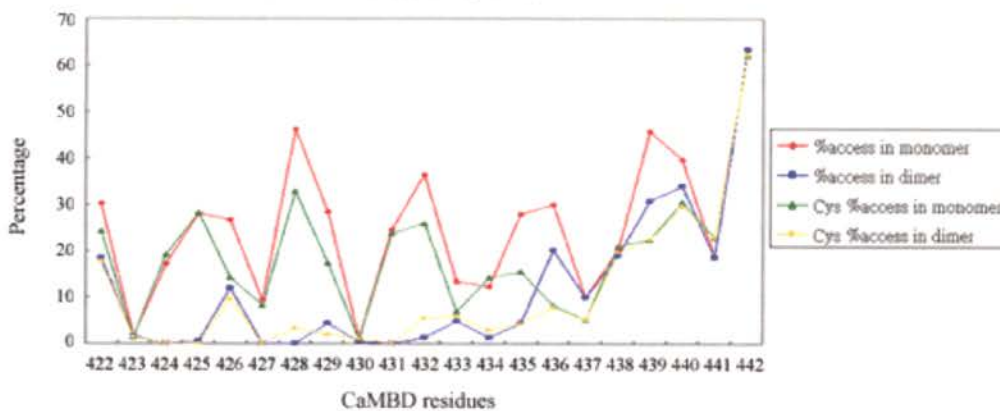
C

PyMPO Reactivity of CaMBD Cysteine Mutants



D

Solvent Accessibility of CaMBD



PyMPO Reactivity of Cysteine-substituted CaMBD

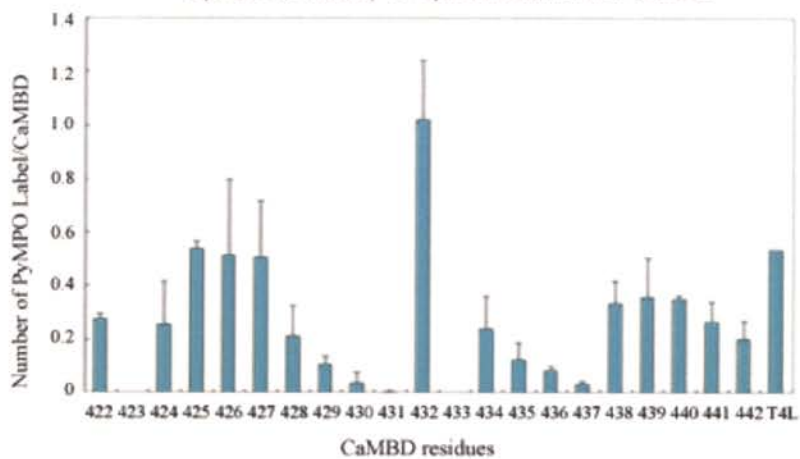
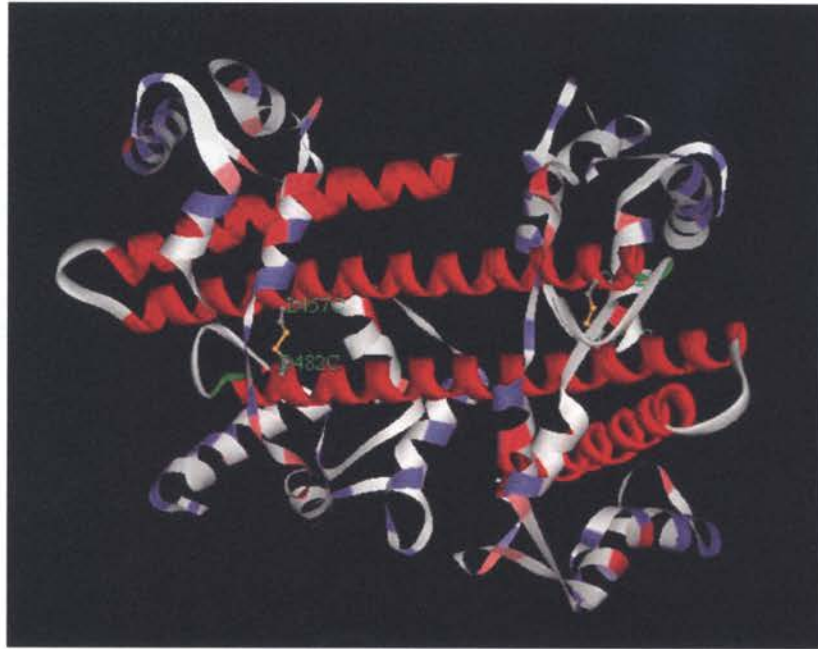


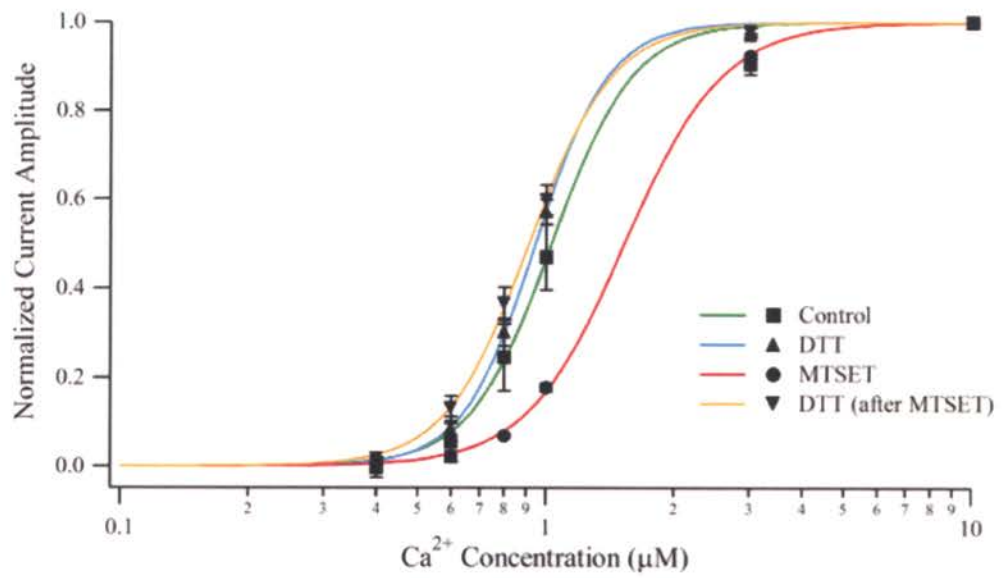
Figure 11. Site-directed fluorescence labeling (SDFL) of adjacent residues of W432 on CaMBD

(A) A ribbon diagram showing adjacent residues of W432 on CaMBD. The model indicates the location of the single tryptophan residue, W432, in the CaMBD of SK2 channel α -subunit, as well as the 20 residues subjected to cysteine substitutions for fluorescence labeling. The distance between W432 and N422 is 19.78 Å, while that between W432 and K442 is 15.82 Å. (B) Reactivity of the purified cysteine-substituted CaMBD free in solution with PyMPO-maleimide. (Upper panels) 2.5 μ g (0.25 nmol) of mutant T438C was reacted at pH 6.8 on ice with 3-fold molar excess of PyMPO-maleimide for 10 min either in the presence or absence of 50 μ M free Ca^{2+} and/or 0.25 nmol CaM. The reaction was quenched by the addition of cysteine to a final concentration of 1 mM, and the samples were then analyzed by SDS-PAGE. Gel was visualized using UV irradiation and documented with Kodak 1D 2.0.2. The picture on the right shows the Coomassie blue staining of the same gel. (Middle panels) Different amounts of T438C were labeled with PyMPO-maleimide in the presence of Ca^{2+} without CaM. (Lower panel) Analysis of data in Middle panels indicates a linear relationship between the protein concentration and the fluorescence intensity. (C) Comparison of the reactivity of the purified cysteine-substituted CaMBD free in solution with PyMPO-maleimide. The number of incorporated PyMPO fluorescence probe per CaMBD (average of three independent experiments) is shown for each cysteine mutant in the presence (+) or absence (-) of Ca^{2+} and/or CaM. The lack of data from the CaMBD A423C and L433C mutants is due to the difficulty in expressing these recombinant proteins. T4 lysozyme (T4L) was used as the negative control, indicating that the variation of the PyMPO reactivity resulting from the presence of Ca^{2+} and/or CaM is unique for the CaMBD peptide. (D) Calculated solvent accessibility based on the crystal structure of CaMBD/ Ca^{2+} /CaM failed to predict the PyMPO reactivity of cysteine-substituted CaMBD. The solvent accessibility for residues N422 to K442 of CaMBD was calculated as the original and cysteine-substituted forms in both monomeric and dimeric CaMBD/ Ca^{2+} /CaM models. DeepView defines the maximum accessibility as the accessible surface area for residue X in an extended pentapeptide GGXGG. Percentage in the Y-axis refers to the relative accessibility of a residue X obtained by comparison of the observed accessibility to this reference value of 100% (Upper panel). None of the four curves fit the bar graph summarizing experimental PyMPO reactivity of cysteine-substituted CaMBD in the presence of both Ca^{2+} and CaM (Lower panel).

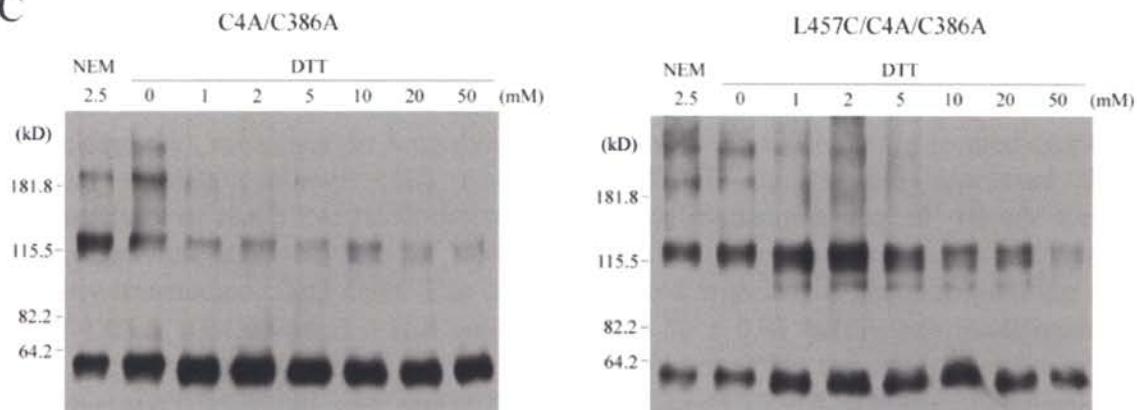
A



B



C



D

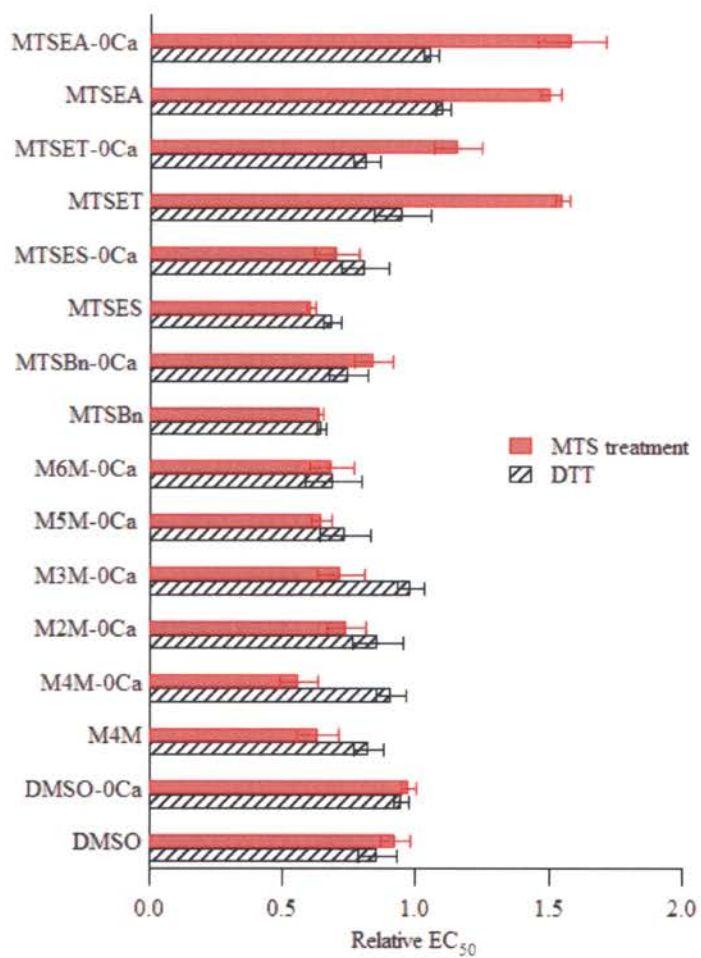
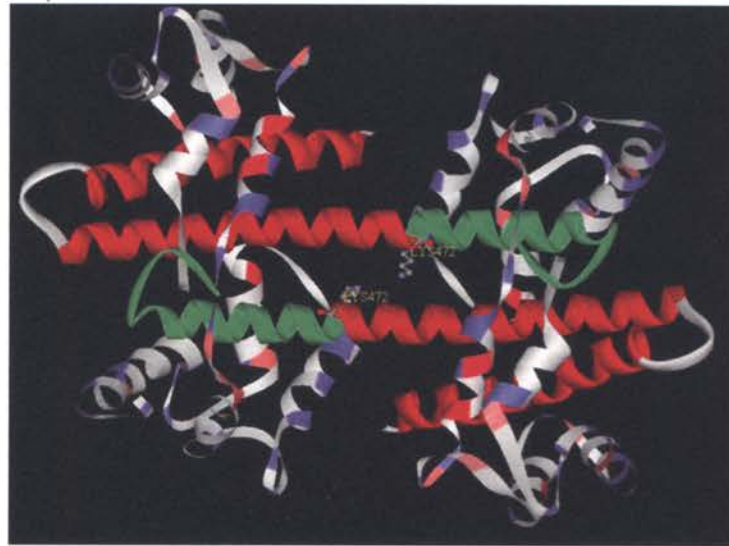


Figure 12. The rSK2 L457C single mutant was able to be modified and crosslinked upon addition of MTS compounds, altering the calcium sensitivity of the channel.

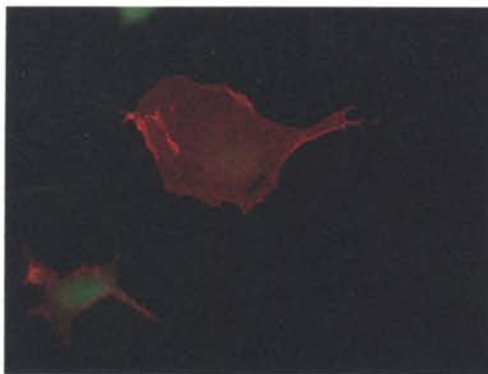
(A) A ribbon diagram showing the dimeric SK channel CaMBD/Ca²⁺/CaM complex. The model indicates the location of L457C and D482C in the CaMBD of SK2 channel α -subunit (*green*), revealing the long distance between two L457 residues located on two individual CaMBD subunits. (B) Reducible MTSET modification decreased the Ca²⁺-sensitivity of rSK2 L457C. Relative current amplitudes measured at -80 mV were plotted versus the intracellular Ca²⁺ concentration for inside-out patches excised from transiently-transfected CHO cells. The data were fitted with a Hill equation yielding an EC₅₀ of $1.03 \pm 0.04 \mu\text{M}$ and a Hill coefficient of 4.59 ± 0.81 before any modification (*green*). Incubation in 10 mM DTT for 3 minutes did not affect the curve significantly; EC₅₀ value was $0.95 \pm 0.01 \mu\text{M}$, and Hill coefficient was 5.13 ± 0.24 (*blue*). Application of 1 mM MTSET for 8 seconds at -80 mV shifted the Ca²⁺-response curve to the right, with values for EC₅₀ of $1.53 \pm 0.02 \mu\text{M}$ and a Hill coefficient of 3.79 ± 0.11 (*red*). Reduction by 3-minute incubation in 10 mM DTT reversed the effect of MTSET modification; EC₅₀ value was $0.91 \pm 0.01 \mu\text{M}$, and Hill coefficient was 4.45 ± 0.14 (*yellow*). (C) The MTS cross-linker with a cross-linking span of 7.8 Å, M4M, induced the formation of relatively stable rSK2 L457C dimers. Membranes were prepared from CHO cells transiently-transfected with C8-tagged intracellular cysteine-free rSK2 and rSK2 L457C. The cross-linking reaction was performed in the presence of 50 μM free Ca²⁺ and 200 μM M4M on ice for 15 minutes, and the products were either preserved by 2.5 mM NEM or reduced by various concentrations of DTT as indicated. Western blotting using the anti-C8 antibody revealed the monomeric 49-kDa rSK2 and a higher molecular weight band, presumably the cross-linked rSK2 dimer, which was more prominent in reactions containing the rSK2 L457C mutant. (D) Summary of alteration in Ca²⁺-sensitivity after MTS compounds cross-linked or modified rSK2 L457C/C4A/C386A channel. EC₅₀ measured after (*red bars*) MTS compound treatment and posterior to DTT reduction (*black shaded bars*) were normalized to that measured before MTS compound treatment. Data from $n \geq 3$ patches were averaged and plotted as mean \pm SEM. In the absence of Ca²⁺, MTS cross-linkers and negatively-charged MTSES increased the Ca²⁺-sensitivity of rSK2 L457C/C4A/C386A channel, whereas positively-charged MTSEA decreased its Ca²⁺-sensitivity.

A

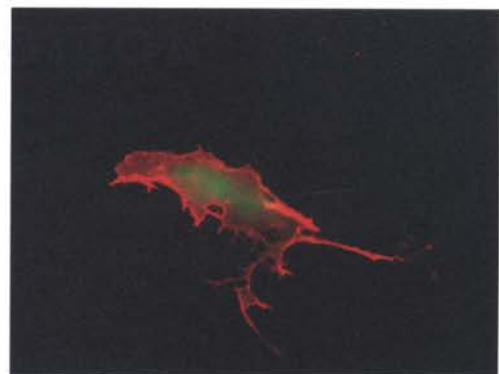


B

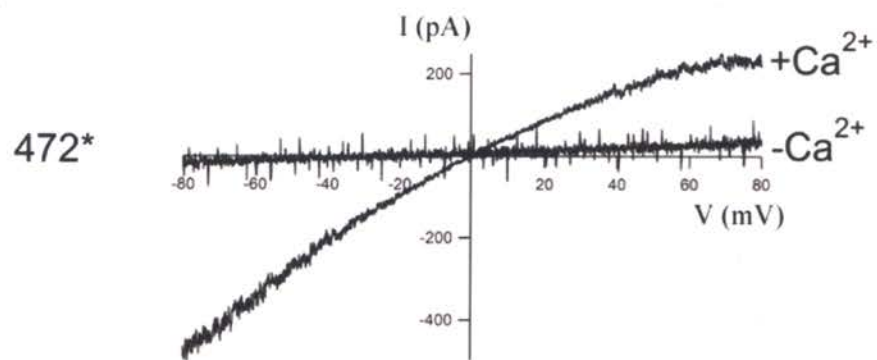
SK2:64/67 + CaM



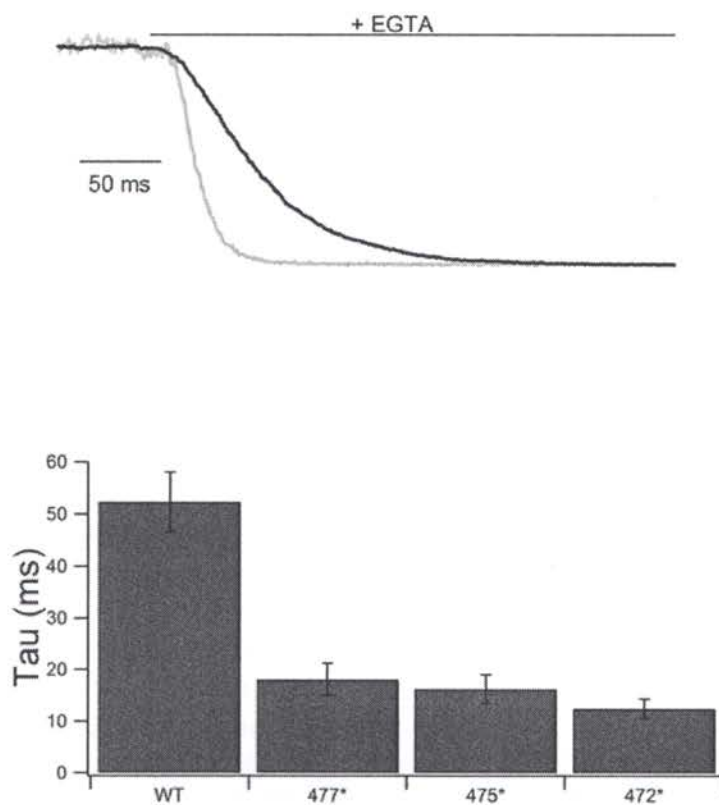
SK2:472* + CaM



C



D



E

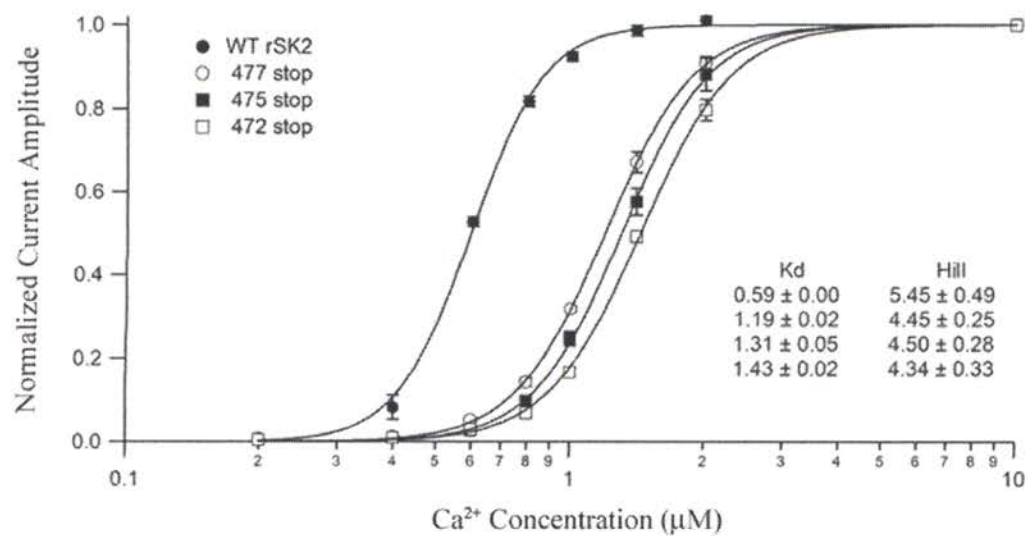


Figure 13. The rSK2 K472* channel harboring a truncation of the C-terminal domain was fully functional, displaying normal Ca^{2+} -gating.

(A) Ribbon diagram of the CaMBD/ Ca^{2+} /CaM dimeric complex showing SK2:472* with the truncated part in green. (B) Immunocytochemistry of COS cells transfected with the indicated combinations of SK2:64/67 or SK2:472* along with CaM and a GFP expression plasmid. SK channel harbors three tandem copies of the myc epitope in the external loop between transmembrane domains 3 and 4. Transfected cells were identified by expression of GFP, channel protein was detected with an anti-myc mouse monoclonal antibody and visualized by Texas Red-conjugated horse anti-mouse secondary antibody, and the signals were merged. In each case, cells were examined without the membrane permeabilization. Like the positive control SK2:64/67 (*left*), SK2:472* (*right*) was detected on the cell surface when transfected with wild type CaM. (C) Currents recorded from representative inside-out patches excised from COS cells cotransfected with SK2:472* and CaM. The patch was excised into Ca^{2+} solution (10 μM , $+\text{Ca}^{2+}$), then exposed to 0 Ca^{2+} solution ($-\text{Ca}^{2+}$). SK2:472* was functional and displayed normal Ca^{2+} -gating. (D) Fast piezo-driven application of EGTA to inside-out patches expressing SK2 wild-type, SK2:477*, SK2:475*, and SK2:472* channels. (*Upper*) Representative current traces of SK2 wild-type (Zagotta et al.) and SK2:477* (*gray*). The holding potential was 80 mV; current was normalized; time calibration is 50 ms. (*Lower*) Time constants for deactivation, determined from mono-exponential fits, were 52.3 ± 5.8 , 18.2 ± 3.1 , 16.2 ± 2.8 and 12.5 ± 1.9 (mean \pm SEM) ms for wild-type, SK2:477*, SK2:475*, and SK2:472* channels, respectively. (E) Normalized Ca^{2+} dose-response relationships. The indicated SK2 channel and CaM were coexpressed. Relative current amplitudes measured at -80 mV from $n \geq 4$ patches for each combination of channel and CaM were averaged and plotted *versus* the intracellular Ca^{2+} concentration. The averaged data were fitted with a Hill equation (*continuous lines*).

Table 1. Alteration of Ca²⁺-sensitivity after cross-linking/modification with MTS compounds

	Control		MTS Compound		DTT	
	EC ₅₀ (μM)	<i>n</i>	EC ₅₀ (μM)	<i>n</i>	EC ₅₀ (μM)	<i>n</i>
C4.386A						
<i>DMSO</i>	0.60 ± 0.11	3.55 ± 0.46 (5)	0.59 ± 0.12	3.46 ± 0.63 (5)	0.59 ± 0.08	3.82 ± 0.42 (4)
			<i>p</i> = 0.53		<i>p</i> = 0.33	
<i>DMSO-0Ca</i>	0.58 ± 0.07	3.65 ± 1.65 (4)	0.59 ± 0.06	3.55 ± 0.74 (4)	0.61 ± 0.05	3.17 ± 0.44 (4)
			<i>p</i> = 0.17		<i>p</i> = 0.31	
<i>M4M</i>	0.53 ± 0.07	3.42 ± 0.67 (5)	0.59 ± 0.11	3.66 ± 0.48 (5)	0.62 ± 0.14	3.18 ± 0.72 (4)
			<i>p</i> = 0.09		<i>p</i> = 0.09	
<i>M4M-0Ca</i>	0.66 ± 0.12	3.58 ± 1.03 (6)	0.70 ± 0.16	4.12 ± 0.60 (6)	0.73 ± 0.15	3.94 ± 0.89 (5)
			<i>p</i> = 0.29		<i>p</i> = 0.37	
<i>M2M-0Ca</i>	0.74 ± 0.19	4.11 ± 0.66 (5)	0.82 ± 0.26	3.89 ± 0.63 (5)	0.90 ± 0.25	4.03 ± 0.30 (4)
			<i>p</i> = 0.17		<i>p</i> = 0.25	
<i>M3M-0Ca</i>	0.63 ± 0.07	3.91 ± 0.69 (5)	0.68 ± 0.04	4.02 ± 0.35 (5)	0.66 ± 0.08	4.21 ± 1.23 (5)
			<i>p</i> = 0.08		<i>p</i> = 0.23	
<i>M5M-0Ca</i>	0.63 ± 0.15	4.28 ± 0.60 (6)	0.70 ± 0.18	4.89 ± 0.66 (6)	0.78 ± 0.15	4.73 ± 0.89 (4)
			<i>p</i> = 0.17		<i>p</i> = 0.03	
<i>M6M-0Ca</i>	0.69 ± 0.17	3.44 ± 0.64 (8)	0.74 ± 0.15	3.72 ± 0.55 (8)	0.78 ± 0.14	3.75 ± 0.48 (8)
			<i>p</i> = 0.06		<i>p</i> = 0.01	
<i>MTSBn-0Ca</i>	0.50 ± 0.05	3.78 ± 0.60 (4)	0.51 ± 0.10	3.29 ± 1.00 (4)	0.60 ± 0.05	3.84 ± 0.01 (2)
			<i>p</i> = 0.93		<i>p</i> = 0.30	

(continued from previous page)

<i>MTSES-0Ca</i>	0.53 ± 0.02	3.54 ± 0.43 (4)	0.52 ± 0.04	3.65 ± 0.29 (4)	0.54 ± 0.07	3.50 ± 0.21 (3)
			<i>p</i> = 0.68		<i>p</i> = 0.99	
<i>MTSET-0Ca</i>	0.51 ± 0.08	3.48 ± 0.68 (6)	0.50 ± 0.10	3.65 ± 0.46 (5)	0.50 ± 0.13	3.60 ± 0.68 (4)
			<i>p</i> = 0.26		<i>p</i> = 0.59	
<i>MTSEA-0Ca</i>	0.56 ± 0.10	4.12 ± 0.49 (3)	0.55 ± 0.16	4.16 ± 0.13 (3)	0.72	4.29 (1)
			<i>p</i> = 0.76			
	Control		MTS Compound		DTT	
	EC₅₀ (μM)	<i>n</i>	EC₅₀ (μM)	<i>n</i>	EC₅₀ (μM)	<i>n</i>
<i>L457C/C4.386A</i>						
<i>DMSO</i>	1.06 ± 0.09	4.24 ± 0.66 (5)	0.98 ± 0.15	3.73 ± 0.88 (5)	0.90 ± 0.16	4.14 ± 0.55 (5)
			<i>p</i> = 0.27		<i>p</i> = 0.13	
<i>DMSO-0Ca</i>	0.99 ± 0.04	4.11 ± 0.51 (4)	0.96 ± 0.04	3.85 ± 0.53 (4)	0.94 ± 0.05	3.57 ± 0.61 (3)
			<i>p</i> = 0.43		<i>p</i> = 0.21	
<i>M4M</i>	0.92 ± 0.05	3.59 ± 0.46 (4)	0.58 ± 0.14	3.42 ± 0.74 (4)	0.76 ± 0.11	3.83 ± 0.45 (4)
			<i>p</i> = 0.02		<i>p</i> = 0.05	
<i>M4M-0Ca</i>	1.16 ± 0.20	3.73 ± 0.73 (7)	0.63 ± 0.14	3.00 ± 0.52 (7)	1.07 ± 0.14	3.18 ± 0.46 (6)
			<i>p</i> = 0.00		<i>p</i> = 0.15	
<i>M2M-0Ca</i>	0.96 ± 0.23	2.80 ± 0.31 (9)	0.68 ± 0.14	3.19 ± 0.45 (9)	0.84 ± 0.12	3.21 ± 0.42 (7)
			<i>p</i> = 0.02		<i>p</i> = 0.15	
<i>M3M-0Ca</i>	0.92 ± 0.13	3.04 ± 0.44 (5)	0.73 ± 0.09	3.63 ± 0.69 (3)	0.92 ± 0.06	3.53 ± 0.72 (2)
			<i>p</i> = 0.03		<i>p</i> = 0.58	

(continued from previous page)

<i>M5M-0Ca</i>	1.04 ± 0.19	3.62 ± 0.43 (4)	0.66 ± 0.12 <i>p</i> = 0.01	4.11 ± 0.38 (4)	0.76 ± 0.25 <i>p</i> = 0.09	3.86 ± 0.39 (4)
<i>M6M-0Ca</i>	0.95 ± 0.12	2.81 ± 0.47 (5)	0.65 ± 0.17 <i>p</i> = 0.02	3.21 ± 0.72 (5)	0.67 ± 0.17 <i>p</i> = 0.07	3.18 ± 0.76 (4)
<i>MTSBn</i>	1.06 ± 0.15	4.20 ± 0.81 (7)	0.68 ± 0.10 <i>p</i> = 0.00	4.94 ± 1.11 (7)	0.70 ± 0.09 <i>p</i> = 0.00	4.86 ± 0.85 (6)
<i>MTSBn-0Ca</i>	1.10 ± 0.24	3.66 ± 0.78 (5)	0.90 ± 0.16 <i>p</i> = 0.09	4.31 ± 0.74 (5)	0.80 ± 0.12 <i>p</i> = 0.03	3.79 ± 0.84 (5)
<i>MTSES</i>	1.12 ± 0.16	3.94 ± 0.40 (6)	0.68 ± 0.11 <i>p</i> = 0.00	3.87 ± 0.09 (6)	0.79 ± 0.18 <i>p</i> = 0.00	4.17 ± 0.15 (4)
<i>MTSES-0Ca</i>	0.98 ± 0.25	3.16 ± 0.42 (4)	0.65 ± 0.04 <i>p</i> = 0.06	3.93 ± 0.95 (4)	0.76 ± 0.04 <i>p</i> = 0.13	3.47 ± 0.55 (4)
<i>MTSET</i>	1.11 ± 0.10	3.41 ± 0.86 (3)	1.72 ± 0.13 <i>p</i> = 0.00	3.51 ± 0.23 (3)	1.04 ± 0.11 <i>p</i> = 0.59	3.70 ± 0.60 (3)
<i>MTSET-0Ca</i>	1.14 ± 0.21	2.68 ± 0.20 (3)	1.32 ± 0.36 <i>p</i> = 0.26	2.50 ± 0.19 (3)	0.93 ± 0.24 <i>p</i> = 0.06	3.05 ± 0.33 (3)
<i>MTSEA</i>	1.09 ± 0.11	3.73 ± 0.20 (4)	1.60 ± 0.13 <i>p</i> = 0.00	3.16 ± 0.04 (3)	1.18 ± 0.16 <i>p</i> = 0.09	3.47 ± 0.15 (3)
<i>MTSEA-0Ca</i>	1.04 ± 0.19	3.71 ± 0.85 (4)	1.62 ± 0.22 <i>p</i> = 0.01	3.00 ± 0.36 (4)	1.22 ± 0.18 <i>p</i> = 0.17	3.40 ± 1.10 (3)

EC₅₀ and Hill coefficient, *n*, determined from fits of the Hill equation to individual experiments. Data are presented as mean ± SD (number of patches). *p* values determined from paired t-test (in comparison with control).

IV. Discussion

SK channels are heteromeric channels comprised of the pore-forming α -subunits and calmodulin. The crystal structure of CaMBD/Ca²⁺/CaM revealed the intricate interaction between the SK2 CaM-binding domain and CaM, which controls the Ca²⁺-activated gating motion of SK channel S6 transmembrane domain. A variety of techniques were utilized in this study to tease out the role of CaM in gating, trafficking, and modulation of SK channels; as well as how well the static crystal structure corresponds to the interplay of CaM and CaMBD during the dynamic gating process. Excised inside-out patch clamp recordings from transiently transfected mammalian cells were used in both section II and III to determine the gating property and Ca²⁺-sensitivity of SK channels with site-directed mutations and truncations. Additionally, immunocytochemistry was used to investigate how the association of CaM to the CaMBD peptide facilitates the trafficking of SK channels to the cell surface. In section III, SDFL and cross-linking experiments of either isolated peptides or complete SK channels were used to examine the dimer-of-dimers gating model for SK channels and the CaM-CaMBD contact sites at the atomic level.

A. CaM Activation Mechanisms

As a ubiquitous Ca²⁺ sensor inside the eukaryotic cells, CaM serves many different functions. Three activation mechanisms are proposed for CaM: relieving autoinhibition, active site remodeling, and dimerization (Hoeflich and Ikura, 2002). SK channels fall in the last category as shown in the crystal structure of CaMBD/Ca²⁺/CaM, and the

constitutive binding of CaM to the CaMBD peptide endows the rapid gating and high Ca²⁺ sensitivity. Interestingly, the constitutive association between CaM and SK channels is not required for gating, as demonstrated in the rSK2 R464E/K467E double charge reversal mutant that has drastically reduced CaM affinity in section II of this dissertation. Loss of Ca²⁺/CaM-activated gating could be remedied by application of the purified recombinant CaM *in trans*, eluding that only the Ca²⁺-dependent binding is necessary for gating (Lee et al., 2003).

Calcium signaling pathways regulate a variety of cellular events such as gene transcription, protein phosphorylation, nucleotide metabolism, and ion transport. In higher vertebrates, a single CaM protein is encoded by multiple, co-expressed genes, and the number of discrete CaM transcripts produced by a single cell is further increased by alternative polyadenylation. CaM mRNAs are targeted to different intracellular compartments and that the translocation of mRNA, instead of the protein, provides a means to enrich the CaM protein in a specific site in the cell. (Ikura and Ames, 2006; Kortvely and Gulya, 2004). Therefore, the ability of SK channels being gated by not constitutively bound CaM provides a possibility of channel function closely regulated by the availability of CaM, which is affected by the metabolic state of the cell. Another wild speculation is that the association and dissociation of CaM *in trans* may also dictate the open and close rates of SK channel, resulting in prolonged activation and deactivation times of Ca²⁺-modulated currents reminiscent of the slow AHP current.

Given that CaM binds very tightly to SK and this binding is required for surface

expression, it seems unlikely that CaM availability will be a determinant of channel activity in the plasma membrane. Yet, the phosphorylation state of CaM could affect the the Ca²⁺ sensitivity of SK channels: high-affinity SK2-CaM(T80A) channels mediated a K⁺ current with fast onset and slow decay kinetics, while the low-affinity SK2-CaM(T80D) channels mediated currents with slow onset and fast decay (Bildl et al., 2004). Therefore, phosphorylation or other post-translational modification of CaM might decrease CaM affinity to SK channel, thereby providing the possibility of CaM dissociation from pre-associated SK channels after facilitating the surface expression of SK channels.

Intriguingly, the compensatory CaM E84R/E87K mutant was unable to achieve the original Ca²⁺ sensitivity despite of resuming the Ca²⁺-independent binding to rSK2 R464E/K467E. Therefore, the constitutive association between CaM and SK channels does not guarantee the efficacy of Ca²⁺-gating. A possible explanation is that CaM E84R/E87K mutant has lower Ca²⁺-binding affinity due to the introduced positive charges of arginine and lysine, which could repulse the divalent Ca²⁺ cations. Another possibility is that the rSK2 R464E/K467E has intrinsic defect in sensing the conformational changes relayed from CaM, and hence is less sensitive to the intracellular Ca²⁺ signal.

B. CaM-facilitated Trafficking of SK Channels

Similar to the CaM-dependent association of SK4/IK1 monomers at their Ct1 domains

(proximal C terminus) regulates channel assembly and surface expression (Joiner et al., 2001), the constitutive association between Ca^{2+} -free CaM and CaMBD facilitated trafficking of the SK2 channel to the cell membrane (Lee et al., 2003). The details of the trafficking facilitation are not known; we speculate that a chaperon-like mechanism is involved, probably through appropriate channel assembly (Joiner et al., 2001; Jones et al., 2005). The tripeptide 'RKR' which functions in K_{ATP} channels as an ER retention signal (Zerangue et al., 1999) is also present in the N-terminal domain of SK2 (LFEKRRKRLSDY). This motif was mutated to 'AAA' and assayed by voltage clamp recordings of inside-out patches excised from transiently transfected CHO cells. However, the mutant channels showed current amplitudes and Ca^{2+} gating comparable to wildtype SK2 channel. Therefore, SK2 channels do not utilize this trafficking signal. Interestingly, when the tetrapeptide 'KRKR' which comprises part of the CK2 binding sequence was mutated to 'AAAA', no current response was detected (Duane Allen, personal communication). Hence, it is possible that the ER retention signal requires the additional basic charge in the context of the SK channel, or that CK2 binding might be essential in SK channel trafficking. Further experiments are necessary to define the subcellular localization of retained SK channels within the cell. Also, it would be interesting to know whether incubating the cells at a permissive temperature such as 27°C could rescue the trafficking defect. Since the CaM availability could be rate-limiting for SK channel surface expression (Persechini and Stemmer, 2002), the cell excitability might be regulated by SK channel current density via the metabolic state-dependent CaM concentration as mentioned in section A.

A recent study demonstrated that activation of cyclic AMP-dependent protein kinase (PKA) with forskolin causes a dramatic decrease in surface localization of the SK2 channel subunit due to direct phosphorylation of the SK2 channel subunit. Mutagenesis and mass spectrometry studies identified four PKA phosphorylation sites: S465 (minor site) and three amino acid residues S568, S569, S570 (major sites) within the C-terminal region; suggesting that PKA phosphorylation is necessary for PKA-mediated reorganization of SK2 surface expression (Ren et al., 2006).

C. Reconcile the Functional Data to the Crystal Structure

The crystal structure of CaMBD/Ca²⁺/CaM failed to precisely predict the solvent accessibility estimated from SDFL experiments, the proximity of substituted cysteines in the cross-linking data, and gating ability of truncated channels which drastically disrupt the dimer-of-dimers (Section III). In contrast, previous functional study identifying CaM E-F hands 1 and 2 as the necessary and sufficient Ca²⁺ sensors for Ca²⁺ gating of SK channels (Keen et al., 1999) corresponds to the CaMBD/Ca²⁺/CaM crystal structure with Ca²⁺ occupying CaM E-F hands 1 and 2 (Schumacher et al., 2001). Accompanying the CaMBD/Ca²⁺/CaM crystal structure, dynamic light scattering (DLS) studies on the CaMBD/CaM complex (relative molecular mass (Mr 29K) of monomer complex 29,000) indicate that it is monomeric in the absence of Ca²⁺ (30K) and dimeric (61K) in the presence of Ca²⁺. This has been confirmed by equilibrium sedimentation analyses (29K and 54K in the absence and presence of Ca²⁺, respectively). Additionally, the compensatory CaM:84/87 mutant rescues the constitutive association between CaM and

rSK2 of the SK2:64/67 double charge reversal mutant (Section II); hence, the contact sites between CaM linker region and CaMBD $\alpha 2$ helix identified by the crystal structure are consistent with the functional data.

Considering that there are still heated arguments over how the new crystal structure of Kv1.2 could interpret the measurements of the motion of the voltage sensor (Tombola et al., 2005), it is not unreasonable to conceive the limit of predicting the dynamic motions of SK channels based solely on the static crystal structure of CaMBD/Ca²⁺/CaM. We suspect that the CaM-CaMBD interaction beyond residue K472 is not reflected by the crystal, and the N-lobe of CaM might conform to a structure other than the dimer-of-dimers during the gating process.

D. Hydrophobic Residues in SK Channels

Although the N- and C-terminal leucine zippers of hIK1 play a vital role in trafficking (Jones et al., 2004; Syme et al., 2003), no comparable leucine residues have been reported for other SK channels. Our finding of charge-dependent alteration in Ca²⁺-sensitivity of MTS reagent-modified rSK2 L457C is thus an unprecedented discovery. Unlike salt bridges, hydrophobic interactions are easily overlooked due to their generally lower impact on the channel structure if a mutation occurs. Yet, the rSK2 L457 position appears to be very sensitive to its micro-electrical environment, adapting drastic different conformations upon adornment by different charged MTS compounds. We suppose that this conservative leucine residue stabilizes the protein-protein interface

between CaM and CaMBD and subsequently ensures to the high Ca^{2+} -sensitivity of SK channels. Other hydrophobic residues of CaM-modulated channels may as well play equivalent roles in the quality control for Ca^{2+} -regulated processes.

E. Future Experiments

As the protein crystallography techniques advance, it is possible to resolve the structure of the complete SK channel in the near future. We expect to learn the protein-lipid interaction between SK channel and surrounding lipids during this development. Further structure-driven experiments on SK channel dynamics, such as biotin-avidin analysis and FRET analysis, will surely ensue. Meanwhile, the interplay between CaM and SK channels should be investigated in a metabolic context. How differential expression of CaM regulates the SK channel density and the resulting cell excitability? What happens if cultured hippocampal neurons are transfected by Ca^{2+} -sensitivity compromised SK channels? The answers to these questions could lead to studies utilizing corresponding time-controlled, tissue-specific transgenic mice, and hence provide more physiological insights of SK channels.

V. Summary and Conclusions

In this dissertation, I have identified that both electrostatic and hydrophobic interactions contribute to the close association between the SK channel CaMBD and CaM. Using electrophysiological recordings and immunochemistry on SK2 double charge reversal mutant R464E/K467E, that has dramatically reduced calmodulin binding affinity due to disrupted salt bridges with E84 and E86 on CaM, I demonstrated that the Ca^{2+} -independent constitutive association of CaM and SK channel subunits is required for surface expression, but not for channel gating. Application of MTS reagents onto SK2 L457C revealed the charge-dependent modulation of Ca^{2+} -sensitivity, and MTS crosslinkers rescued the decreased Ca^{2+} -sensitivity of SK2 L457C. In addition, the interaction sites between the SK channel CaMBD and CaM were site-directed cysteine-substituted on both isolated peptides and the complete channel. Neither the solvent accessibility nor proximity of substituted cysteines exactly reflected the predictions based upon the structural data. Furthermore, a C-terminal truncation predicted to abolish Ca^{2+} gating resulted in fully functional Ca^{2+} -gated channels. Therefore, despite several previously reported consistencies between structural data of CaMBD/ Ca^{2+} /CaM and functional SK channels, the ‘dimer-of-dimers’ model for SK channel gating may need some revision. This dissertation contributes to our knowledge of the interaction between SK channel CaMBD and CaM. Further physiological insights of SK channels would benefit from understanding how CaM-gating of SK channels is modulated by metabolic signals.

VI. References

- Abacioglu, Y. H., Fouts, T. R., Laman, J. D., Claassen, E., Pincus, S. H., Moore, J. P., Roby, C. A., Kamin-Lewis, R., and Lewis, G. K. (1994). Epitope mapping and topology of baculovirus-expressed HIV-1 gp160 determined with a panel of murine monoclonal antibodies. *AIDS Res Hum Retroviruses* *10*, 371-381.
- Abel, H. J., Lee, J. C., Callaway, J. C., and Foehring, R. C. (2004). Relationships between intracellular calcium and afterhyperpolarizations in neocortical pyramidal neurons. *J Neurophysiol* *91*, 324-335.
- Adelman, J. P., and Herson, P. S. (2004). Making scents of olfactory adaptation. *Nat Neurosci* *7*, 689-690.
- Alger, B. E., and Nicoll, R. A. (1980). Epileptiform burst afterhyperpolarization: calcium-dependent potassium potential in hippocampal CA1 pyramidal cells. *Science* *210*, 1122-1124.
- An, W. F., Bowlby, M. R., Betty, M., Cao, J., Ling, H. P., Mendoza, G., Hinson, J. W., Mattsson, K. I., Strassle, B. W., Trimmer, J. S., and Rhodes, K. J. (2000). Modulation of A-type potassium channels by a family of calcium sensors. *Nature* *403*, 553-556.
- Angers, S., Salahpour, A., Joly, E., Hilaiet, S., Chelsky, D., Dennis, M., and Bouvier, M. (2000). Detection of beta 2-adrenergic receptor dimerization in living cells using bioluminescence resonance energy transfer (BRET). *Proc Natl Acad Sci U S A* *97*, 3684-3689.
- Babu, Y. S., Sack, J. S., Greenhough, T. J., Bugg, C. E., Means, A. R., and Cook, W. J. (1985). Three-dimensional structure of calmodulin. *Nature* *315*, 37-40.

- Bildl, W., Strassmaier, T., Thurm, H., Andersen, J., Eble, S., Oliver, D., Knipper, M., Mann, M., Schulte, U., Adelman, J. P., and Fakler, B. (2004). Protein kinase CK2 is coassembled with small conductance Ca²⁺-activated K⁺ channels and regulates channel gating. *Neuron* *43*, 847-858.
- Blunck, R., Starace, D. M., Correa, A. M., and Bezanilla, F. (2004). Detecting rearrangements of shaker and NaChBac in real-time with fluorescence spectroscopy in patch-clamped mammalian cells. *Biophys J* *86*, 3966-3980.
- Bond, C. T., Herson, P. S., Strassmaier, T., Hammond, R., Stackman, R., Maylie, J., and Adelman, J. P. (2004). Small conductance Ca²⁺-activated K⁺ channel knock-out mice reveal the identity of calcium-dependent afterhyperpolarization currents. *J Neurosci* *24*, 5301-5306.
- Bond, C. T., Maylie, J., and Adelman, J. P. (1999). Small-conductance calcium-activated potassium channels. *Ann N Y Acad Sci* *868*, 370-378.
- Bond, C. T., Maylie, J., and Adelman, J. P. (2005). SK channels in excitability, pacemaking and synaptic integration. *Curr Opin Neurobiol* *15*, 305-311.
- Bond, C. T., Sprengel, R., Bissonnette, J. M., Kaufmann, W. A., Pribnow, D., Neelands, T., Storck, T., Baetscher, M., Jerecic, J., Maylie, J., *et al.* (2000). Respiration and parturition affected by conditional overexpression of the Ca²⁺-activated K⁺ channel subunit, SK3. *Science* *289*, 1942-1946.
- Bradley, J., Bonigk, W., Yau, K. W., and Frings, S. (2004). Calmodulin permanently associates with rat olfactory CNG channels under native conditions. *Nat Neurosci* *7*, 705-710.
- Bruening-Wright, A., Schumacher, M. A., Adelman, J. P., and Maylie, J. (2002).

Localization of the activation gate for small conductance Ca²⁺-activated K⁺ channels. *J Neurosci* 22, 6499-6506.

Cai, K., Itoh, Y., and Khorana, H. G. (2001). Mapping of contact sites in complex formation between transducin and light-activated rhodopsin by covalent crosslinking: use of a photoactivatable reagent. *Proc Natl Acad Sci U S A* 98, 4877-4882.

Careaga, C. L., and Falke, J. J. (1992). Thermal motions of surface alpha-helices in the D-galactose chemosensory receptor. Detection by disulfide trapping. *J Mol Biol* 226, 1219-1235.

Chen, T. Y., and Yau, K. W. (1994). Direct modulation by Ca(2+)-calmodulin of cyclic nucleotide-activated channel of rat olfactory receptor neurons. *Nature* 368, 545-548.

Chin, D., and Means, A. R. (2000a). Author correction. *Trends Cell Biol* 10, 428.

Chin, D., and Means, A. R. (2000b). Calmodulin: a prototypical calcium sensor. *Trends Cell Biol* 10, 322-328.

Coetzee, W. A., Amarillo, Y., Chiu, J., Chow, A., Lau, D., McCormack, T., Moreno, H., Nadal, M. S., Ozaita, A., Pountney, D., *et al.* (1999). Molecular diversity of K⁺ channels. *Ann N Y Acad Sci* 868, 233-285.

Deisseroth, K., Heist, E. K., and Tsien, R. W. (1998). Translocation of calmodulin to the nucleus supports CREB phosphorylation in hippocampal neurons. *Nature* 392, 198-202.

DeMaria, C. D., Soong, T. W., Alseikhan, B. A., Alvania, R. S., and Yue, D. T. (2001). Calmodulin bifurcates the local Ca²⁺ signal that modulates P/Q-type Ca²⁺ channels. *Nature* 411, 484-489.

Deschenes, I., Neyroud, N., DiSilvestre, D., Marban, E., Yue, D. T., and Tomaselli, G. F. (2002). Isoform-specific modulation of voltage-gated Na(+) channels by calmodulin. *Circ*

Res 90, E49-57.

Dombkowski, A. A. (2003). Disulfide by Design: a computational method for the rational design of disulfide bonds in proteins. *Bioinformatics* 19, 1852-1853.

Dong, J., Shi, N., Berke, I., Chen, L., and Jiang, Y. (2005). Structures of the MthK RCK domain and the effect of Ca²⁺ on gating ring stability. *J Biol Chem* 280, 41716-41724.

Doughty, J. M., Plane, F., and Langton, P. D. (1999). Charybdotoxin and apamin block EDHF in rat mesenteric artery if selectively applied to the endothelium. *Am J Physiol* 276, H1107-1112.

Dunham, T. D., and Farrens, D. L. (1999). Conformational changes in rhodopsin. Movement of helix f detected by site-specific chemical labeling and fluorescence spectroscopy. *J Biol Chem* 274, 1683-1690.

Edgerton, J. R., and Reinhart, P. H. (2003). Distinct contributions of small and large conductance Ca²⁺-activated K⁺ channels to rat Purkinje neuron function. *J Physiol* 548, 53-69.

Ehlers, M. D., Zhang, S., Bernhardt, J. P., and Huganir, R. L. (1996). Inactivation of NMDA receptors by direct interaction of calmodulin with the NR1 subunit. *Cell* 84, 745-755.

Erickson, M. G., Alseikhan, B. A., Peterson, B. Z., and Yue, D. T. (2001). Preassociation of calmodulin with voltage-gated Ca(2+) channels revealed by FRET in single living cells. *Neuron* 31, 973-985.

Erickson, M. G., Liang, H., Mori, M. X., and Yue, D. T. (2003). FRET two-hybrid mapping reveals function and location of L-type Ca²⁺ channel CaM preassociation. *Neuron* 39, 97-107.

Fabiato, A., and Fabiato, F. (1979). Calculator programs for computing the composition of the solutions containing multiple metals and ligands used for experiments in skinned muscle cells. *J Physiol (Paris)* 75, 463-505.

Farrens, D. L., Altenbach, C., Yang, K., Hubbell, W. L., and Khorana, H. G. (1996). Requirement of rigid-body motion of transmembrane helices for light activation of rhodopsin. *Science* 274, 768-770.

Finley, M., Arrabit, C., Fowler, C., Suen, K. F., and Slesinger, P. A. (2004). betaL-betaM loop in the C-terminal domain of G protein-activated inwardly rectifying K(+) channels is important for G(beta gamma) subunit activation. *J Physiol* 555, 643-657.

Gardos, G. (1958). The function of calcium in the potassium permeability of human erythrocytes. *Biochim Biophys Acta* 30, 653-654.

Geiser, J. R., van Tuinen, D., Brockerhoff, S. E., Neff, M. M., and Davis, T. N. (1991). Can calmodulin function without binding calcium? *Cell* 65, 949-959.

Grunwald, M. E., Yu, W. P., Yu, H. H., and Yau, K. W. (1998). Identification of a domain on the beta-subunit of the rod cGMP-gated cation channel that mediates inhibition by calcium-calmodulin. *J Biol Chem* 273, 9148-9157.

Grunwald, M. E., Zhong, H., Lai, J., and Yau, K. W. (1999). Molecular determinants of the modulation of cyclic nucleotide-activated channels by calmodulin. *Proc Natl Acad Sci U S A* 96, 13444-13449.

Gu, N., Vervaeke, K., Hu, H., and Storm, J. F. (2005). Kv7/KCNQ/M and HCN/h, but not KCa2/SK channels, contribute to the somatic medium after-hyperpolarization and excitability control in CA1 hippocampal pyramidal cells. *J Physiol* 566, 689-715.

Hamilton, S. L., and Reid, M. B. (2000). RyR1 modulation by oxidation and calmodulin.

Antioxid Redox Signal 2, 41-45.

Hammond, R. S., Bond, C. T., Strassmaier, T., Ngo-Anh, T. J., Adelman, J. P., Maylie, J., and Stackman, R. W. (2006). Small-conductance Ca²⁺-activated K⁺ channel type 2 (SK2) modulates hippocampal learning, memory, and synaptic plasticity. *J Neurosci* 26, 1844-1853.

Herrera, G. M., Heppner, T. J., and Nelson, M. T. (2000). Regulation of urinary bladder smooth muscle contractions by ryanodine receptors and BK and SK channels. *Am J Physiol Regul Integr Comp Physiol* 279, R60-68.

Herrera, G. M., Pozo, M. J., Zvara, P., Petkov, G. V., Bond, C. T., Adelman, J. P., and Nelson, M. T. (2003). Urinary bladder instability induced by selective suppression of the murine small conductance calcium-activated potassium (SK3) channel. *J Physiol* 551, 893-903.

Hille, B. (2001). *Ion channels of excitable membranes*, third edition (Sunderland, MA, Sinauer Associates, Inc.).

Hirschberg, B., Maylie, J., Adelman, J. P., and Marrion, N. V. (1998). Gating of recombinant small-conductance Ca-activated K⁺ channels by calcium. *J Gen Physiol* 111, 565-581.

Hoeflich, K. P., and Ikura, M. (2002). Calmodulin in action: diversity in target recognition and activation mechanisms. *Cell* 108, 739-742.

Horenstein, J., Wagner, D. A., Czajkowski, C., and Akabas, M. H. (2001). Protein mobility and GABA-induced conformational changes in GABA(A) receptor pore-lining M2 segment. *Nat Neurosci* 4, 477-485.

Hsu, Y. T., and Molday, R. S. (1993). Modulation of the cGMP-gated channel of rod

photoreceptor cells by calmodulin. *Nature* 361, 76-79.

Ikura, M., and Ames, J. B. (2006). Genetic polymorphism and protein conformational plasticity in the calmodulin superfamily: two ways to promote multifunctionality. *Proc Natl Acad Sci U S A* 103, 1159-1164.

Ikura, M., Clore, G. M., Gronenborn, A. M., Zhu, G., Klee, C. B., and Bax, A. (1992). Solution structure of a calmodulin-target peptide complex by multidimensional NMR. *Science* 256, 632-638.

Ishii, T. M., Maylie, J., and Adelman, J. P. (1997a). Determinants of apamin and d-tubocurarine block in SK potassium channels. *J Biol Chem* 272, 23195-23200.

Ishii, T. M., Silvia, C., Hirschberg, B., Bond, C. T., Adelman, J. P., and Maylie, J. (1997b). A human intermediate conductance calcium-activated potassium channel. *Proc Natl Acad Sci U S A* 94, 11651-11656.

Jacobson, D., Herson, P. S., Neelands, T. R., Maylie, J., and Adelman, J. P. (2002). SK channels are necessary but not sufficient for denervation-induced hyperexcitability. *Muscle Nerve* 26, 817-822.

Janz, J. M., and Farrens, D. L. (2004). Rhodopsin activation exposes a key hydrophobic binding site for the transducin alpha-subunit C terminus. *J Biol Chem* 279, 29767-29773.

Jiang, Y., Lee, A., Chen, J., Cadene, M., Chait, B. T., and MacKinnon, R. (2002). Crystal structure and mechanism of a calcium-gated potassium channel. *Nature* 417, 515-522.

Joiner, W. J., Khanna, R., Schlichter, L. C., and Kaczmarek, L. K. (2001). Calmodulin regulates assembly and trafficking of SK4/IK1 Ca²⁺-activated K⁺ channels. *J Biol Chem* 276, 37980-37985.

Joiner, W. J., Wang, L. Y., Tang, M. D., and Kaczmarek, L. K. (1997). hSK4, a member of

a novel subfamily of calcium-activated potassium channels. *Proc Natl Acad Sci U S A* *94*, 11013-11018.

Jones, H. M., Hamilton, K. L., and Devor, D. C. (2005). Role of an S4-S5 linker lysine in the trafficking of the Ca(2+)-activated K(+) channels IK1 and SK3. *J Biol Chem* *280*, 37257-37265.

Jones, H. M., Hamilton, K. L., Papworth, G. D., Syme, C. A., Watkins, S. C., Bradbury, N. A., and Devor, D. C. (2004). Role of the NH2 terminus in the assembly and trafficking of the intermediate conductance Ca²⁺-activated K⁺ channel hIK1. *J Biol Chem* *279*, 15531-15540.

Keen, J. E., Khawaled, R., Farrens, D. L., Neelands, T., Rivard, A., Bond, C. T., Janowsky, A., Fakler, B., Adelman, J. P., and Maylie, J. (1999). Domains responsible for constitutive and Ca(2+)-dependent interactions between calmodulin and small conductance Ca(2+)-activated potassium channels. *J Neurosci* *19*, 8830-8838.

Khawaled, R., Bruening-Wright, A., Adelman, J. P., and Maylie, J. (1999). Bicuculline block of small-conductance calcium-activated potassium channels. *Pflugers Arch* *438*, 314-321.

Klevit, R. E., Blumenthal, D. K., Wemmer, D. E., and Krebs, E. G. (1985). Interaction of calmodulin and a calmodulin-binding peptide from myosin light chain kinase: major spectral changes in both occur as the result of complex formation. *Biochemistry* *24*, 8152-8157.

Kobashi, K. (1968). Catalytic oxidation of sulfhydryl groups by o-phenanthroline copper complex. *Biochim Biophys Acta* *158*, 239-245.

Kohler, M., Hirschberg, B., Bond, C. T., Kinzie, J. M., Marrion, N. V., Maylie, J., and

- Adelman, J. P. (1996). Small-conductance, calcium-activated potassium channels from mammalian brain. *Science* 273, 1709-1714.
- Kortvely, E., and Gulya, K. (2004). Calmodulin, and various ways to regulate its activity. *Life Sci* 74, 1065-1070.
- Lakowicz, J. R. (1999). *Principles of Fluorescence Spectroscopy*, 2nd edn (New York, Plenum Publishers).
- Lamers, J. M., and Stinis, J. T. (1983). Inhibition of Ca²⁺-dependent protein kinase and Ca²⁺/Mg²⁺-ATPase in cardiac sarcolemma by the anti-calmodulin drug calmidazolium. *Cell Calcium* 4, 281-294.
- Lancaster, B., and Nicoll, R. A. (1987). Properties of two calcium-activated hyperpolarizations in rat hippocampal neurones. *J Physiol* 389, 187-203.
- Lee, W. S., Ngo-Anh, T. J., Bruening-Wright, A., Maylie, J., and Adelman, J. P. (2003). Small Conductance Ca²⁺-activated K⁺ Channels and Calmodulin: CELL SURFACE EXPRESSION AND GATING. *J Biol Chem* 278, 25940-25946.
- Liang, H., DeMaria, C. D., Erickson, M. G., Mori, M. X., Alseikhan, B. A., and Yue, D. T. (2003). Unified mechanisms of Ca²⁺ regulation across the Ca²⁺ channel family. *Neuron* 39, 951-960.
- Liu, D. T., Tibbs, G. R., and Siegelbaum, S. A. (1996). Subunit stoichiometry of cyclic nucleotide-gated channels and effects of subunit order on channel function. *Neuron* 16, 983-990.
- Logsdon, N. J., Kang, J., Togo, J. A., Christian, E. P., and Aiyar, J. (1997). A novel gene, hKCa4, encodes the calcium-activated potassium channel in human T lymphocytes. *J Biol Chem* 272, 32723-32726.

Loo, T. W., and Clarke, D. M. (2001). Determining the dimensions of the drug-binding domain of human P-glycoprotein using thiol cross-linking compounds as molecular rulers. *J Biol Chem* 276, 36877-36880.

Madison, D. V., and Nicoll, R. A. (1984). Control of the repetitive discharge of rat CA 1 pyramidal neurones in vitro. *J Physiol* 354, 319-331.

Marcotti, W., Johnson, S. L., and Kros, C. J. (2004). A transiently expressed SK current sustains and modulates action potential activity in immature mouse inner hair cells. *J Physiol* 560, 691-708.

Marrion, N. V., and Tavalin, S. J. (1998). Selective activation of Ca²⁺-activated K⁺ channels by co-localized Ca²⁺ channels in hippocampal neurons. *Nature* 395, 900-905.

McCormack, K., Tanouye, M. A., Iverson, L. E., Lin, J. W., Ramaswami, M., McCormack, T., Campanelli, J. T., Mathew, M. K., and Rudy, B. (1991). A role for hydrophobic residues in the voltage-dependent gating of Shaker K⁺ channels. *Proc Natl Acad Sci U S A* 88, 2931-2935.

Meador, W. E., Means, A. R., and Quirocho, F. A. (1992). Target enzyme recognition by calmodulin: 2.4 A structure of a calmodulin-peptide complex. *Science* 257, 1251-1255.

Michikawa, T., Hirota, J., Kawano, S., Hiraoka, M., Yamada, M., Furuichi, T., and Mikoshiba, K. (1999). Calmodulin mediates calcium-dependent inactivation of the cerebellar type 1 inositol 1,4,5-trisphosphate receptor. *Neuron* 23, 799-808.

Molday, R. S. (1996). Calmodulin regulation of cyclic-nucleotide-gated channels. *Curr Opin Neurobiol* 6, 445-452.

Mori, M., Konno, T., Ozawa, T., Murata, M., Imoto, K., and Nagayama, K. (2000). Novel interaction of the voltage-dependent sodium channel (VDSC) with calmodulin: does

VDSC acquire calmodulin-mediated Ca²⁺-sensitivity? *Biochemistry* 39, 1316-1323.

Mori, M. X., Erickson, M. G., and Yue, D. T. (2004). Functional stoichiometry and local enrichment of calmodulin interacting with Ca²⁺ channels. *Science* 304, 432-435.

Murphy, M. E., and Brayden, J. E. (1995). Apamin-sensitive K⁺ channels mediate an endothelium-dependent hyperpolarization in rabbit mesenteric arteries. *J Physiol* 489 (Pt 3), 723-734.

Nadif Kasri, N., Bultynck, G., Sienaert, I., Callewaert, G., Erneux, C., Missiaen, L., Parys, J. B., and De Smedt, H. (2002). The role of calmodulin for inositol 1,4,5-trisphosphate receptor function. *Biochim Biophys Acta* 1600, 19-31.

Ngo-Anh, T. J., Bloodgood, B. L., Lin, M., Sabatini, B. L., Maylie, J., and Adelman, J. P. (2005). SK channels and NMDA receptors form a Ca²⁺-mediated feedback loop in dendritic spines. *Nat Neurosci* 8, 642-649.

Oliver, D., Klocker, N., Schuck, J., Baukrowitz, T., Ruppersberg, J. P., and Fakler, B. (2000). Gating of Ca²⁺-activated K⁺ channels controls fast inhibitory synaptic transmission at auditory outer hair cells. *Neuron* 26, 595-601.

Ordaz, B., Tang, J., Xiao, R., Salgado, A., Sampieri, A., Zhu, M. X., and Vaca, L. (2005). Calmodulin and calcium interplay in the modulation of TRPC5 channel activity. Identification of a novel C-terminal domain for calcium/calmodulin-mediated facilitation. *J Biol Chem* 280, 30788-30796.

Palfi, A., Kortvely, E., Fekete, E., Kovacs, B., Varszegi, S., and Gulya, K. (2002). Differential calmodulin gene expression in the rodent brain. *Life Sci* 70, 2829-2855.

Palfi, A., Vizi, S., and Gulya, K. (1999). Differential distribution and intracellular targeting of mRNAs corresponding to the three calmodulin genes in rat brain. A

quantitative in situ hybridization study. *J Histochem Cytochem* 47, 583-600.

Persechini, A., and Stemmer, P. M. (2002). Calmodulin is a limiting factor in the cell. *Trends Cardiovasc Med* 12, 32-37.

Petersen, M. T., Jonson, P. H., and Petersen, S. B. (1999). Amino acid neighbours and detailed conformational analysis of cysteines in proteins. *Protein Eng* 12, 535-548.

Peterson, B. Z., DeMaria, C. D., Adelman, J. P., and Yue, D. T. (1999). Calmodulin is the Ca²⁺ sensor for Ca²⁺-dependent inactivation of L-type calcium channels. *Neuron* 22, 549-558.

Pfleger, K. D., and Eidne, K. A. (2005). Monitoring the formation of dynamic G-protein-coupled receptor-protein complexes in living cells. *Biochem J* 385, 625-637.

Pitt, G. S., Zuhlke, R. D., Hudmon, A., Schulman, H., Reuter, H., and Tsien, R. W. (2001). Molecular basis of calmodulin tethering and Ca²⁺-dependent inactivation of L-type Ca²⁺ channels. *J Biol Chem* 276, 30794-30802.

Qian, X., Nimigean, C. M., Niu, X., Moss, B. L., and Magleby, K. L. (2002). Slo1 tail domains, but not the Ca²⁺ bowl, are required for the beta 1 subunit to increase the apparent Ca²⁺ sensitivity of BK channels. *J Gen Physiol* 120, 829-843.

Ren, Y., Lyndon, B. F., Alexander, J. C., Lubin, F. D., Adelman, J. P., Pfaffinger, P. J., Schrader, L. A., and Anderson, A. E. (2006). Regulation of surface localization of the small-conductance Ca²⁺-activated potassium channel, SK2 through direct phosphorylation by cyclic amp-dependent protein kinase. *J Biol Chem*.

Rodney, G. G., Williams, B. Y., Strasburg, G. M., Beckingham, K., and Hamilton, S. L. (2000). Regulation of RYR1 activity by Ca(2+) and calmodulin. *Biochemistry* 39, 7807-7812.

- Sah, P. (1996). Ca²⁺-activated K⁺ currents in neurones: types, physiological roles and modulation. *Trends Neurosci* 19, 150-154.
- Sailer, C. A., Hu, H., Kaufmann, W. A., Trieb, M., Schwarzer, C., Storm, J. F., and Knaus, H. G. (2002). Regional differences in distribution and functional expression of small-conductance Ca²⁺-activated K⁺ channels in rat brain. *J Neurosci* 22, 9698-9707.
- Saimi, Y., and Kung, C. (2002). Calmodulin as an ion channel subunit. *Annu Rev Physiol* 64, 289-311.
- Schonherr, R., Lober, K., and Heinemann, S. H. (2000). Inhibition of human ether a go-go potassium channels by Ca²⁺/calmodulin. *Embo J* 19, 3263-3271.
- Schreiber, M., and Salkoff, L. (1997). A novel calcium-sensing domain in the BK channel. *Biophys J* 73, 1355-1363.
- Schumacher, M. A., Crum, M., and Miller, M. C. (2004). Crystal structures of apocalmodulin and an apocalmodulin/SK potassium channel gating domain complex. *Structure* 12, 849-860.
- Schumacher, M. A., Rivard, A. F., Bachinger, H. P., and Adelman, J. P. (2001). Structure of the gating domain of a Ca²⁺-activated K⁺ channel complexed with Ca²⁺/calmodulin. *Nature* 410, 1120-1124.
- Schutz, C. N., and Warshel, A. (2001). What are the dielectric "constants" of proteins and how to validate electrostatic models? *Proteins* 44, 400-417.
- Schwindt, P. C., Spain, W. J., Foehring, R. C., Stafstrom, C. E., Chubb, M. C., and Crill, W. E. (1988). Multiple potassium conductances and their functions in neurons from cat sensorimotor cortex in vitro. *J Neurophysiol* 59, 424-449.
- Shah, V. N., Wingo, T. L., Weiss, K. L., Williams, C. K., Balsler, J. R., and Chazin, W. J.

- (2006). Calcium-dependent regulation of the voltage-gated sodium channel hH1: Intrinsic and extrinsic sensors use a common molecular switch. *Proc Natl Acad Sci U S A*.
- Shao, L. R., Halvorsrud, R., Borg-Graham, L., and Storm, J. F. (1999). The role of BK-type Ca^{2+} -dependent K^{+} channels in spike broadening during repetitive firing in rat hippocampal pyramidal cells. *J Physiol* 521 Pt 1, 135-146.
- Skene, J. H. (1990). GAP-43 as a 'calmodulin sponge' and some implications for calcium signalling in axon terminals. *Neurosci Res Suppl* 13, S112-125.
- Smith, J. S., Rousseau, E., and Meissner, G. (1989). Calmodulin modulation of single sarcoplasmic reticulum Ca^{2+} -release channels from cardiac and skeletal muscle. *Circ Res* 64, 352-359.
- Stackman, R. W., Hammond, R. S., Linardatos, E., Gerlach, A., Maylie, J., Adelman, J. P., and Tzounopoulos, T. (2002). Small conductance Ca^{2+} -activated K^{+} channels modulate synaptic plasticity and memory encoding. *J Neurosci* 22, 10163-10171.
- Stocker, M. (2004). Ca^{2+} -activated K^{+} channels: molecular determinants and function of the SK family. *Nat Rev Neurosci* 5, 758-770.
- Stocker, M., Hirzel, K., D'Hoedt, D., and Pedarzani, P. (2004). Matching molecules to function: neuronal Ca^{2+} -activated K^{+} channels and afterhyperpolarizations. *Toxicon* 43, 933-949.
- Stocker, M., Krause, M., and Pedarzani, P. (1999). An apamin-sensitive Ca^{2+} -activated K^{+} current in hippocampal pyramidal neurons. *Proc Natl Acad Sci U S A* 96, 4662-4667.
- Stocker, M., and Pedarzani, P. (2000). Differential distribution of three Ca^{2+} -activated K^{+} channel subunits, SK1, SK2, and SK3, in the adult rat central nervous system. *Mol Cell Neurosci* 15, 476-493.

Strassmaier, T., Bond, C. T., Sailer, C. A., Knaus, H. G., Maylie, J., and Adelman, J. P. (2005). A novel isoform of SK2 assembles with other SK subunits in mouse brain. *J Biol Chem* 280, 21231-21236.

Swensen, A. M., and Bean, B. P. (2003). Ionic mechanisms of burst firing in dissociated Purkinje neurons. *J Neurosci* 23, 9650-9663.

Syme, C. A., Hamilton, K. L., Jones, H. M., Gerlach, A. C., Giltinan, L., Papworth, G. D., Watkins, S. C., Bradbury, N. A., and Devor, D. C. (2003). Trafficking of the Ca²⁺-activated K⁺ channel, hK1, is dependent upon a C-terminal leucine zipper. *J Biol Chem* 278, 8476-8486.

Taylor, M. S., Bonev, A. D., Gross, T. P., Eckman, D. M., Brayden, J. E., Bond, C. T., Adelman, J. P., and Nelson, M. T. (2003). Altered Expression of Small-Conductance Ca²⁺-Activated K⁺ (SK3) Channels Modulates Arterial Tone and Blood Pressure. *Circ Res*.

Tombola, F., Pathak, M. M., and Isacoff, E. Y. (2005). How far will you go to sense voltage? *Neuron* 48, 719-725.

Toutenhoofd, S. L., and Strehler, E. E. (2000). The calmodulin multigene family as a unique case of genetic redundancy: multiple levels of regulation to provide spatial and temporal control of calmodulin pools? *Cell Calcium* 28, 83-96.

Trudeau, M. C., and Zagotta, W. N. (2002). Mechanism of calcium/calmodulin inhibition of rod cyclic nucleotide-gated channels. *Proc Natl Acad Sci U S A* 99, 8424-8429.

Trudeau, M. C., and Zagotta, W. N. (2003). Calcium/Calmodulin Modulation of Olfactory and Rod Cyclic Nucleotide-gated Ion Channels. *J Biol Chem* 278, 18705-18708.

- Tse, A., and Hille, B. (1992). GnRH-induced Ca^{2+} oscillations and rhythmic hyperpolarizations of pituitary gonadotropes. *Science* 255, 462-464.
- Tse, A., Tse, F. W., and Hille, B. (1995). Modulation of Ca^{2+} oscillation and apamin-sensitive, Ca^{2+} -activated K^{+} current in rat gonadotropes. *Pflugers Arch* 430, 645-652.
- Varnum, M. D., and Zagotta, W. N. (1997). Interdomain interactions underlying activation of cyclic nucleotide-gated channels. *Science* 278, 110-113.
- Verkade, P., Schrama, L. H., Verkleij, A. J., Gispen, W. H., and Oestreicher, A. B. (1997). Ultrastructural co-localization of calmodulin and B-50/growth-associated protein-43 at the plasma membrane of proximal unmyelinated axon shafts studied in the model of the regenerating rat sciatic nerve. *Neuroscience* 79, 1207-1218.
- Villalobos, C., Shakkottai, V. G., Chandy, K. G., Michelhaugh, S. K., and Andrade, R. (2004). SKCa channels mediate the medium but not the slow calcium-activated afterhyperpolarization in cortical neurons. *J Neurosci* 24, 3537-3542.
- Wen, H., and Levitan, I. B. (2002). Calmodulin is an auxiliary subunit of KCNQ2/3 potassium channels. *J Neurosci* 22, 7991-8001.
- Wissmann, R., Bildl, W., Neumann, H., Rivard, A. F., Klocker, N., Weitz, D., Schulte, U., Adelman, J. P., Bentrop, D., and Fakler, B. (2002). A helical region in the C terminus of small-conductance Ca^{2+} -activated K^{+} channels controls assembly with apo-calmodulin. *J Biol Chem* 277, 4558-4564.
- Wolfart, J., Neuhoff, H., Franz, O., and Roeper, J. (2001). Differential expression of the small-conductance, calcium-activated potassium channel SK3 is critical for pacemaker control in dopaminergic midbrain neurons. *J Neurosci* 21, 3443-3456.

- Xia, X. M., Fakler, B., Rivard, A., Wayman, G., Johnson-Pais, T., Keen, J. E., Ishii, T., Hirschberg, B., Bond, C. T., Lutsenko, S., *et al.* (1998). Mechanism of calcium gating in small-conductance calcium-activated potassium channels. *Nature* 395, 503-507.
- Xia, X. M., Zeng, X., and Lingle, C. J. (2002). Multiple regulatory sites in large-conductance calcium-activated potassium channels. *Nature* 418, 880-884.
- Xu, J., Yu, W., Wright, J. M., Raab, R. W., and Li, M. (1998). Distinct functional stoichiometry of potassium channel beta subunits. *Proc Natl Acad Sci U S A* 95, 1846-1851.
- Yamaguchi, N., Xu, L., Pasek, D. A., Evans, K. E., Chen, S. R., and Meissner, G. (2005). Calmodulin regulation and identification of calmodulin binding region of type-3 ryanodine receptor calcium release channel. *Biochemistry* 44, 15074-15081.
- Yus-Najera, E., Santana-Castro, I., and Villarroel, A. (2002). The identification and characterization of a noncontinuous calmodulin-binding site in noninactivating voltage-dependent KCNQ potassium channels. *J Biol Chem* 277, 28545-28553.
- Zagotta, W. N., Olivier, N. B., Black, K. D., Young, E. C., Olson, R., and Gouaux, E. (2003). Structural basis for modulation and agonist specificity of HCN pacemaker channels. *Nature* 425, 200-205.
- Zamponi, G. W. (2003). Calmodulin lobotomized: novel insights into calcium regulation of voltage-gated calcium channels. *Neuron* 39, 879-881.
- Zerangue, N., Schwappach, B., Jan, Y. N., and Jan, L. Y. (1999). A new ER trafficking signal regulates the subunit stoichiometry of plasma membrane K(ATP) channels. *Neuron* 22, 537-548.
- Zhang, M., Houamed, K., Kupersmidt, S., Roden, D., and Satin, L. S. (2005).

Pharmacological properties and functional role of K_{slow} current in mouse pancreatic beta-cells: SK channels contribute to K_{slow} tail current and modulate insulin secretion. *J Gen Physiol* 126, 353-363.

Zhang, S., Ehlers, M. D., Bernhardt, J. P., Su, C. T., and Huganir, R. L. (1998). Calmodulin mediates calcium-dependent inactivation of N-methyl-D-aspartate receptors. *Neuron* 21, 443-453.

Zuhlke, R. D., Pitt, G. S., Deisseroth, K., Tsien, R. W., and Reuter, H. (1999). Calmodulin supports both inactivation and facilitation of L-type calcium channels. *Nature* 399, 159-162.